Université catholique de Louvain
Ecole Polytechnique de Louvain
(Louvain School of Engineering)
Institute of Information and Communication Technologies,
Electronics and Applied Mathematics (ICTEAM)

B - 1348 Louvain-la-Neuve Belgique

Quantitative electroencephalography and applications in the assessments of conscious states and in Brain Computer Interfaces

Rémy Lehembre

Thesis presented for the Ph.D. degree
in Applied Sciences

Ph.D. committee:

Benoit MACQ (UCL/ICTEAM) - Supervisor
Christophe DE VLEESCHOUWER (UCL/ICTEAM)
Michel VERLEYSEN (UCL/ICTEAM)
Quentin NOIRHOMME (ULG/CSG)
Steven LAUREYS (ULG/CSG)
Andrea SODDU (ULG/CSG)

July 2012

Abstract

Probing consciousness is a major challenge in the evaluation of patients with disorders of consciousness (DOC). Improvement of behavioral scales have led to more accurate bedside assessments but are still bound to variability due to different factors such as the subjectivity and experience of the assessor and the fluctuations of the patient state. Brain imaging techniques such as positron emission tomography (PET) functional MRI (fMRI), diffusion tensor imaging (DTI) or electroencephalography (EEG) provide different and complementary information on metabolism, haemodynamic function, tissue organization and electrical activity of the brain. Measurements obtained from these methods can lead to objective assessments and quantification of correlates of consciousness. This thesis aims at exploring electrophysiological markers of consciousness in three different settings. First mechanisms of consciousness are explored in healthy subjects during ketamine induced loss of consciousness. Second by studying differences in resting state EEG of patients in vegetative/unresponsive wakefulness state (VS/UWS) and patients in minimally conscious state (MCS). Finally by investigating voluntary control through a Brain Computer Interface (BCI) device.

The thesis is divided in two parts, the first part introduces the anatomy of the brain and the physiological processes underlying EEG generation, in particular the hierarchy of the neocortex. Then in chapter 3, the different EEG patterns observed in DOC are illustrated with the different electrophysiological techniques used to assess DOC patients such as quantitative electroencephalography (qEEG), event related potentials (ERP) and brain computer interfaces (BCI). Chapter 4 is an non exhaustive overview of signal processing techniques and their adaptation to qEEG.

In the second part, the three studies conducted during this thesis are presented. Chapter 5 explores ketamine induced loss of consciousness in healthy volunteers. A concomitant increase in theta and gamma frequencies at the scalp and source level in frontal and parietal cortices was observed. Assessment of effective connectivity with dynamical causal modelling (DCM) showed a difference in intra-cortical connectivity. In chapter 6, scalp level differences in power spectra and connectivity measurements could discriminate VS/UWS patients from MCS patients. VS/UWS patients displayed slow oscillations while MCS patients had more power and higher connectivity in higher frequencies. Finally, chapter 7 presents a comparative study between

source reconstruction based classification of upcoming finger movement and classification with common spatial patterns (CSP). The source reconstruction approach did not improve classification rates achieved with CSP at the scalp level in the studied dataset.

Acknowledgements

En premier lieu je voudrais remercier Michel Verleysen d'avoir accepté la présidence du jury de cette thèse ainsi que Christophe de Vleeschouwer d'en avoir accepté le rôle de secrétaire.

Merci à Benoît Macq, qui en proposant un large éventail de sujets originaux m'a permis tout d'abord de faire un travail de fin d'études passionnant. Ses encouragements et son soutien à continuer dans la recherche ont été indispensables.

Je ne remercierai jamais assez Steven Laureys de m'avoir accueilli si chaleureusement au sein du Coma Science Group. J'ai pu bénéficier de l'aide de toute une équipe pluridisciplinaire couvrant un large éventail de compétences dans une ambiance toujours stimulante.

Merci à Quentin Noirhomme, je nous vois encore avec Cédric en train de rédiger notre projet FRIA sur cette terrasse d'un café irlandais près de Schuman. C'est grâce à tes conseils précieux que j'ai pu obtenir la bourse et par la suite c'est par ton intermédiaire que j'ai pu venir poursuivre mes travaux à Liège. Une chose est sûre, je n'aurai pas fini sans ton aide.

Grazie ad Andrea per tutto l'incoraggiamento costantemente rinnovato. I molti caffè ingerito, l'ospitalità, corsi di italiano, viaggi ciclotrone-chu (se si sommano tutti questi viaggi ti devo un biglietto per un giro del mondo)... Forza Italia !

Merci à Mélanie Boly de m'en avoir appris un bon paquet sur l'EEG et la conscience et ce toujours dans la bonne humeur.

Merci à Christophe Phillips, toujours de bon conseil.

Merci à tous les membres du Coma Science Group qui m'ont permis de finir ma thèse dans un environment de travail captivant et stimulant: Camille (encore une part de pizza Roberto ?), Marie-Aurélie, Dina, Aurore, Damien, Peter, Athéna, Audrey, Marie, Zulay, Ithabi, Olivia, Patcho, Caroline, Vanessa, Lizette et Audrey.

Merci à toutes les personnes du Centre de Recherches du Cyclotron ainsi que les membres de l'ICTEAM.

Merci à Zayd qui m'en a appris plus d'une sur des sujets aussi différents que la photo, la bd et l'eeg...

Merci à Vincenzo pour son hospitalité et les découvertes musicales, bon courage pour la fin de ta thèse !

Merci à Anhahita et Fabien pour toutes les chouettes discussions !

Merci à Jean-Julien, Christian et Andrew pour tous les eNTERFACES et bons moments passés ensemble.

La musique m'a accompagnée tout au long de cette thèse, je garde un souvenir mémorable de cette tournée des pavés ainsi que de ce caddy'ac tour avec Rony Rone et les Balltraps. Un tout grand merci à toute la famille Wisnia et à la famille Leseigneur pour leur accueil à chaque fois mémorable à Carsac! Merci le Mat pour toutes les manoucheries et merci mon Ron pour ces belles aventures ("Le grand saut dans le grand n'importe quoi").

Merci à Aidan & the Italian Weather Ladies: Aidan, Fabrice et Simon, "Keep finding things that make you smile" pour tous les moments de musique privilégiés...

Et puis un merci particulier et rythmique à Augustin, j'espère avoir encore souvent l'occasion de faire partie de the best rhythm sexction of the world...

Merci à Armistead Burwell Smith IV

Merci à mes collègues du bureau a.157 à LLN : Teh (sacré Jimi), Antonin (whou hwou hou huu huu) , Suzanne (Allez Roger !), Julien (Vive l'Amérique), Jérôme (La phrase du jour..)

Merci à la famille de Vieusart : Gaetan, Anne et Hanaé-Lou et les voisins Marthe, Guillaume, Isaline, Clément (et le/la troisième!) pour les moments magiques et hors du temps, les BBQs et le soleil !

Merci à Sébastien pour la constante bonne humeur !

Merci à Elsa et Ara pour tous les bons moments passés et à venir...et bientôt un petit bonhomme!

Merci aux immortels, Will (Le gálactico !!) Tuan (je te dois un canapé vu comme j'ai trop souvent squatté le tien), BBR (Bouge ton .... et fait le rebondir... !), Renaud ("Tu t'en ai toujours sorti, je vois pas pourquoi tu t'en sortirais pas").

Merci Ced, on a fait un sacré bout de chemin, t'as cartonné pour ta thèse mais faudra encore t'améliorer un peu pour les 20km (jek jek).

Merci à Luc et Rosemonde pour toutes ces petites choses qui font déjà une montagne, à Pauline et Quentin (fiou, quelle différence de bosser sur un vrai bureau..!)

Merci à ma famille: Christian, Bernadette, Aymeric et Coryse, j'espère me rattraper rapidement sur tout ce temps où j'ai été peu disponible !

Last but not least: Merci Marie.

à Emilie...

Contents

List of Figures

Notations and Acronyms

Mathematical notations

j	imaginary unit: $j = \sqrt{-1}$
x	a scalar
$\hat{\boldsymbol{x}}$	a unit vector
$\mathrm{Re}(x)$	the real part of x
$\mathrm{Im}(x)$	the imaginary part of x
$\exp(x)$	the exponential of x
$\arctan(x)$	the arc tangent of x
$\lvert x \rvert$	the absolute value or norm of x
$\mathbf{x}$	a vector
$\otimes$	the convolution operator
x_m	the m^{th} entry of vector $\mathbf{x}$: $\mathbf{x} = [x_0, x_1, \ldots, x_{K-1}]^T$
$\mathbf{x}^T$	the transpose of vector $\mathbf{x}$
$\mathbf{X}$	a matrix
$\mathbf{X}^T$	the transpose of matrix $\mathbf{X}$
$\mathbf{X}^{-1}$	the inverse of matrix $\mathbf{X}$
$\mathbf{I}_N$	the $N \times N$ identity matrix
$p(x)$	the probability distribution of variable x

Acronyms

DMN : Default Mode Network
DOC : Disorders of consciousness
C : Coherency
ECN : External Control Network
EEG : Electroencephalography
IC : Imaginary part of Coherency
MCS : Minimally Conscious State
PLI : Phase lag Index
VS\UWS : Vegetative State \ Unresponsive Wakefulness Syndrome

Introduction

1

The inside of your head is not this gray and white matter you were told of. It is a landscape of springs and branches, a house of fire, even better : the mighty city of your invention [1]

My thesis is about deciphering brain electrical signals, and finding patterns that correlates with consciousness, "the mighty city of your invention". The goal of the present thesis is to use electrophysiological features to better comprehend the state of patients with disorders of consciousness (DOC), to be able to differentiate DOC states and to provide means of communications for patients with DOC.

This first chapter introduces different neuroimaging techniques and explains why there is a regain of interest in electrophysiological measurements of the brain. Then a general definition of consciousness is given based on wakefulness and awareness and different states of consciousness are described accordingly. Finally, the goals of this thesis are presented as well as the outline.

1.1 Measuring the brain

The brain is the control siege of the human body. It receives inputs from the peripheral nervous system through the spinal cord and integrates all information for decision making. Information is carried throughout the brain in varying forms, electrical (nerve impulses), chemical (neurotransmitters), blood flow (hormones). Pathological damage (stroke injury, tumor, anoxia or other diseases such as Alzheimer) can interrupt information flow hence alter the normal functioning of the brain, leading to deficits in motor control, cognitive processing, memory impairments and disorders of consciousness. While in most cases the symptoms can easily

[1] "L'intérieur de votre tête n'est pas cette masse grise et blanche que l'on vous a dite. C'est un paysage de sources et de branches, une maison de feu, mieux encore, la ville miraculeuse qu'il vous plaira d'inventer." Paul Nougé, Belgian poet, 1895 1967, freely translated by R.Lehembre

be detected, it is often challenging to determine the underlying neurological causes. Due to the complex and fragile aspect of the brain, a physician can hardly examine the brain internally without risking further dammage. Nowadays, physicians have different tools at their disposal to evaluate and measure the structure and brain functions. All of these tools can provide images of the brain but have very different spatial and temporal resolution. The following is a non exhaustive description of current neuroimaging techniques separated in two categories, structural and functional neuroimaging. Features (spatial and temporal resolution, invasiveness and price/usability) of each technique are depicted in figure 1.1.

1.1.1 Structural neuroimaging

The first class of neuroimaging tools concerns all technique that gives an image of the structure of the brain. There are thee main structural imaging tools, the Computed Tomography (CT), Magnetic Resonance Imaging (MRI) and Diffusion Tensor Imaging (DTI).

1. Computed Tomography (CT) CT anatomical scans are slightly invasive as they require the use of ionizing radiation (X-rays). They deliver precise images highly useful in the detection of lesions, hematomas and give unique highlights on intracerebral calcification. They are mainly used for medical purposes.

2. Magnetic Resonance Imaging (MRI) MRI scans are obtained by placing a subject in a strong magnetic field. Although this field is 30000 times the magnetic field of the earth, it is harmless for the human body, hence MRI scans are considered as non invasive. Although they have similar spatial resolution than CT scans, they provide better contrasted images suited for examining soft tissues. They are best used to detect abnormalities in brain tissues such as tumors.

3. Diffusion Tensor Imaging (DTI) DTI images provide information on the flow of water molecules. Since these molecules are mainly found in axons, DTI reveals the state of the white matter and connections between brain areas. DTI is non invasive as it can be obtained in MRI scanner and is useful to assess white matter injuries such as axonal shearing

1.1.2 Functional neuroimaging

This category of tools includes all the techniques that provide a quantified measure of the brain such as Positron Emission Tomography (PET), Electroencephalography (EEG), Magnetoencephalography (MEG), functional Magnetic Resonance Imaging (fMRI), Near infrared spectroscopy (NIRS), local field potentials (LFP) or single unit activity (SUA).

1. Positron Emission Tomography (PET):PET scans provide a three dimensional image of the brain by measuring the emissions of biologically active molecules that have been labeled radioactively and are injected into the bloodstream. PET scans give spatially precise information on the brain metabolism. However the time resolution is limited and the method is invasive.

2. Electroencephalography (EEG): Although the spatial resolution of EEG is low compared to other modalities, it still has unmet time resolution (ms) allowing to track neural dynamics. Furthermore it is inexpensive, non invasive, and is available worldwide. In this thesis, only EEG is used, multimodal integration of information from different brain imaging modalities will be the scope of further research.

3. Local Field Potentials (LFP): Microelectrodes are placed in the extracellular medium surrounding neurons. The potential created by postsynaptic currents of a large number of neurons is recorded by the electrode. LFPs provide a similar measure than EEG with fine spatial resolution but is highly invasive.

4. Single Unit Activity (SUA): Spike potentials of individual neurons can be recorded by inserting microelectrodes inside the brain. This method provides a high spatial and temporal resolution but is highly invasive.

5. functional Magnetic Resonance Imaging (fMRI): measures neural activity with a 2-3 second resolution through the blood oxygen level dependent (BOLD) effect. Indeed, neural activity calls for increase oxygen supply and oxygenated hemoglobin increases the MR signal hence providing a map of neuronal activity.

6. Near infrared spectroscopy (NIRS): measures the activity of targeted brain regions by monitoring blood hemoglobin levels. It is based on the fact that absorption and transmission coefficients of near infrared light gives information on hemoglobin concentrations. NIRS is non invasive

1.1.3 EEG meets new challenges

The emergence, in the 1980s and early 1990, of modern neuroimaging tools such as PET and fMRI has only shadowed EEG for a short time. Indeed while the spatially precise images offered by PET and fMRI give a reliable information on 'where' an action takes place inside the brain they cannot answer the question of 'when' this action occurs. Hence, EEG is regaining interest in the neuroimaging community as advances both at the hardware and signal processing level are aiming to improve the spatial resolution with high density EEG and modern feature extraction techniques. We searched in medline the number of publications retrieved for the the

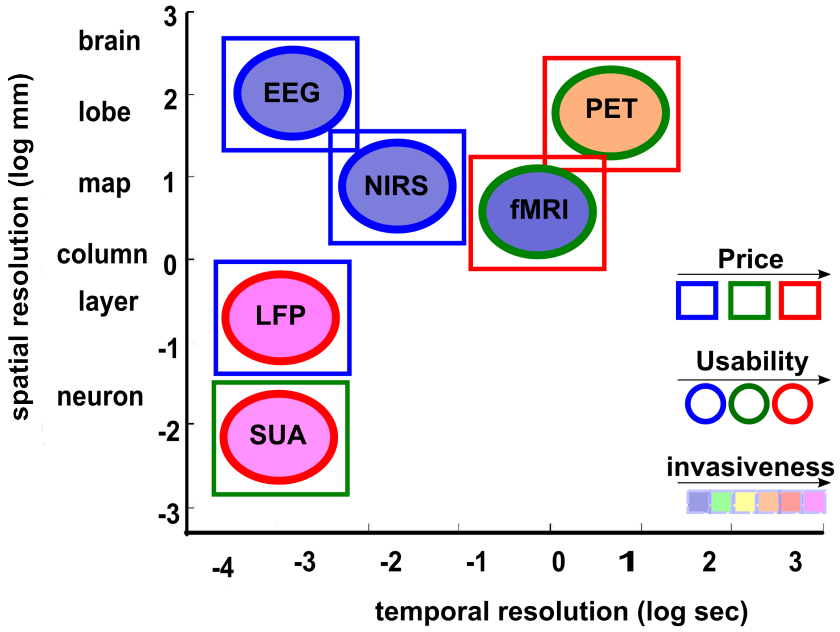

Figure 1.1 Neuroimaging techniques displayed according to their temporal (horizontal axis) and spatial (vertical axis) resolution. The color of the square around the name of each methods indicates it's price (blue corresponds to the cheapest and red to the most expensive) and the color of the circle indicates the usability which depends on different factors such as portability, installation time and surgical operation. Finally the invasiveness of each method is indicated by the filling color of each circles.

keywords "EEG", "fMRI" and "PET" in two methodologically oriented journals, Human Brain Mapping and NeuroImage. Interestingly we found similar trends in the two journals: there is a higher number of PET related publications until 1997-1998 when fMRI related publications take the lead until nowadays. The number of EEG related publications are trailing behind until 2004-2005 when they exceed PET related publications and continue to grow until now (see figure 1.1). This shows that while fMRI might be considered nowadays as the most popular neuroimaging technique in research, EEG currently meets new challenges with constantly improving methodology for describing brain signals at the following levels:

1. Time series : EEG holds a large variety of patterns which can describe the state in which a patient is (see chapter 3). Extracting frequency information from the time series give quantitative measures for statistical studies. Clinical aspects of EEG patterns are presented in section 3.2

2. Event related potentials : investigating the timing and waveform of a neural response to a specific stimulus is achieved by averaging repeated trials time-

locked to the stimulus onset. ERP enable to probe specific brain function. The use of ERPs in DOC are presented in section 3.4

3. Connectivity : Brain areas are said to be segregated (resp. integrated) if their activity is independent (resp. dependent) from other brain areas. Connectivity measurements between brain areas provide information on the integration level of cortical networks. An immense collection of connectivity measurements has fostered this last decade providing means of studying networks of areas. A non exhaustive description of this class of methods is available in section 4.3

4. Localization : Improving the spatial resolution of EEG measurements rely on an ill-posed source reconstruction problem. Based on the available sensors placed on the scalp (current high density nets use up to 256 electrodes), one can reconstruct the activity of thousands of sources on the cortical mantle. The different methods for reconstructing source activity are described in section 4.4

5. Brain Computer Interfaces : Control of external devices solely relying on EEG brain signals is possible with brain computer interfaces. These devices are particularly useful for disabled persons who cannot rely on traditional communication pathways. State of the art BCI results in DOC are described in section 3.5.

1.2 What is consciousness ?

1.2.1 General definition

For centuries, men have attempted to find a definition of consciousness. Recently, a group of neuroscientists stated that it is not possible yet to define consciousness : "We have no idea how consciousness emerges from the physical activity of the brain and we do not know whether consciousness can emerge from non-biological systems, such as computers... Consciousness has not yet become a scientific term that can be defined. Currently we all use the term consciousness in many different and often ambiguous ways. Precise definitions of different aspects of consciousness will emerge... but to make precise definitions at this stage is premature." [1]. While a precise definition is currently out of hand, it is generally accepted that consciousness requires the presence of wakefulness and awareness. Wakefulness is the condition of being awake. Awareness can be divided in two components : awareness of self and awareness of the environment. These two components are not simultaneously experienced, instead, they activate different anti correlated networks, the default mode network (DMN) (awareness of self) and the external control network (ECN) (awareness of the environment) as illustrated in figure 1.3. When the DMN

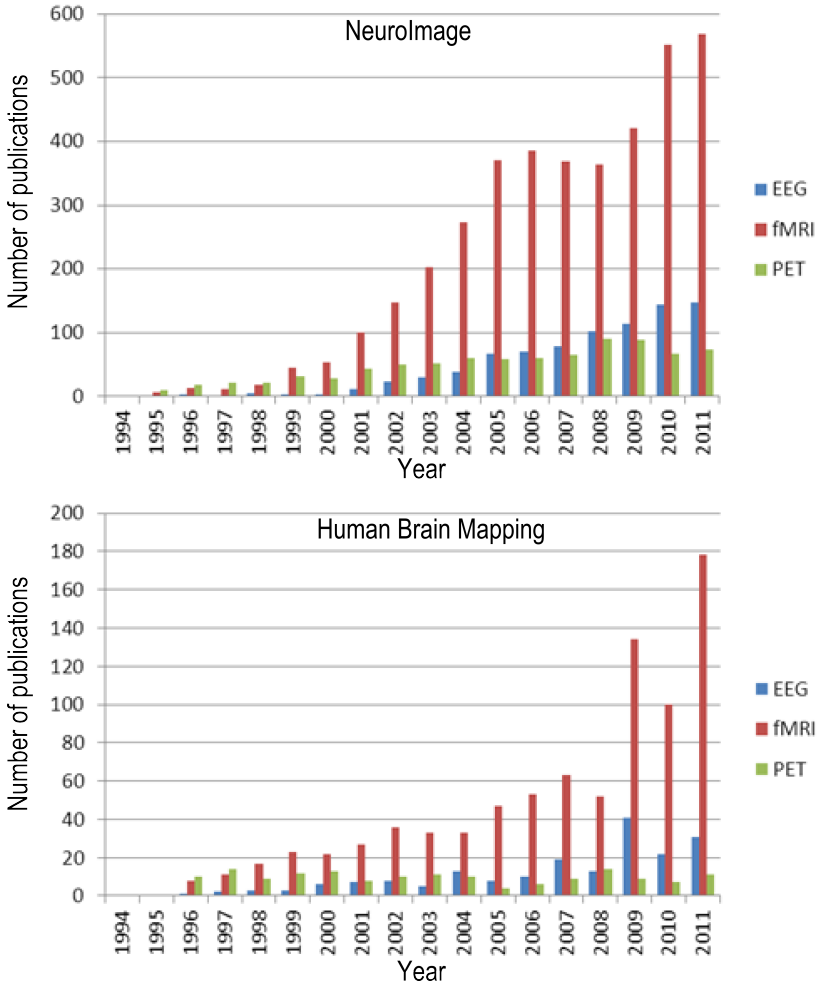

Figure 1.2 Number of publications retrieved in medline when searching for the key words "EEG", "fMRI" and "PET" between 1994 and 2011 for two methodological journals, NeuroImage (top) and Human Brain Mapping (bottom). The first issue of NeuroImage appeared in 1992, and the first issue of Human Brain Mapping appeared in 1996

is activated, a subject orients his thoughts to his inner self and experiences a state of "daydreaming", recalling past memories or projecting to future events. When the ECN is activated, the subject interacts with his environment through all his senses.

1.2.2 Altered states of consciousness

In the absence of wakefulness and/or awareness, a person is in an altered state of consciousness. Altered state can be normal or pathological. We all experience loss of consciousness in our every day life when falling asleep. Our wakefulness and awareness decrease in drowsiness, light sleep, REM and deep sleep. Total loss of consciousness can be artificially induced in healthy subjects with general anesthesia. There are different pathological altered state or disorders of consciousness (DOC) either caused by a trauma or an ischemia [2]. After an accident, a patient is often in coma, neither awake nor aware. Hopefully, the patient might recover and regain a normal life after a few days. This is however not always the case, and patients might open their eyes and awake from coma but with impaired cognitive function. The state in which the patient has no sense of his environment and no self awareness is termed Vegetative State or Unresponsive Wakefulness (VS/UWS). If the patient displays minimal sense of awareness of his environment he is in a minimally conscious state. A particular case when the injury only affects the brain stem is called the Locked-in Syndrome (LIS). In this case the patient is conscious but is locked in his body and generally cannot communicate except with blinks. The different states of consciousness are illustrated in figure 1.3.

1.3 Contributions of the thesis

This thesis contributes in expanding the palette of applications of EEG signal processing techniques in the three following cases:

1. Understanding the mechanisms associated with loss of consciousness can be achieved on an empirical basis with healthy subjects by monitoring brain activity under general anesthesia. We therefore investigated electrophysiological correlates of loss of consciousness under ketamine sedation not only at the scalp level and at the source level but also using modern dynamical causal modelling techniques showing that ketamine sedation preferentially involves cortico-cortical mechanisms.

2. Clinical EEG recordings of two groups of DOC patients were recorded and analyzed. Quantified measures of power and connectivity in different frequency

[2] shortage of blood supply to the brain cells, which can be caused for example by a cerebrovascular accident

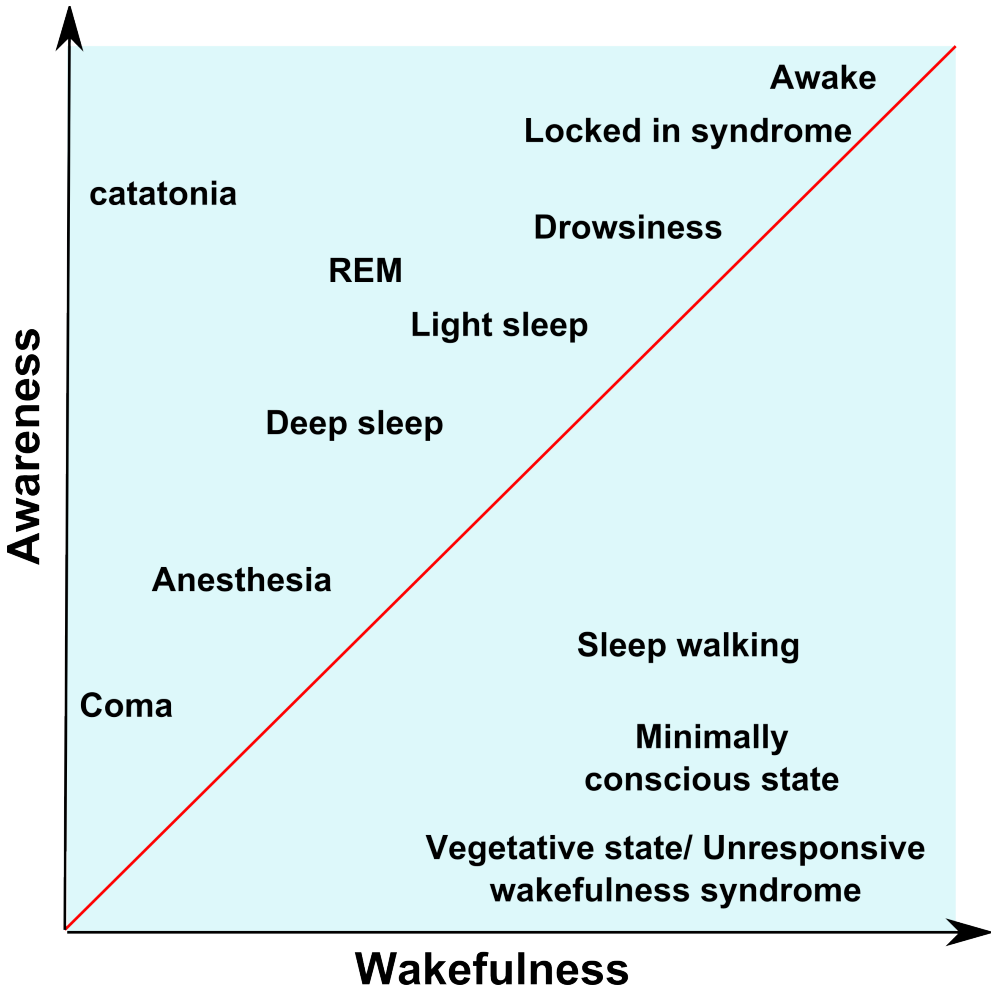

Figure 1.3 States of consciousness are plotted against their wakefulness and awareness components. Both awareness and wakefulness are high in wake healthy subjects and locked in patients. Wakefulness and awareness gradually decrease in healthy subjects going to drowsiness, light sleep, rapid eye movement (REM) and deep sleep. Anesthesia and coma are associated with quasi inexistent wakefulness and awareness. Vegetative state/Unresponsive wakefulness syndrome is considered as a wakeful state without awareness and minimally conscious states are also wakeful states but with a minimum level of awareness.

band were computed and showed differences between the VS/UWS and the MCS group. EEG measurements can thus potentially give indications on the diagnosis and prognosis of DOC patients.

3. Brain Computer Interfaces offer an alternative communication tool for patients with altered states of consciousness. The quality and usefulness of BCIs is measured in terms of bit rate, i.e. the quantity of information that a user delivers. One possible way of improving bit rates in BCIs is to improve the classification accuracy of brain features. Extraction of more discriminant features potentially allows better classification rates. We therefore investigated the use of source reconstruction methods and compared it's appreciation against state of the art statistical tool. In the studied BCI configuration, source reconstruction methods did not yield any improvements.

1.4 Synopsis of the Thesis

The objective of this thesis is to explore electrophysiological mechanisms of consciousness and to provide means of communication to patients in altered states of consciousness. The thesis is separated in two parts. The first parts introduces electroencephalography (chapter 2) and then describes in chapter 3 the different electrophysiological tools used to assess consciousness in patients with disorders of consciousness (DOC), these ranges from standard clinical EEG, quantitative EEG, evoked potentials and Brain Computer interfaces (BCI). An overview of qEEG methods is presented in chapter 4. In the second part of the thesis, three different applications are presented. First, mechanisms of consciousness are analyzed in ketamine induced loss of consciousness in healthy volunteers. Then a study aiming to find discrepancies between two groups of DOC patients is described (chapter 6). Finally, a comparison of the use of standard BCI methods with the use of inverse problem for feature extraction in a finger tapping task is presented in chapter 7.

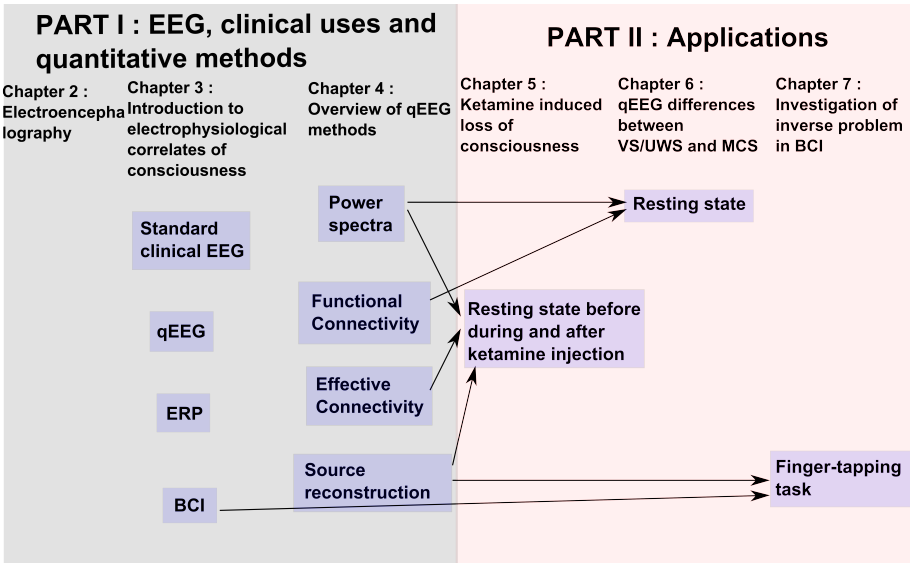

Figure 1.4 The first part of the thesis first presents different uses of EEG DOC patients before overviewing qEEG methods. Three different applications aiming at understanding mechanisms of consciousness are presented in the second part. First the use of source reconstructions methods for feature extractions in a BCI setting is presented. Then extraction qEEG values from resting state data is performed aiming to find differences between VS/UWS and MCS patients. Finally mechanisms of ketamine loss of consciousness are studied using dynamical causal modelling

Part I

Electroencephalography, clinical uses and quantitative methods

Electroencephalography

2

Men ought to know that from nothing else but the brain come joys, delights, laughter and sports, and sorrows, griefs, despondency, and lamentations [1]

This chapter is an introduction to the brain and electroencephalography. After a short history on how our ancestors viewed the brain, the general structure of a neuron and the different families of neurons are presented (section2.2). Then we will detail the structure and function of the brain (section2.3). Finally mechanisms of EEG generation are presented (section 2.4) as well as technical aspects of EEG recording (section2.5)

2.1 History

Although Hippocrates had foreseen the brain as the center of the body 24 century ago, many of his fellows thought that it was the heart or even the liver that was the center of emotions. The role and functionalities of these three organs remained unclear and widely debated until the renaissance when practitioners studied their anatomy in details. It is only in the 17th century, that Nicolas Steno ruled out the heart from being the siege of emotions by demonstrating that it is solely a muscle acting as a pump providing blood to the entire body. Leonardo da Vinci provided detailed drawings made after brain dissections. His aim was to find the siege of the soul or *sensus communis*, a place that anatomist Mondino de Liuzzi thought to be in the center of the brain and that René Descartes thought to be in the pineal gland. Hence, knowledge on the anatomy of the brain gave indications on where auditory, visual and mental processing took place but did not provide full understanding on how it was functioning. Scientists needed an instrument to measure the activity of the brain while it is functioning. A first step towards this direction came when Luigi

[1] Hippocrates

Galvani (1737-1798) discovered that living cells produce electricity, as measured on frog legs. These results led one century later to the first electrocortical measurements which are credited to Richard Caton (1842-1926) who placed the electrodes of a galvanometer directly in contact with the cortex of craniotomised animals. But the first non invasive recording of EEG signals on a human being were made by german neurologist Hans Berger (1873-1941). Originally, Berger was investigating the existence of mental energy, a form of energy that could be exchanged between persons in a telepathic way. Instead, his discovery led to a new clinical tool giving insights on brain processes with a millisecond resolution. His series of reports published under the title 'On the Electroencephalogram of man' [2] already described alpha waves, epileptic discharges, sleep spindles. He is the first having studied fluctuations of consciousness.

In the following chapter, details on neurons will be provided and the structure of the brain will be presented. Then the mechanisms of EEG generation will be detailed and a description of the different EEG waves will be given. Finally the objectives and outline of this thesis will be given.

2.2 The neuron

A human brain has an average of 10^{11} neurons. The understanding of neuron structure and function is essential for further comprehension of EEG signals, hence they are described hereunder. Although there are different types of neurons they all share a common three part structure made of a body cell or soma, dendrites and one axon. Neurons have important metabolic needs, thus they are surrounded by glial cells which feed them, provide oxygen and insulation. In most cases, neurons receive information through the dendrites and send information through the axon. There are no physical connections between neurons, they communicate by sending chemical messengers, the neurotransmitters, through a small gap, called the synapse, between the membrane of the axon terminal (presynaptic membrane) and the membrane of the dendrite (postsynaptic membrane). Although most synapses are axodendritic (information flows from the axon of the emitting neuron to the dendrite of the receiving neuron), there are other types of synapses namely axosomatic, axoaxonal, dendrodendritic, dendrosomatic and somasomatic synapses.

2.2.1 How neurons communicate

At rest, a neuronal cell has a membrane potential of approximately -65mV. This potential results from the concentration of potassium (K^+) and chloride (Cl^-) ions inside the cell and of sodium (Na^+) and calcium (Ca^+) ions outside the cells. Ion channels in the membrane allow ion exchange through the membrane thus polariz-

ing or depolarizing the cell. Two potentials are to be distinguished, the postsynaptic potential and the action potential.

The postsynaptic potential A neuron is constantly listening to other neurons and as neurotransmitters cross the synapse and bind to receptors of the postsynaptic membrane, they open ions channels which changes the membrane potential and induce a postsynaptic potential. Postsynaptic potentials can either be excitatory or inhibitory whether they induce a positive or negative change.

The action potential Post-synaptic potentials have gradual variations, but when the variation reaches a threshold of about 10 mV (varies according to the neuron type), it triggers the opening of ion channels leading to a massive influx of (Na^+) ions inside the cell, hence depolarizing the neuron. Due to voltage dependent ion channel mechanisms, the (Na^+) ion channels will then close and (K^+) ion channel will open letting (K^+) ions outside of the cell which regains it's resting membrane potential. This fast depolarization is called the action potential or spike and will propagate through the axon of the neuron to reach synaptic junctions with other neurons, release neurotransmitters in the synapse cleft which will in turn bind with receptors of the post-synaptic membrane and so on.

2.2.2 Different types of neurons and cortical columns

In order to better understand mechanisms of EEG generation which will be discussed in section 2.4 and cortical models used in dynamic causal modeling (DCM) (section 4.3.2), it is useful to review the different types of cortical neurons and the different types of neurotransmitter they produce. Neurons can be grouped in three families, afferent, efferent and interneurons. Afferent neurons convey information to a brain region, as for example sensory neurons which convey informations on tissues or organs of the body. Efferent neurons send information from a brain region, such as motor neurons which transmits orders to effector cells. Finally interneurons which have limited spatial extent, connect principal cells inside a brain region and allow a higher computational complexity. There are also three main types of neurotransmitters, those with excitatory action such as glutamate, those with inhibitory action such as γ-aminobutyric acid (GABA), and those with mixed effects. The function of a neuron depends of it's location in a cortical column. Cortical columns are vertical processing unit placed side by side throughout the cortex. Most columns in the cortex share n identical 6-layer structure. Layer I is the outermost layer and is mainly composed of axons and dendrites from deeper layers. Some of these axons extend to other neighboring columns. The limited amount of body cells are from inhibitory interneurons connecting to dendrites of neurons from deeper layers. Layer II, the

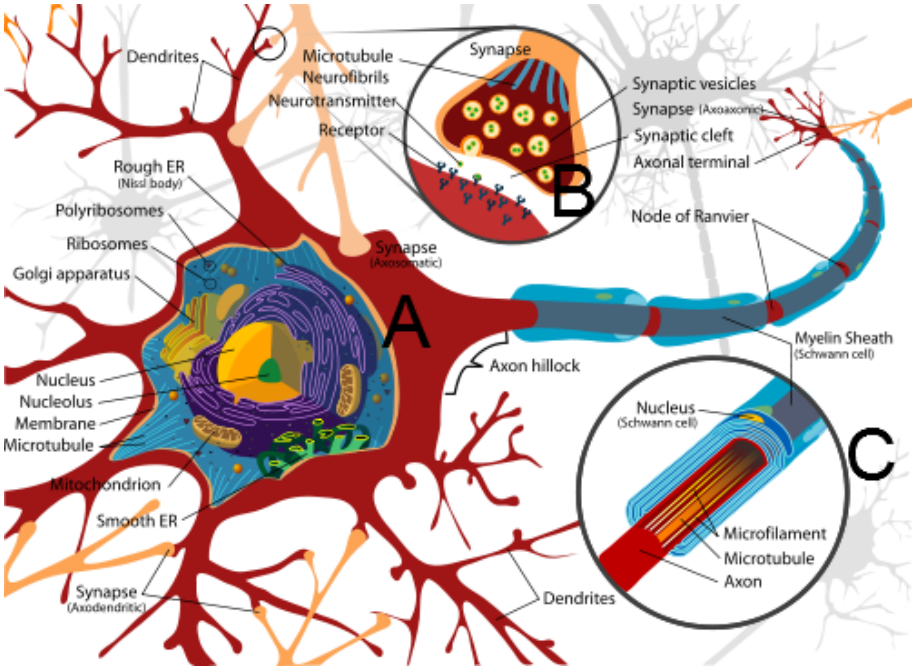

Figure 2.1 Neuron illustration with A) The neuron, a three part cell composed of 1) the soma or body cell including the nucleus and surrounded by a membrane, 2) dendrites listening to other neurons at synaptic bridges 3) the axon which is larger than the dendrites and allow a fast propagation of action potentials to remote neurons B) The synaptic connection showing neurotransmitters released from the presynaptic membrane in the synaptic cleft and binding to receptors at the postsynaptic membrane C) Axon detail. This is a file from the Wikimedia Commons. Commons is a freely licensed media file repository

external granular cell layer and layer III, the external pyramidal cell layer, both contain small pyramidal cells and some interneurons. Neurons in these two layers make cortico-cortical connections with other cortical columns and project their axons to the corpus callosum for cross hemispheric connections. Layer IV is the internal granular cell layer and is composed of excitatory spiny stellate cell and interneurons. Layer IV is the input layer of signals coming from the thalamus. Layer V is the internal pyramidal cell layer which mainly hosts large pyramidal cells and some inhibitory interneurons such as chandelier cells. The axons of pyramidal cells in layer V project through the white matter and connect to deeper brain regions such as the brainstem and basal ganglia. Finally layer VI is the multiform layer and is composed of various neurons, pyramidal cells projecting to the thalamus and interneurons projecting to other cortical columns throughout the neocortex. Layer VI is also an input layer for signals coming from the thalamus. Cortical columns are illustrated in figure 2.2.

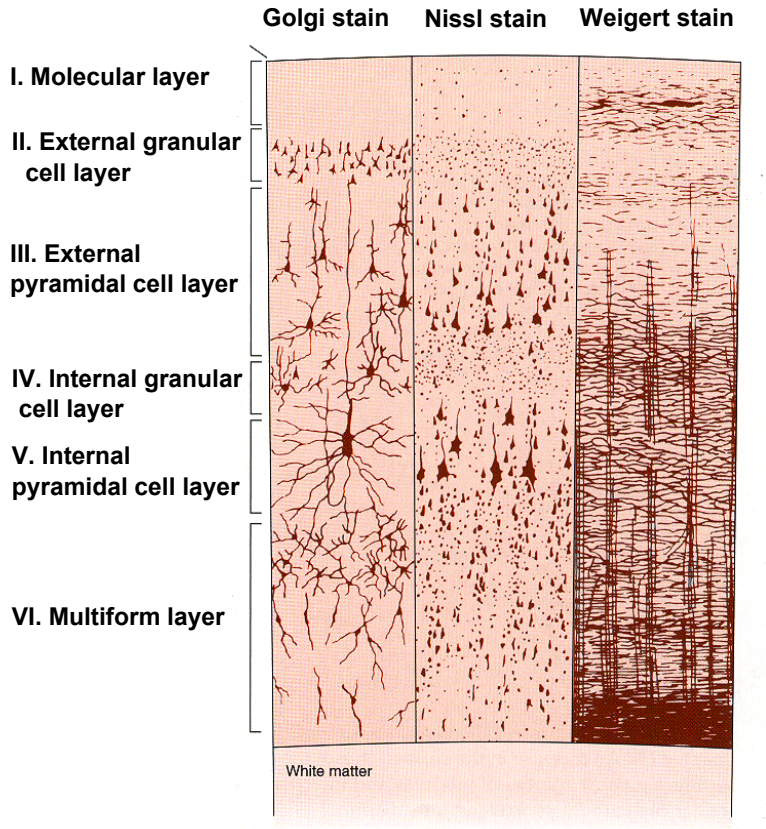

Figure 2.2 Three views of a column cell and the 6 layer structure. Body cells and dendritic arborescence are clearly visible with the Golgi stain while the Nissl stain mainly shows body cells and proximal dendrites. Note the triangular shaped somata of pyramidal cells in layers III and V. Finally the Weigert stain reveals axonal projections in the cortical column. Figure modified from Richard B Wells 2005 unpublished

Name	Family	Location in a column	type	Neurotransmitter
Pyramidal	Efferent	Layer III & V	Excitatory	Glutamate
Spiny Stellate cells	Interneuron	Layer IV	Excitatory	Glutamate
Basket cells	Interneuron	Layer II & IV	Inhibitory	GABA
Chandelier cells	Interneuron	Layer V	Inhibitory	GABA

Table 2.1 List of neurons and their specifications in a cortical column

Roughly, a cortical column is made of 65% of pyramidal cells, 20% of spiny stellate cells and 15% of inhibitory interneurons such as baket cells and chandelier cells. Table 2.1 lists the major neurons in a cortical column and their location.

2.3 The brain

The brain is the central part of the nervous system. It receives and process information provided by the different sensory inputs of the body in order to take necessary actions. It controls the pace of the heart, triggers motor actions and maintains homeostasis (the regulation of various body parameters such as temperature, blood oxygen level etc...). The brain has the ability to learn and memorize information through changes in synaptic properties.

2.3.1 Structure

The brain receives information from the spinal cord which contains all the nerves corresponding to the muscles of our body. The spinal cord arrives to the brainstem which is composed of the medulla oblongata, the pons and the midbrain. The brainstem is responsible of all automatic functions for survival (breathing, heartbeat..). Hence damage to the brainstem is life threatening. Close to the brainstem and situated in the back of the brain is the cerebellum (little brain in latin) which is the center of movement coordination. It receives orders from higher levels of the cortex and processes them in order to give precise controls on every muscle required for movement achievement. Above the brainstem, almost in the core of the brain, sits the thalamus, acting as relay dispatching information from lower levels structures to the desired region of the cortex. The hypothalamus is located just under the thalamus and helps maintain homeostasis. Near the thalamus and hypothalamus, the amygdala analyses information in search of potentially harmful situations and alarms the rest of the brain in case of danger. The hippocampus is the storing place of short term memories. Finally, above and around these structures is the cerebral cortex. It is composed of gray and white matter, the gray matter is composed of body cells and the white matter of axons and glial cells projecting to other parts of the brain. Damage to gray matter will disrupt the functioning of corresponding areas while

white matter lesions will disrupt connections between regions. The most superficial part of the cortex, closest to the skull is called the neocortex, neo stands for new as this part developed last according to evolution. The neocortex is 2 to 4 mm thick and is composed of gray matter, essentially body cells. It is the home of high level functions. The neocortex is divided in four principle lobes, the frontal, parietal, occipital and temporal lobes. The frontal lobe hosts language processing abilities, the parietal lobe includes the sensorimotor area which controls movement, the occipital lobe contains the primary visual cortex while the temporal lobe is the siege of the primary auditory cortex. The brain is illustrated in figure 2.3

2.4 Mechanisms of EEG generation

Action potentials do not contribute directly to EEG...But post-synaptic potentials do As we have seen in section 2.2.1, when a neuron fires, it sends an action potential, a very fast (1ms) spike of high amplitude. This potential propagates along the axon but also outside of the membrane cells. However it is rapidly attenuated by extracellular fluids, blood vessels and slow ion movements. The passive neuron acts like a capacitive low pass filter, hence the attenuation of extracellular currents is selective and the action potential is heavily attenuated outside the cell. Furthermore, due to the fast shape of the action potential, the probability that many neurons fire at the same time is low therefore action potentials from different neurons have little chance of adding up (except in epileptic pathologies). On the contrary, post-synaptic potentials vary slowly and gradually, and although they have smaller amplitudes than action potentials, extracellular currents created by these potentials from a high number of neurons can add up and become sufficiently high to be measured with electrodes at the scalp level.

Orientation of cells is important The cortex is folded in gyri and sulcus. Electrodes can record currents originating from both, but only from neurons with parallel orientation. Hence EEG records mainly activity in gyri as currents originating from sulcus regions can cancel out (see figure 2.4). Since pyramidal neurons are aligned in parallel, they are the main eeg generators.

2.5 EEG Recording

Conventional EEG recording consists in placing either individual electrodes or multiple electrodes held together with a cap. Electrode nomenclature and placement is ruled by the 10-20 international system. It is based on anatomical location and on percentage of distances. Electrodes are named with respect to their position and have the letter F for frontal, C for Central, P for parietal, O for occipital or a

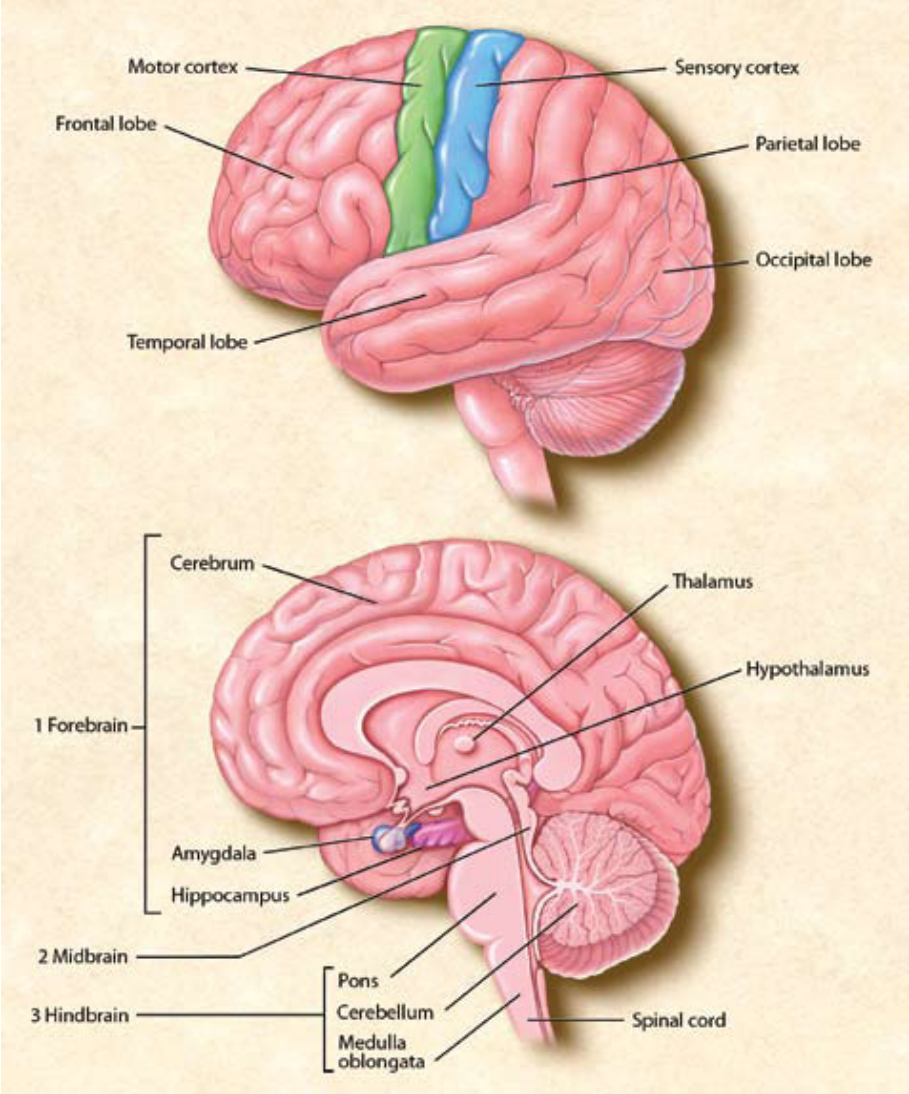

Figure 2.3 Illustration of the brain. Top : Cerebral cortex is divided in four lobes, the frontal lobe, the parietal lobe, the occipital lobe, and the temporal lobe. The motor cortex governs movements and the sensory cortex treats information coming from the five senses. Bottom : Internal structures of the brain. Illustration by Lydia V. Kibiuk, Baltimore, MD

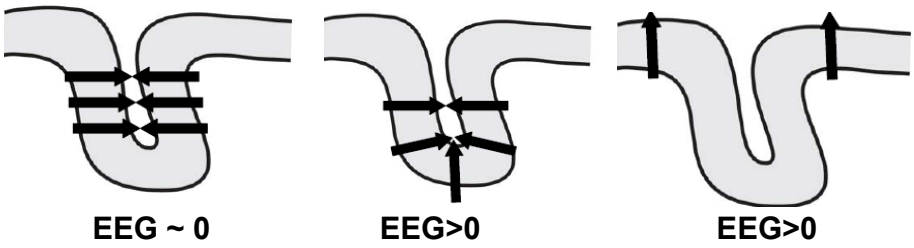

Figure 2.4 Illustration of EEG contributors. Left, currents from dipole in opposite orientation cancel out resulting in no contribution. Center, mix of opposite dipoles and dipoles in same orientation although not parallel, small contribution to EEG. Right, optimal orientation of dipoles, maximum contribution to the EEG

letter combination such as FC for a position between frontal and central. Additionally, letters are followed by a number (even for electrodes on the right hemisphere and odd for electrodes on the left hemisphere) or by the letter Z (for electrodes on the midline). The 10-20 system was originally designed for 19 electrodes, but has been revised to the 10-10 system in order to include more electrodes. The need of high spatial sampling for a better accuracy of source reconstruction methods yielded high density recording systems with up to 256 electrodes. Recording a good quality EEG requires practice and rigorous placement of electrodes and gel. A noise free environment and cooperative patient are also mandatory as EEG recordings are often contaminated by biological or apparatus related artefacts. Once recorded, EEG analysis requires some practice as different references and volume conduction can lead to differences of interpretation.

Unwanted noises and artefacts The electroencephalogram (EEG) does not only detect electrical fields generated by cerebral activity but also fields generated by muscular activity such as eye or eyelids movements, or fields generated by electrical apparatus. In clinical environments, patients in altered states of consciousness are often surrounded by many different electronic equipments withstanding their vital functions. They have little control of their movements and can be spastic. Furthermore they do not control their level of sudation which can potentially be the cause of artifacts which should be minimized during the recording. It is of good practice to simultaneously record respiration, heartbeats, and muscular activity in order to better track artifacts and eventually remove them from the signal.

Reference The measured signal results from a potential difference between two electrodes. It is therefore not possible to use only one electrode. Two different kinds of montages can be used, a bipolar montage in which the electrodes are paired two by two, or a referential montage where all the electrodes are coupled to a single

electrode called the reference. In a bipolar montage, it can be considered that the recorded signal stems from an imaginary position located between the two electrodes. When using a reference, one must check that it is not positioned in a region where a signal of interest is to be recorded. Common positions for the reference are the ear lobes, the mastoids, possibly coupled, the nose or a position on the midline. The choice of the reference electrode has an influence on the shape of the recorded signal, notably for evoked potentials. Bipolar montages are less sensitive to artifacts but will not detect events which are common in two coupled electrodes. A referential montage does not have this drawback but is however more sensitive to artifacts. As it will be discussed in section 4.3.1, the use of a reference adds artifactual correlations which can lead to misinterpretation of connectivity measures.

Volume Conduction Propagation of electromagnetic waves in the brain medium is of the order of $10^5 ms^{-1}$ [3]. This implies that potential changes are measured simultaneously at any point in the brain. Therefore due to diffusion of currents through the brain medium, different electrodes measure contributions from the same sources and have an artificially correlated signal which can lead to misinterpretations especially in connectivity studies. This is the so called volume conduction problem.

Electrophysiological correlates of consciousness

3

The brain, the masterpiece of creation, is almost unknown to us [1]

This chapter corresponds to a publication to appear in *Archives Italienne de Biologie* [4]. It reviews current uses of electrophysiological measurements in deciphering brain states in patients with disorders of consciousness. First visual patterns observed on EEG traces are enumerated and their prognosis and diagnosis value are described (section 3.2). We then review the latest developments in the quantification of EEG features aiming at characterizing different brain states in DOC (section 3.3). We then address how specific brain functions can be tested using event related potentials and how active paradigms can unveil voluntary cognitive processing of DOC patients (section 3.4). When a patient with DOC demonstrates residual cognitive processing but cannot communicate through traditionnal pathways (speech or movements), brain-based communication tools coined brain computer interfaces are tested section 3.5.

3.1 Introduction

The electroencephalography (EEG) has a long history of use in the intensive care unit, and there is a well documented literature on EEG abnormalities in comatose patients and patients in vegetative state (VS) or newly coined unresponsive wakefulness syndrome (UWS) [5]. The use of EEG as a diagnostic tool is subject to controversies [6], but the prognostic value of EEG patterns when combined with the etiology is well acknowledged [7]. However, the study of patients with disorders of consciousness (DOC) has experienced an important turn with the definition in 2002 of the minimally conscious state (MCS) as a state "characterized by inconsistent but clearly discernable behavioral evidence of consciousness and can be distinguished by coma and VS/UWS by documenting the presence of specific behavioral features

[1] Nicolaus Steno, 1669

not found in either of these conditions" [8]. This new definition has triggered the challenge to untangle VS/UWS and MCS patients. At bedside, behavioral scales such as the Coma Recovery Scale-Revised (CRS-R) [9] are used to assess patients. This evaluation can give hints on the prognosis as MCS patients have better recovery chances than VS/UWS patients. Still, behavioral assessments are subjective and not always accurate [10] hence the need of objective multimodal assessments covering all aspects of brain functioning, ranging from the metabolism assessed with positron emission tomography (PET), the structural images captured with the magnetic resonance imaging (MRI), the hemodynamic response obtained with functional MRI, the structural changes in the white matter observed with diffusion tensor imaging (DTI) and the dynamics of cortical activations measured with EEG. In the following only EEG aspects of coma, VS/UWS and MCS patients will be covered. Aside of standard clinical measurements, different applications have originated from EEG. For example, quantitative EEG (qEEG) consists in numerical computations of parameters from the EEG such as power spectra, connectivity values or entropy. These parameters offer better validity than visual scoring [11] and subsequently they can be used to train classifiers in order to separate groups of patients in different states. Next, evoked potentials, allows the assessment of specific cortical functions by measuring responses to repeated given stimuli. Furthermore, the past twenty years have seen advances in the field of brain computer interfaces (BCI) using the EEG. Direct communication from the brain to a computer has been demonstrated [12] [13]. Such devices can be of great help to assess consciousness in severe brain injured patients with DOC. In the following, standard clinical EEG patterns in coma and related states will be reviewed and illustrated. Second, the investigation of qEEG methods will be presented followed by a description of oscillatory brain activity in response to stimuli, i.e. event related potentials (ERPs). Finally, advances in brain computer interfaces and their applications at bedside will also be discussed.

3.2 Standard Clinical EEG

The EEG is often mandatory in the neurological management. A routine clinical EEG recording lasts approximately seven to thirty minutes. Electrode failure and artifacts are common issues impeding the quality of the recording; hence its duration must be long enough to allow the practitioner to determine the background activity or main rhythm of the patient. Moreover, some physiologic or even pathologic events could be missed if the recording duration is too short. To unravel some of these features, clinical EEG often involve provocative tests such as photic, auditory or painful stimulation. Visual inspection of the EEG traces can give insights on the origin and severity of the encephalopathy. First of all the clinician must identify the predominant rhythm. Healthy wake adults display at rest a posterior and symmetric alpha rhythm which oscillates between 8 and 12 Hz depending on the subject. The

amplitude of the alpha rhythm increases when the eyes are closed and decreases in case of stress. The distribution and amplitude of the alpha rhythm can differ between individuals, some do not exhibit any alpha rhythm (approximately 2% of the world population [14]), others might have an alpha rhythm of low amplitude. While most individuals have an alpha rhythm mainly distributed over posterior regions, in some subjects it can be concentrated on occipital leads and in others it might be more widely distributed [15]. An irregular beta rhythm (13-30 Hz) of smaller amplitude can be superimposed on the alpha rhythm, especially when the eyes are opened or when the subject is attentive to the environment. Those beta rhythms are also often present in case of benzodiazepine intake. When the subject is tired and drowsy, slower waves appear, and theta (4-7Hz) becomes the predominant rhythm. In deep sleep states, the predominant rhythm is delta (0.5-4Hz) (see Figure 3.1.I, 3.1.II and 3.1.III for alpha, theta and delta waves).

Following a brain injury, whether it is of traumatic or anoxic origin, the EEG can be altered and display abnormalities. A visible main effect is a slowing of the brain activity proportional to the severity of the injury. If cerebral suffering is diffuse, the predominant rhythm is no longer posterior alpha but diffuse theta or delta. In some cases of severe brain lesions alpha or theta activity can be observed but it does not resemble a normal adult alpha activity as it is frontally distributed and not reactive to stimuli such as eye opening or closing. These rhythms are coined alpha-coma or theta-coma [16] (see Figure 3.1.VII for an illustration of alpha coma). Along with the diffuse slowing commonly observed in DOC patients, several additional patterns have been reported. In case of supratentorial lesions, polymorphic focal delta rhythm can be visible over the damaged regions [17]. If there is asymmetric brain damage, the EEG will likely also be asymmetric; the electrogenesis of one hemisphere can appear almost normal whereas that of the other is severely impaired. Still a precise location of a lesion cannot be achieved with the EEG as its spatial resolution is low. When the lesions are infratentorial, the EEG can display a close to normal activity as it is sometimes but not always the case in locked-in patients (LIS) [18] [19] [20] [21] [22] [23]. Another pattern found in DOC patients is termed burst suppression, where bursts of slow waves mingled with high frequency transients are followed by periods of flat EEG (see figure 3.1.VIII). When the entire recording is flat or isoelectric, i.e. there is no cerebral activity of more than two micro volts; the patient can be in a state of electrocerebral inactivity [24] (see Figure 3.1.IX). In this case, repeated recordings are necessary because an inactive EEG can be reversible as it is the case after drug intoxication for example. Furthermore, some VS/UWS patients can have an inactive EEG since they no longer have cortical activity while brainstem electrical activity is not detected by standard EEG recording [17]. Along with these abnormal patterns, the EEG recording can be very useful to detect epileptiform activity which can take different forms such as continuous generalized paroxysmal activity (figure 3.1.VI), paroxystic bursts, periodic

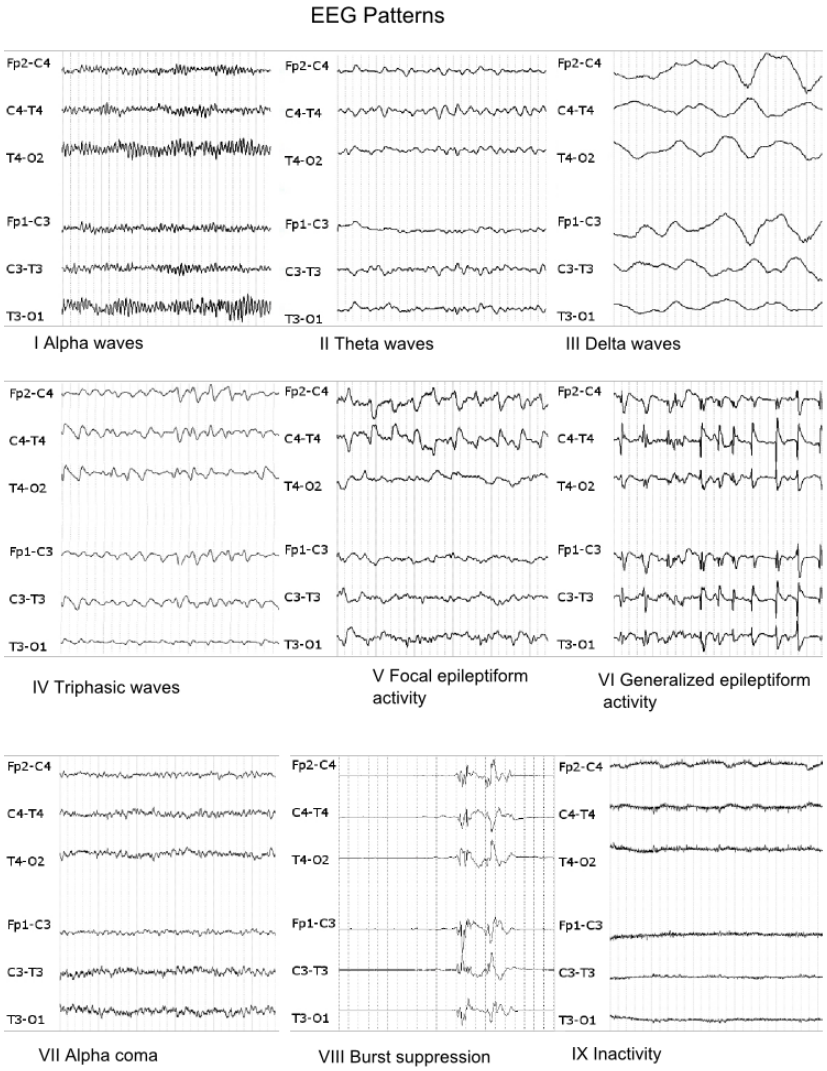

Figure 3.1 Nine different EEG patterns of five second duration in a "standard zero" bipolar montage with three electrodes on the right hemisphere (Fp2-C4, C4-T4 and T4-02) and three electrodes on the left hemisphere (Fp1-C3, C3-T3 and T3-01). I. Alpha waves in a healthy subject, the eeg is symmetric and there is a posterior distribution of the alpha waves (higher amplitude at T4-02, T3-01). II. Theta waves of 4 cycles per second showing a general slowing of the brain electrical activity. III. Delta waves oscillating at one cycle per second. It can be seen in deep sleep or coma. IV. Triphasic waves, a distinctive but non-specific pattern linked to a moderate alteration of consciousness. V. Focal epileptiform activity is a sign of underlying brain lesions; here it is well seen in the fronto-central right hemisphere (Fp2-C4, C4-T4). VI. Generalized epileptiform activity. Rhythmic spike waves are well visible on all electrodes. VII. Alpha coma, a pattern of bad prognosis is visible within 72 hours following the injury. It consists in diffuse irregular waves of 8-12 Hz. VIII. Burst-suppression, a pattern associated with a poor prognosis corresponds to brief periods of bursts followed by periods of electrical silence (<10uV). It often precedes cerebral death. IX. Inactivity is described as no cerebral electrical activity (<2uV). Except in cases of severe intoxication or hypothermia, it is irreversible.

lateralized epileptic discharges (figure 3.1.V), or focal sharp waves which can indicate epileptic discharges due to a lesion. In the case of therapeutic hypothermia after cardiac arrest, the brain activity can be followed in real time and help guide the treatment [25]. The scoring of an EEG recording is subjective and therefore dependent on the investigator. To assess the severity of the state of DOC patient, Synek suggested the use of a scale consisting of five grades and including sub-grades [26]. The number of the grade increases with the severity of the injury, grade one being associated with regular alpha and some theta, while grade two has a predominant theta that may be either reactive or non- reactive. Grade three includes predominant delta and/or spindles reactive or non reactive. Grade four is reached when there is either burst suppression activity or alpha/theta coma or low amplitude activity (<20 μV). Finally grade five corresponds to electro-cerebral silence (<2 μV). Another scale was introduced by Young and colleagues to improve inter-observer agreement [27]. Furthermore, nomenclatures have been proposed to formalize the reading of an EEG trace [28]. Establishing a diagnostic solely based on a single standard EEG is difficult since the patterns are not specific of the etiology and the same subject can have varying patterns in short intervals. A study based on patients in persistent VS/UWS concluded that there was no possible diagnostic use of EEG [29] due to its heterogeneous and varying aspect. It can still be used to confirm the diagnosis of brain death and can still be of diagnostic importance in some cases of complete LIS patients. Despite the limited diagnostic role of standard EEG recording, a prognosis is possible but challenging as one specific pattern can be found in encephalopathy of different origins. Furthermore, the outcome does not depend uniquely on the brain affection itself but on the overall condition of the patient. EEG information needs therefore to be backed up by etiology in order to have insights on the prognosis. For example, in the case of cardiac arrest coma, reactivity is an important feature for good prognosis; indeed a recent study showed that in the case of cardiac arrest, 10 out of 11 patients with reactivity evolved positively while only one out of 18 patients that presented a non reactive EEG had a good outcome [30]. General scales such as the Synek scale also gave a significant correlation with the variation of the level of cognitive function between admission and after 3 months in traumatic and non-traumatic patients [31]. In the case of coma due to cardiac arrest, burst suppression patterns are of bad prognosis [15]. There has been much debate on the prognosis value of alpha or theta coma. It was found that unreactive alpha or theta coma is of bad prognosis but a reactive alpha or theta coma can be associated with a better outcome [32]. EEG variation carries a better prognosis then an unvaried EEG, and the presence of sleep patterns in night recordings of patients are of better prognosis then if absent [33]. Furthermore, recent unpublished data including 5 VS/UWS and 6 MCS show that only MCS patients have sleep patterns, more precisely rapid eye movement sleep and slow waves cycles while the VS/UWS patients did not. Sleep patterns could therefore be used as a diagnostic tool.

3.3 Quantitative EEG

Standard EEG scores can be different from one reader to another. Furthermore not all the information contained in the EEG can be unveiled by visual inspection of the EEG traces and only qualitative information can be retrieved. With the advent of digital EEG technology, the computation of complex parameters has been made possible hence providing objective measures leading to a quantitative analysis of the EEG (qEEG). For instance, one can compute the power spectral density (i.e. the distribution of the power of a signal in the frequency domain) at each electrodes thus giving local power at each frequency. The level of consciousness of a patient can be monitored with measures of signal complexity such as entropy. Levels of connectivity between electrodes can be assessed with measures of synchronization, coherence or mutual information [34] [35]. Furthermore, using an inverse model, one can project the information at the sensor level to a source level and hence localize specific activity in the brain such as epileptic focus. To quantitatively analyze an EEG trace, a preprocessing step is required. The EEG must be band passed to remove slow direct current drifts due to gel drying and to remove high frequencies such as muscle artifacts and line noise. Then, segments containing artifacts such as eye blinks or other movements are marked for removal. Artifacts removal can be automated using Independent Component Analysis (ICA) which decomposes the signal into independent components [36]. A component containing eye blinks or muscle tone can be removed and the signal rebuilt from the remaining components. The advantage of using ICA is that segments that would have otherwise been discarded can be used for further analysis, but the drawback is that it is unknown whether if neural information is lost in the process. Once artifact free segments of one or more seconds have been extracted, power or connectivity is computed on each segment and mean as well as standard deviation values are obtained. Statistical analysis can then be performed allowing the diagnosis and prognosis of groups of patients. For an overview of qEEG, see Tong and Takhor [37]. The power spectral density can be computed with the fast Fourier transform or with a wavelet transform computed on the extracted segments [37]. It can be expressed in absolute power (μV^2) or in relative power (%) for each individual electrode or on a selected number of electrodes of a region of interest. In patients with DOC, power in higher bands such as alpha and beta decreases while power in lower bands such as delta and theta increases in relationship with the severity of the disorder [38] [39]. Measures of signal complexity such as the bispectral index (BIS, Aspect Medical Systems, Newton, USA) were initially developed for anesthesia monitoring [40] [41] but can be used to evaluate consciousness levels in DOC patients. The BIS, a unit less measure ranging from 0 (isoelectric EEG) to 100 (normal activity) derives from a combination of temporal, frequency parameters and bispectral measures. It can be seen as a black box which parameters have been empirically set and optimized on a large database of EEG

recordings during anesthesia [42]. In sleep, BIS values gradually decrease [43]. In DOC patients, one study found correlations between BIS values and scores of the Glasgow Coma Scale [44]. However, although statistically significant, these correlations were highly variable and thus difficult to use as a diagnostic tool. Another study showed that at the group level, VS/UWS patients have significantly lower BIS than MCS patients although BIS values do not allow the diagnosis of patients at the individual level [45], still measures of BIS have a prognosis value as patients with a higher BIS recovered better. Other flexible methods based on entropy have been designed in order to synthesize the EEG information into one number. The Datex-Ohmeda S/5 entropy monitoring (GE Healthcare, Helsinki, Finland) for instance implements a time-frequency balanced spectral entropy which gives an information on the complexity of the EEG. A recent study showed a 48% reduction of the entropy in VS/UWS patients compared to controls while in MCS patients it was only reduced by 18% [46]. More importantly, entropy could discriminate VS/UWS and MCS patients with a specificity and sensitivity of 90% in the acute setting, it is therefore a candidate tool for diagnosis. Furthermore this study corroborates the idea that VS/UWS have a decrease of neural network complexity, as suggested by results presented with yet another entropy measurement, the approximate entropy (ApEn) [47]. ApEn also showed prognostic capabilities in a group of VS/UWS patients, low values were associated with bad outcome while higher values led to MCS, partial or total recovery. Moreover, testing of ApEn under three conditions, eyes closed, auditory and painful stimuli, yielded similar results, and could quantify the degree of complexity suppression as a function of loss of consciousness [48]. The EEG can also quantify connectivity between brain regions [49]. Connectivity is disrupted in patients suffering from DOC [50], it provides complimentary information of diagnostic and prognostic importance [51]. Coupling parameters between electrodes provide a connectivity measure between underlying regions. A broad array of methods can be used to assess this coupling, correlation in the time domain, coherence which is a linear correlation between two signals as a measure of frequency, or non linear methods such as mutual information. Such measures require careful interpretation as they are entailed to two inherent problems of the EEG, the reference problem and the volume conduction problem. Indeed, a single reference adds a common component to all the signals of all electrodes which will subsequently appear coupled. To address this problem, bipolar montages are used which provide reference free electrodes with the drawback of reducing the number of available electrodes. Volume conduction also adds artificial coupling between electrodes. Indeed, electrical currents produced by neural assemblies diffuse through the cerebrospinal fluid and the bone and are measured by different electrodes simultaneously, giving rise to correlated electric signals. Hence, correlation and coherence measures are affected by these biases which will typically result in high values of connectivity in neighboring electrodes. Still, coherence is well-known, and easy to use, it is therefore the most

used method to assess connectivity in clinical settings. A case study on a VS/UWS patient with severe asymmetric brain damage revealed a drop of coherence in the damaged hemisphere [52]. A decrease in coherence has also been observed in MCS patients [53]. Advanced connectivity methods aiming to answer the volume conduction problem and offering more information such as the directionality of the connection have been proposed such as the imaginary part of coherency [54], the phase lag index [55] or granger causality [49]. A preliminary study using the phase lag index and the imaginary part of coherency showed that MCS patients had stronger connections in theta and alpha band than VS/UWS patients at the group level [39]. Likewise, granger causality showed that patients in severe neurocognitive disorders (SND), an upper boundary of MCS significantly displayed more connections than MCS patients. Furthermore, a classifier based on the number of connections computed with granger causality achieved a 100% accurate classification into MCS and SND class of the 16 (7 MCS, 9 SND) patients included in the study [56]. Finally, in qEEG can also be included approaches that allow the reconstitution of cerebral activity using source reconstruction methods [57]. These methods are based on models of ranging complexity, from spherical brain models to realistic models based on magnetic resonance images. All parameters computed at the electrode level can also be computed at the source level, resulting in a better spatial resolution and providing a 3D visualization of the activity of the brain. Source reconstruction techniques require however a minimum of 32 electrodes, and 64 or more being recommended [57]. A prospective study including 50 VS/UWS patients showed correlations between the level of recovery at three months and the power of occipital sources in the alpha range [58]. Recovery level, either MCS or complete recovery of consciousness could also be differentiated.

3.4 Event related potentials

Since the electroencephalography (EEG) cannot quantify small changes induced by sensory, motor or cognitive activities, more subtle functional variations can be investigated by averaging the EEG activity, according to the onset of a repeated stimulus. Averaging increases the signal to noise ratio therefore revealing activity that is time-locked to the stimulus while other non-stimulus related activity is averaged out. Event Related Potentials (ERP) reflects therefore the time course of information processing from low-level peripheral receptive structures to high-order associative cortices. ERPs are frequently used in clinical routine and can be classified in two categories : short latency or exogenous components, and cognitive or endogenous components [59].

3.4.1 Short-Latency ERPs

Short-latency ERPs or exogenous ERPs are elicited within a time range between 0 and 100 ms after the presentation of a stimulus. They correspond to the activation of the ascending pathways to the primary cortex and are affected by the physical properties of the stimulus. The absence of exogenous components is a marker of poor outcome [60], most patients who do not present these components bilaterally die or end their life in a vegetative state. The presence of short-latency ERP is however not sufficient to be a good predictor of recovery since well-preserved potentials are recorded in patient who never recover. Brainstem auditory evoked potentials (BAEP) are most often used with sounds ("clicks") using headphone. They are evoked in the first 10 ms revealing the activity from the auditory nerve to the inferior colliculus [61]. The absence of BAEPs is also a reliable marker of bad outcome when there is no evidence of peripheral auditory injury. However, the presence of normal BAEPs does not indicate a good outcome [62] [63] [64] [65]. Somatosensory evoked potentials (SEP) are elicited by sensory electrical stimulation of the median nerve at the wrists. Bilateral absence of SEPs in coma patients is strongly related with unfavourable outcome (i.e. death or VS/UWS) especially in patients with hypoxia-ischemia etiology [66] [67] [68] [69]. For a large scale review including 2891 patients [70]. All patients with good outcome have developed normal SEPs but they are also present in patients with unfavorable outcome [66] [71] [72] [73]. Likewise, middle-latency auditory-evoked potentials (MLAEPs) appearing between 10 and 50 ms and possibly related to the activation of primary auditory cortex and thalamus is strongly associated, when absent, with poor outcome in post-anoxic coma [74]. Finally, visual evoked potentials, elicited using flashing LEDs, are less used at the intensive care because these are not systematically present even in healthy subjects [75].

3.4.2 Cognitive ERPs

Cognitive ERPs or endogenous ERPs are obtained after 100 ms of the presentation of a stimulus and reflect the activity of both cortical and subcortical structures, including associative areas [75]. They depend on the psychological significance of the stimulus and are linked to the level of arousal or attention but also to the experimental condition. Using passive paradigms, cognitive ERPs assess residual cognitive functions and with active paradigms, they can be used to detect sign of consciousness in severe brain injured patients. Moreover, ERPs generally appear to be good predictors of favorable outcome [76]. Five cognitive components have been measured in DOC patients: the N1 component in response to a stimulus, the mismatch negativity and the P3 in response to novelty, and the N400 and P600 components in response to a semantic change.

3.4.3 Passive paradigms

The N1 component is a negative inflection that appears around 100 ms in response to any auditory stimulus [77], showing an activation of the auditory cortex [78]. The presence of a N1 in comatose patients indicates that the primary auditory cortex is functionally preserved. Some studies suggest that the presence of the N1 component is a good marker of recovery [65] [79] [80]) whereas others suggest that its absence does not appear to be a predictor of bad outcome [81] [82].

The mismatch negativity (MMN) is another negative component that appears around 100-250 ms after any auditory change in a monotonous sequence of sounds (i.e., an oddball paradigm) [83], involving the primary auditory and prefrontal cortices [84]. Its low amplitude implies that many repetitions are needed to observe a response. As subjects do not need to be attentive to the sound to detect a MMN, it indicates an automatic response generated by a comparison process between the afferent input and a memory trace developed by the repetitive stimulation. MMN is however not present in every healthy subjects. As most of healthy subjects, a few patients with DOC are likely to process sound deviance, mainly when their state is not due to anoxia. Many studies showed a high prognostic value for recovery, all etiology confounded [85] [65] [80] [86] [87] [74]. Using the subject's own name, another study also showed a prognostic values of the MMN in recovery of consciousness from coma and VS/UWS patients (i.e., 4 of the 5 patients showing a MMN response recovered to MCS 3 months later, the other 5 patients without MMN response failed to show any clinical improvement) [88]. Comparing VS/UWS to MCS patients, Kotchoubey et al. reported a MMN in 65% and 34% of them respectively, with complex tones eliciting a MMN more frequently than pure tones [86]. In 10 VS/UWS patients, MMN amplitude has been shown to be increased with recovery of consciousness, when patients switched to MCS [89]. However, MMN cannot be used to differentiate between VS/UWS and MCS patients [86] [90].

The P3 is a positive component generated when subjects detect a rare and unexpected stimulus in a regular train of standard stimuli (i.e., oddball paradigm) [91]. MMN and P3 are two different brain responses generated by similar stimuli (deviant or novel) but they differ by their latency after a stimulus. For a visual potential, P3 appears around 300 ms after the presentation of the stimulus and for an auditory potential it may appear after 500 or 600 ms. The P3 corresponds to the activation of a fronto-parietal network [92]. Note again that as the MMN, not all healthy subjects present a P3. Even if simple sounds can generate a P3 or a MMN, they can also be produced by more complex stimuli with emotional valence that influences the amplitude of the evoked potential [93] [94] [79] leading to a larger number of post comatose patients exhibiting P3 response [95] [96]. For example, the patient's own name, which is a salient attention-grabbing stimulus, is more likely to generate a P3 than a simple sound ("click") [97] [98]). As the MMN, in passive

paradigms, P3 component does not allow to distinguish between VS/UWS and MCS patients [86] [97] [75] [90]. Indeed, delayed P3 responses have been observed following an own name stimulus in both VS/UWS and MCS patients, suggesting partially preserved semantic processing in non-communicative brain-damaged patients [97]. The presence of P3 in patients with impaired consciousness in the acute stage seems also related to a good prognosis [99] [100] [81] [82] [79] [101]. Similarly to the MMN component, the presence of a P3 component has also been found to correlate with recovery of consciousness in 34 post-traumatic VS/UWS patients [102].

The last component is the N400 which is a negative potential appearing about 400 ms after the presentation of a word. Its amplitude is increased if the stimulus is discordant (phonological or semantic mismatch) with respect to the context (word or sentence) [103]. Semantic incongruence can also lead to a P600 which is a positive inflection 600 ms after the stimulus. Any positive or negative change can therefore be considered in the treatment of incongruence. Medial and lateral temporal cortex, as well as the left frontal and parietal cortex seem to contribute to N400 response [104] [105]. These inflections were observed in inattentive healthy subjects suggesting that like the MMN and the P3, N400 and P600 are also the result of an automatic process [106] [75]. A N400 response to incongruous words has been reported in some VS/UWS and in a majority of MCS patients suggesting that semantic processes can be relatively preserved in DOC patients [107]. Similarly, recognition of affective prosody has been observed in 6 of 27 VS/UWS and MCS patients as well as in three LIS patients [108], suggesting residual detection of affective mismatch due to violations of emotional context of stimulation in DOC patients.

3.4.4 Active paradigms

While passive paradigms help to detect residual brain activity in severely brain injured patients, the use of new active paradigms (i.e. tasks requiring patient's participation instead of passive listening) can help to determine if the patient is conscious or not. If the patient is conscious, EEG signal can be used to assess the possibility of a functional communication through brain computer interfaces (BCI) [109] [110]. The recent case of a 21-year old comatose woman who failed to show any motor sign of consciousness after 49 days following a basilar artery thrombosis [111] illustrates the practical utility of demonstrating voluntary brain activity in non-clinical means. Only EEG evoked-potential based on command following (i.e., counting her own name in a list of names) permitted to make the diagnosis of complete locked-in syndrome (characterized by tetraplegia, anarthria and paralysis of eye motility). Indeed, in the active condition, when asking to count her own name, the P3 response observed was larger than while passively listening. This active own name paradigm using P3 was also employed on a larger number of DOC patients. Schnakers et al. studied 22 severely brain injured patients which were instructed to count the

number of times they heard their own name. Some MCS patients, including patients only showing visual tracking without behavioral command following, showed an increase of the P3 responses when counting their own name compared to when listening to the names passively, documenting again command following based on brain activity only. VS/UWS patients did not demonstrate such responses [98]. Similarly, EEG-based evidence of conscious processing (i.e., count a deviant sound sequence in a series of beeps) was demonstrated in 3 out of 4 MCS patients while no voluntary modulation of evoked potentials was observed in 4 VS/UWS patients [112].

3.5 Brain Computer Interfaces

Brain-computer interfaces (BCI) are systems allowing the brain to communicate with the outside world without going through the peripheral nerves and muscles. They convert directly the brain activity into control signals for electronic devices [12] [113]. BCI based on EEG brain activity can use different components such as the P3, the sensorimotor rhythms (SMRs) or the slow cortical potentials (SCPs). The most widely component used in BCI is the P3. The advantage of using the P3 is that it allows up to 36 different commands with visual stimuli. A visual BCI has been developed using a matrix composed of letters [114] where the rows and columns are illuminated one by one. Subjects have to focus their attention on the letter they want to spell, generating a P3 response after each illumination of the letter. With this device, users can spell up to 8 letters per minute with an accuracy of 80%. Communication could be established in 5 out of 6 patients with amyotrophic lateral sclerosis (ALS). Four of them continued to use this system to communicate with the external world in a daily routine [115]. This paradigm has also been adapted to the auditory modality (e.g., for blind people), although the performances achieved are lower and higher concentration is required [116] [117]. Another auditory BCI has been developed for a binary communication (yes/no answer) [118] where users hear a sequence of four stimuli (i.e., yes, no, stop, go) presented in a random order. In order to answer a question, participants have to focus on either "yes" or "no" when hearing the sequence. A stable P3 response corresponding to the answer (yes/no) has been observed in healthy volunteers but also in ALS patients, with a lower reliability [118]. The first BCI study used with DOC patients was also carried out with this last paradigm in order to test its reliability as a diagnostic tool ("is the patient conscious?"). Results showed the benefits of the system to improve detection of consciousness in DOC patients. Two LIS patients were also evaluated, one showed reliable ability to use the BCI but not the other patient, suggesting that the system does not confirm the absence of consciousness in case of negative results [119]. Other auditory BCI for communication have also been proposed for ALS and locked in patients [117] [120]. A very recent paradigm, the P3-Brain Painting, has been developed to paint pictures using P3 brain activity only enabling ALS and LIS patients to ex-

press themselves creatively [121]. Changes in sensorimotor rhythms (SMRs) or mu rhythms have also been employed in BCIs. SMRs refer to an EEG activity of 8-15 Hz recorded in the primary sensorimotor cortex [12], usually accompanied by a beta activity of 18-26 Hz. This activity can be reduced or desynchronized using preparation, execution, or imagination of movement, particularly in the contralateral motor cortex. An increase in the rate (or synchronization) occurs after the execution of a movement and during relaxation [122]. The advantage is that these components do not require the actual execution of the movement but kinesthetic imagination is enough to make them appear [123]. It is however only possible to integrate two commands, more commands leading to a decrease in classification accuracy. In healthy subjects, many BCIs based on SMRs have shown good results for writing words in both visual [124] and auditory [125] modality. A completely paralyzed patient was also able to use a BCI based on SMRs to communicate through a virtual keyboard with a set of letters [126] [127]. To select a letter, the patient had to perform a mental task (i.e. movement imagery) and after several months, he was able to control the keyboard with an accuracy of 70%. The SMRs were also used recently with DOC patients showing the ability of a patient clinically diagnosed as VS/UWS to respond to the command (imagine squeezing the right hand versus imagine moving all toes) [128]. Finally, slow cortical potentials (SCPs) are the lowest frequencies generated by the cortex that can be used for BCI. They consist in slow potential shifts lasting 300 ms to several seconds. Negative SCPs are usually associated with movement involving cortical activation, while positive SCPs are associated with a reduction in cortical activity [129]. Again, this system involves only 2 commands. Subjects learn to control their brain activity through operant conditioning and are subsequently able to move an object on a screen [130]. People with ALS in advanced stages have been able, after training, to use this device to write words by increasing or decreasing their brain activity to select a target letter [131].

EEG analysis methods

4

The great topmost sheet of the mass, that where hardly a light had twinkled or moved, becomes now a sparkling field of rhythmic flashing points with trains of traveling sparks hurrying hither and thither. The brain is waking and with it the mind is returning. It is as if the Milky Way entered upon some cosmic dance. Swiftly the head mass becomes an enchanted loom where millions of flashing shuttles weave a dissolving pattern, always a meaningful pattern though never an abiding one; a shifting harmony of subpatterns.[1]

The goal of this chapter is to introduce signal processing techniques to extract "meaningful patterns" or features of electrophysiological activity. Time frequency features allows the extraction of the time-varying spectra of the signal at each electrode location (section 4.2). This can also be done at the source level once an inverse solution has been applied on the scalp data. Functional connectivity features provide information on the correlation between signals at the electrode level or at the source level (section 4.3.1). While they are useful to question functional interactions between regions, they do not give information on what *causes* the observed data. This is achieved with effective connectivity, using models of cortical structure to infer parameters on their interactions (section 4.3.2). Finally shifting from scalp measurements to source space is achieved through different families of inverse solutions based on a priori hypotheses (section 4.4).

4.1 Introduction

Following the discovery of the brain's electrical activity by Berger [2] in 1929, scientists and clinicians have studied electrical traces visually on paper. However, the electroencephalogram contains a vast quantity of information that is not discernible by visual inspection. Advances in signal analysis methods, brain imaging, and com-

[1] Sherrington, 1942, Man on his Nature

puter performances have allowed a large palette of technical tools to unveil the hidden mysteries of the EEG, these patterns and subpatterns that Sherington poetically described. This new panel of methods is coined quantitative electroencephalography (qEEG) [37] and allows feature extraction, classification of EEG signals and statistical assessments of databases. In this chapter, a non-exhaustive overview of qEEG will be presented to give the reader a broad perspective of available techniques and how they relate. First spectral estimation methods can extract power in different frequency bands, starting with spectral estimation methods and time-frequency transforms. Then connectivity methods will be introduced, separated in two families, functional and effective connectivity. Finally source reconstruction approaches will be described. We will put an emphasis on the methods used in the three applications presented in the second part of the thesis.

4.2 Spectral and time-frequency analysis of EEG

Spectral power and how it spatially distributes over the scalp is often used as a feature in clinical studies and in classification of brain signals in the context of BCIs. The quality of the spectral estimation is therefore crucial in extracting the most representative features. Since the EEG has excellent time resolution, tracking the evolution of spectral content over time can reveal micro states information. In the following we will first overview time-frequency methods such as short-time Fourier and Wavelet transform. Then the Hilbert transform will be introduced and a recent non linear method coined Hilbert-Huang transform. Finally parametric methods will be described, namely autoregressive modelling. A short discussion on the pros and cons of these methods will close this section.

4.2.1 Fourier Transform

In the 19th century, French mathematician Joseph Fourier demonstrated that a periodic function can be decomposed in a linear combination of complex periodic exponential functions. It is only a century later that this remarkable property could be exploited with the fast Fourier transform algorithm proposed by Cooley and Tukey [132]. The Fourier Transform $F(\omega)$ of a time evolving function $f(t)$ is defined as follows :

$$\begin{aligned} F(\omega) &= \int_{-\infty}^{+\infty} f(t) \exp^{-j\omega t} dt \\ f(t) &= \int_{-\infty}^{+\infty} F(w) \exp^{j\omega t} d\omega \end{aligned} \tag{4.1}$$

where ω [rad/s] is the angular frequency. Since the integral is taken between minus and plus infinity, the Fourier transform requires the signals to be stationary. Stationarity means that the frequency content of the signal does not change with time. This is not the case with EEG signals. Indeed, the EEG has frequency changes for physiological and technical reasons. First, there is a slow frequency drift due to the slowly

changing impedance between the electrodes and the scalp because the electrode gel dries out. Secondly, the EEG changes with the state in which the subject is. Stationarity can be assumed by using short time sliding windows hence dividing the EEG into finite time segments that have a close to constant frequency content. The choice of the windowing function should be made to obtain a narrow bandwidth, the best signal to noise ratio possible and to avoid side lobes [133]. The short time Fourier transform can be written as :

$$Sf(u,\omega) = \int_{-\infty}^{+\infty} f(t)w(t-u)\exp^{-j\omega t}\,dt \tag{4.2}$$

where w(t) is a windowing function. It is possible to obtain a time-frequency transform on the entire time scale of the signal by sliding the window function samples by samples. However the frequency resolution is fixed and determined by the size of the window and the number of points used for the Fourier Transform. A more flexible approach is viewed in the next paragraph and is coined the Wavelet Transform.

4.2.2 Wavelet Transform

First mentioned in 1909 in an appendix of Haar's thesis, the term wavelet gained important coverage in the 80s with the work of researchers spanning different fields of interest. The main idea behind the wavelet transform is to use a different and more flexible basis than the set of sines and cosines used in the Fourier Transform. Indeed by scaling and translating a mother wavelet, it is possible to gain a desired resolution in time and frequency. The wavelet transform Wf(s,u) of a time varying function f(t) is expressed as follows:

$$Wf(s,u) = \int_{-\infty}^{+\infty} f(t)\frac{1}{\sqrt{s}}\psi^*(\frac{t-u}{s})dt \tag{4.3}$$

where s and u are the dilation and translation parameters of a mother wavelet ψ^* Wavelet analysis is most useful when the user has a priori information on a the waveform to analyze. For instance in ERP analysis, P300 potentials can be seen as a mexican hat waveform. However in resting state data, wavelets are not necessarily suited as their resolution change with frequency and this can cause interpretation problems.

4.2.3 The Hilbert Transform

The Hilbert transform of a time varying signal $x(t)$ is defined as follows:

$$x_a(t) = Hx(t) = \frac{1}{\pi}P.V.\int_{-\infty}^{+\infty}\frac{x(t')}{t-t'}dt' \tag{4.4}$$

The Hilbert transform provides instantaneous frequency and amplitude measurements. This is achieved by using the concept of analytical signal:

$$x_a(t) = x(t) + j\hat{x}(t) \tag{4.5}$$

where $x_a(t)$ is the complex signal associated with $x(t)$ and $\hat{x}(t)$ is the Hilbert transform of $x(t)$. Understanding of the analytical signal is best made in the frequency domain as $X_a(f)$, the Fourier transform of $x_a(t)$ is the positive and doubled part of $X(f)$, the Fourier transform of $x(t)$:

$$\begin{aligned} X_a(f) &= 0 \ \ for\ f < 0 \\ X_a(f) &= X(0) \ \ for\ f = 0 \\ X_a(f) &= 2X(f) \ \ for\ f > 0 \end{aligned} \tag{4.6}$$

In the time domain, the analytical signal can be viewed as a product of an instantaneous amplitude and an instantaneous frequency:

$$x_a(t) = A(t)\exp^{j\phi(t)} \tag{4.7}$$

In order for the instantaneous frequency to be accurate, the analyzed signal must have a narrow frequency band. In qEEG studies, the signal at the electrodes will first be bandpassed in frequency bands of interest before studying there instantaneous amplitude and phase. The use of the Hilbert transform will be further discussed in conjunction with coherency measurements in section 4.3.1

4.2.4 The Hilbert-Huang Transform (HHT)

The Hilbert-Huang Transform first introduced by Huang in 1998 [134] differs considerably from the previous methods in the sense that it does not use predefined basis functions, instead, it decomposes the data into a sum of finite function empirically calculated. This step is called the empirical mode decomposition (EMD). This method although not used in the current thesis could prove useful applied to EEG signals [135] [136].

4.2.5 Parametric modelling

Parametric modelling consists in estimating parameters of a model that will best fit the data in the time domain. These methods are best suited for the analysis of short EEG segments. A frequency domain transfer function is computed from the estimated parameters and gives access to the spectrum of the signal of interest. The most popular parametric method is the autoregressive (AR) model and is defined for a single channel EEG signal $y(t)$ as follows:

$$y(t) = -\sum_{k=1}^{p} a_k y(t-k) + x(t) \tag{4.8}$$

where p is the model order, a_k are the parameters to estimate and $x(t)$ white noise with zero mean and unity variance. Hence, in this model, the current sample is a linear combination of previous sample values. The number of previous sample values used is determined by the model order. The autoregressive model can be extended to the case of multi-channel recordings. It is then called multivariate autoregressive analysis (MVAR) and is described as follows for multiple channels at time t :

$$\mathbf{y}(t) = -\sum_{k=1}^{p} \mathbf{A}_k \mathbf{y}(t-k) + \mathbf{x}(t) \tag{4.9}$$

$\mathbf{A}_k$ is a $p * p$ matrix of coefficients each representing a specific time-lag. As will be seen in section 4.3.1, the MVAR modelling is a convenient formulation to compute different measures of connectivity between different electrode sites. Model order can either be obtained empirically or by using the akaike criterion (AIC). For example, for a signal of length N, the optimal order p is given by minimizing :

$$AIC(p) = N \ln(\rho_p) + 2p \tag{4.10}$$

with ρ the model error variance :

$$\rho_p = \sum_{n=0}^{N-1} |e_p(n)|^2 \tag{4.11}$$

which is obtained from the model error:

$$e_p(n) = \sum_{k=0}^{p} a_p(k) x(n-k) \tag{4.12}$$

Different algorithms can be used to compute the coefficients of AR or MVAR models such as Yule-Walker or the Berg methods. For complete details on parametric modelling, the reader will consult the book by Proakis and Manolakis [137]

4.2.6 Discussion

When taken with default parameters, Fourier, wavelet and Hilbert are comparable [138]. Computing phase relationships can be done with similar results either with Hilbert Transform or Wavelet transform [139]. The use of either method should be justified with a priori knowledge of the data under analysis. Indeed specific waveforms will be better analyzed with well suited wavelets. In part II of the present thesis, Fourier transform is used to compute the spectra of EEG data. The Hilbert transform is used to obtain instantaneous phase and amplitudes of EEG signals in order to compute connectivity measurements (chap. 6). MVAR models are used in DCM to derive connectivity patterns (chap. 6).

4.3 Connectivity

The view that we have of the brain has evolved accordingly to the society we live in. In the 1940s it was viewed as a telephonic hub where a central operator would connect requested phone calls to the desired hub. It was then considered as a computer, a highly hierarchized processing unit. Nowadays with the bloom of the internet and the world wide web, it is viewed as a widely connected network with each connection playing an important role. It is thus crucial to study interactions between different brain areas. There are three levels (modes) of connectivity in the brain, structural, functional and effective connectivity. Structural (or anatomical) connectivity evaluates the presence of physical connections, i.e direct links between two neurons represented by axonal connections. Quantifying these connections at the microscopic level in terms of synaptic strength is highly invasive and challenging. Visualizing structural connectivity can be achieved with diffusion weighted imaging or diffusion weighted imaging of the cortico-spinal tract. More recent techniques such as diffusor tensor imaging (DTI) provide a macro scale tractography displaying axonal fibers interconnecting two regions. This method is particularly useful in the diagnosis and prognosis of patients with brain disorders. Although very informative, anatomical connectivity cannot alone explain all the processes taking place in the brain. Indeed, the presence of a connection does not imply that information will be processed through it. Complex mechanisms drive connection recruitment processes [140]. Hitherto, connection selection is context dependent, synaptic strengths can vary according to the task and thus elicit specific pathways. Also, connections show plasticity as the structure and the transmission properties of a synapse are subject to change either slowly or rapidly. Connections can be favored with specific mechanisms such as learning reinforcement [141]. Therefore functional and effective connectivity complements anatomical connectivity by informing whether or not two neural sources are truly interacting. The boundaries between functional and effective connectivity are not always easy to comprehend [142] [143] as these terms are used for most neuroimaging and electrophysiological techniques in different experimental settings and studying mechanisms having different time and spatial extents. Nevertheless, two currently formal definitions are stated below.

Functional connectivity is defined as *the correlations between spatially remote neurophysiological events* [144] [1]. It can be studied with neuroimaging techniques such as fMRI or with electrophysiological measurements. Functional connectivity gives an information on the correlation between two time series but does not explain underlying neuronal mechanisms. It is most useful when the experimenter does not have the control on what caused the data, however results can be difficult to interpret. Methods for measuring functional connectivity with EEG data are described in section 4.3.1

Effective connectivity is defined as *the influence one neural system exerts over another* [145]. This influence can be quantified through the parameters of an explicit generative model. A flourishing algorithmic literature has provided tools to measure effective connectivity in neuroimaging and electrophysiological data for different experimental settings. One of these tools is coined Dynamic Causal Modelling (DCM) and uses Bayesian model selection to choose the model that best explains the data. DCM is described in section 4.3.2

4.3.1 Functional connectivity

Assessing functional connectivity for electrophysiological measurements can be achieved by computing the connectivity between electrode sites. Although this might look trivial at first sight, EEG specific peculiarities impede the interpretation of connectivity measures. Indeed, due to electrical current diffusion, different electrodes pick up redundant information and can appear artificially correlated. The use of a reference also adds redundancy to the data. To pinpoint the problem of common sources, a large palette of techniques (see [49] and [146] for reviews) has been developed in the past ten years to compute connectivity. In the following paragraphs we review some of these methods, using the classical coherence measure as starting point.

4.3.1.1 Coherency/Coherence

Coherence is a simple measure of correlation between two signals in the frequency domain. Let x and y be two signals at different electrode location, the coherence between x and y at frequency f, is given by the ratio between the cross-spectrum of the two signals and their auto-spectra:

$$C_{xy}(f) = \frac{W_{xy}(f)}{W_{xx}(f)W_{yy}(f)} \tag{4.13}$$

The algorithm implemented in matlab's function 'mscohere' is based on the computation of the FFT of the two signals to obtain their frequency representation. However, as we have seen in section 4.2 there are different ways of computing the spectra of a signal, each leading to a different measure of coherence, for example wavelet-coherence, hilbert-coherence or coherence based on autoregressive parameters. If we now write the signals in term of their analytical signal obtained with the Hilbert Transform, we can extract their instantaneous phase $\phi(t_k)$ and instantaneous amplitude $A(t_k)$:

$$z(t) = x(t) + j\widetilde{x}(t) = A(t)e^{j\phi(t)} \tag{4.14}$$

where $x(t)$ represents the real signal while $\widetilde{x}(t)$ is the Hilbert transform of $x(t)$, a complex value. The instantaneous amplitudes and phases were computed directly

from the real signal and the corresponding Hilbert transform:

$$\begin{aligned} A(t) &= \sqrt{|x(t)|^2 + |\widetilde{x}(t)|^2} \\ \phi(t) &= \arctan(\tfrac{\widetilde{x}(t)}{x(t)}) \end{aligned} \tag{4.15}$$

The cross spectrum can now be written as:

$$S_{xy}(f) = \left\langle r_x r_y \exp(i\delta\phi) \right\rangle \tag{4.16}$$

where $\langle\rangle$ denotes the mean over time. Coherency is than expressed as:

$$C(f) = \frac{\left\langle A_x A_y e^{i\delta\phi} \right\rangle}{\sqrt{A_x^2 A_y^2}} \tag{4.17}$$

Most EEG clinical studies use coherence as a measure of connectivity between electrode sites. However, interpretation of coherence values must be done carefully since they can be contaminated by artifactual correlations between electrodes caused by the reference and by volume conduction. It has been shown that coherence values are high for neighboring electrodes then decrease accordingly with inter-electrode distances [34], [147] [148]. Furthermore, changes in coherence between two electrodes can be a reflection of power or phase variations at the reference site [149], [150]. Finally, coherence measures the correlation of both phase and amplitude simultaneously; it is therefore difficult to assess their individual contribution.

4.3.1.2 Phase Synchrony

Evaluating phase and amplitude separately is done with phase-locking statistics [151]. This method extracts the phase locking values between two signals at different electrodes sites and tests with repeated conditions the hypothesis whether or not the two signals are phase-locked to each other. In order to obtain the phase locking values, the signals are first band-passed before extracting the instantaneous amplitudes and phase. In [151], this is done by bandpassing the signals $s(t)$ at each electrode around frequency f and by convoluting the bandpassed signal $s(t,f)$ with a Gabor wavelet $G(t,f)$:

$$C(t,f) = s(t,f) * G(t,f) \;\; with \;\; G(t,f) = \exp(-\frac{t^2}{2\sigma_t^2}) \exp(j2\pi f t) \tag{4.18}$$

The phase and the amplitude are then taken from the real and imaginary part of $C(t,f)$:

$$A(t,f) = \sqrt{\mathrm{Re}(C(t,f))^2 + \mathrm{Im}(C(t,f))^2} \tag{4.19}$$

$$\phi(t,f) = \arctan(\frac{\mathrm{Im}(C(t,f))}{\mathrm{Re}(C(t,f))}) \tag{4.20}$$

The phase locking value is then defined as the average value over all trials of the phase differences $\Delta\phi(t,n) = \phi_1(t,n) - \phi_2(t,n)$at time t:

$$PLV_t = \frac{1}{N}\sum_{1}^{N}(\exp(j\Delta\phi(t,n))) \tag{4.21}$$

When two electrodes are consistently synchronized across trials, the PLV value is close to 1 while it is close to 0 when there is no synchronization. In order to test for statistical significance, a surrogate data is built by shuffling the data from one electrode, and the two sets of PLV from the real and surrogate data are compared. This step allows to discard false positives due to background synchronous activity. This method is intended for event related paradigms where time-locked events are under study. Hence it cannot be used for steady state responses. Two related techniques have been proposed, the first one is the Empirical Mode Decomposition phase locking analysis [152] and used the EMD to extract the phases of the signals, the second one is coined mean phase coherence [153] and is similar to the phase locking value albeit that it uses the Hilbert transform to extract the instantaneous phase and amplitudes and the average is made over time instead that over the trials at a given time point. It is suggested that the use of wavelet or Hilbert transform is not a critical choice and both can be used with similar results [139]. The phase locking value and the mean phase coherence can take values between 0 (no synchronization) and 1 (perfect synchronization). These two methods provide a more specific connectivity measure than coherence, as they only use phase as a measure of synchrony. However they require the signal to be first bandpassed into narrow frequency ranges using filters that do not alter the phase. They are not adequate to study broadband synchronizations. Furthermore they do not answer neither the volume conduction problem nor the reference problem.

4.3.1.3 Imaginary part of coherency (IC)

Reducing the impact of volume conduction is the aim of the measure proposed by Nolte and colleagues [54]. They introduced a modified measure of coherence that only takes into account the imaginary part of the coherency (IC). The motivation under this choice is that the volume conductions are instantaneous i.e. zero-lagged, in consequence of which they only contribute to the real part of coherency. Therefore keeping solely the imaginary part of coherency grants that the measured synchronies are a reflexion of true brain interactions. The drawback however is that some neural information which is also zero-lagged might be lost in the process of removing the real part of coherency. The IC can be computed by taking the imaginary part of Eq. 4.17:

$$IC = \frac{\langle A_x A_y \sin(\Delta\phi)\rangle}{\sqrt{A_x^2 A_y^2}} \tag{4.22}$$

One additional benefit of IC over standard coherence is that it is asymmetric. Hence it provides an additional information on which region of the brain is driving another. Differences between coherence and imaginary part of coherency are illustrated in figure 4.1 for the alpha band of a healthy subject at rest. The large circle represents the head and the triangle represents the nose. Each smaller circle is positioned at an electrode location and displays the values of coherence between the current electrode (represented by the dot inside the circle) and all the other electrodes. The effect of volume conduction is easily seen for the coherence measurements as the values are arbitrarily high and they decrease with electrode distance. However measures with the imaginary part of coherency appear more interpretable and allow long range synchronies. Indeed, frontal electrodes can have the highest connectivity value with posterior electrodes. IC is used in chapter 6 to find differences in connectivity between VS/UWS and MCS patients.

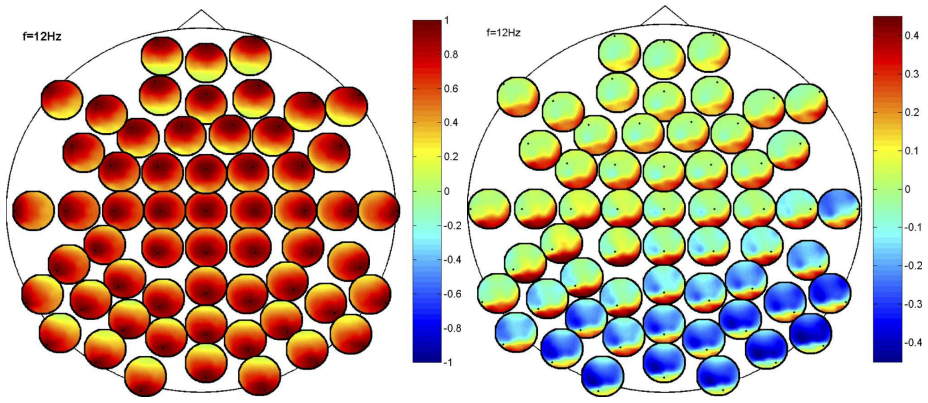

Figure 4.1 Resting state connectivity patterns as assessed with coherence (left) and imaginary part of coherency (right). The large circle represents the head and the triangle represents the nose. Each smaller circle is positioned at an electrode location and displays the values of coherence between the current electrode (represented by the dot inside the circle) and all the other electrodes. The effect of volume conduction is easily seen for the coherence measurements as the values are arbitrarily high and they decrease with electrode distance. However measures with the imaginary part of coherency appear more interpretable and allow long range synchronies. Indeed, frontal electrodes can have the highest connectivity value with posterior electrodes. (Figures modified from [54])

4.3.1.4 Phase Lag Index (PLI)

Another method to minimize the influence of the volume conduction is termed the Phase Lag Index (PLI) [55]. While, the IC removes common source synchronies by removing zero-lagged contributions, it still depends on the amplitudes which can be contaminated. The PLI depends neither on the amplitudes nor on the amplitudes of the phases and takes only into account non-zero lagged phase coupling. The main

concept behind the PLI is to consider that the phase distribution of truly interacting source should be asymmetric. This means that for a given time window, successive phase differences between two electrode sites should be repeatedly either smaller or greater than zero. All phases differences that center around zero should be discarded. Mathematically this translates in the following equation:

$$PLI = \langle sign[\Delta\phi(t_k)] \rangle \tag{4.23}$$

The PLI is the mean of the sign of successive phase differences. It is comprised between 0 (no coupling or coupling with a 0 mod π phase difference) and 1 (perfect coupling). The directionality of the coupling can be obtained if we don't take the absolute value of the PLI. The interpretation of the PLI is straightforward, two regions are perfectly coupled if one region is constantly in phase advance or in phase delay with another region. Two regions with constant but 0 mod π phase delays are not considered as coupled. Similarly to the IC, while removing an important part of artificial coupling due to common sources, the PLI might also remove true brain interactions. The PLI is used in chapter 6 to find differences in connectivity between VS/UWS and MCS patients.

4.3.1.5 Partial directed coherence

All the connectivity measures introduced until now only considered coupling between pairs of electrodes. Using MVAR modelling gives access to the covariance structure of all available channels. This is particularly useful when the coupling between two channels is driven by a third signal, hence it provides a better understanding of the observed coupling. A multichannel simultaneous coupling analysis will provide a different but sounder overview of the network then pair by pair analysis [154].The PDC is obtained by transforming the time domain MVAR representation of a signal (see eq. 4.9) to the frequency domain:

$$\mathbf{S}(f) = \mathbf{H}(f) \sum \mathbf{H}^H(f) \tag{4.24}$$

where $\sum$ is the noise covariance matrix, $\mathbf{H}(f)$ is the transfer function matrix and $\mathbf{H}^H(f)$ is the hermitian transpose of the transfer matrix. The transfer function is obtained from the Fourier transform of the coefficient matrix $\mathbf{A}$: $\mathbf{H}(f) = \overline{\mathbf{A}}(f) = [\mathbf{I} - \mathbf{A}(f)]^{-1}$. Let $\overline{a}_{i,j}$ be the i, j^{th} element of $\overline{\mathbf{A}}$, then the PDC measure from the signal at electrode j to the signal at electrode i is defined as :

$$PDC(f) = \frac{\overline{a}_{i,j}(f)}{\sqrt{\overline{\mathbf{a}}_j^H(f)\overline{\mathbf{a}}_j(f)}} \tag{4.25}$$

Therefore the PDC from signal j to signal i is the relative coupling strength of signal j to signal i compared to all the connections of signal j with other signals at all the other electrode locations [155] [156].

4.3.1.6 Directed transfer function

The directed transfer function is slightly different than the PDC as it is based on the elements of the transfer matrix **H**:

$$DTF(f) = \frac{H_{i,j}(f)}{\sqrt{\mathbf{h}_j H(f) \mathbf{h}_j(f)}} \tag{4.26}$$

The DTF is computationally more expensive as it requires a supplementary matrix inversion. While the PDC normalizes the connection strength with respect to all outflow connections, the DTF normalizes the connection strength with regard to all inflow connections [157] [158].

The PDC and DTF when computed as above provide spectral connectivity estimations of stationary signal and thus cannot track changes in the EEG as they arrive. This limitation can be overcome by using adaptive MVAR modelling [159].

4.3.2 Effective connectivity

In this section, we will introduce dynamic causal modelling for electrophysiological measurements. DCM was first introduced for fMRI in 2003 [160] and since then has been adapted for EEG/MEG for different settings such as event related potentials [161], steady state response [162] or induced response [163]. DCM aims at finding the model that best explains a given set of data using Bayesian model selection. Once a model has been chosen, parameter estimation of the selected model can inform differences between conditions. Models consist in interacting cortical sources located in different regions of the brain. In most DCM studies a cortical source follows Jansen's and Rit model [164] consisting of three layers of cell : inhibitory cells in agranular layers, excitatory spiny cells in granular layers and excitatory pyramidal cells in agranular layers. These three layers communicate between them via intrinsic connections. A cortical source communicates with other cortical sources via extrinsic connections. There are three types of extrinsic connections, forward, backward and lateral. Forward (or bottom-up) connections originate from agranular pyramidal cells and connect to the spiny cells in granular layers. Backward (or top down) connections connect excitatory pyramidal cells from agranular layers to excitatory or inhibitory cells from agranular layers. Finally lateral connections originate from excitatory pyramidal cells and connect to any other layer. Connections are illustrated in figure 4.3.

Neural Model Each subpopulation of neurons inside a column can be viewed as a block where two operations take place : first p(t), the average pulse density of action potentials incoming from other subpopulations are transformed to an average post

synaptic membrane potential, v(t), which is in turn transformed through a second operation into an average pulse density fired by the neurons of the studied subpopulation. These two steps are enumerated hereunder :

1. The first operation is achieved by a convolution of a parameterized impulse response function $h_{e/i}(t)$ and the arriving input $u(t)$:

$$v(t) = h_{e/i}(t) \otimes p(t) \tag{4.27}$$

The impulse response function $h_{e/i}(t)$ either models an inhibitory synapse (h_i) or a excitatory synapse (h_e):

$$h_{e/i}(t) = H_{e/i}\kappa_{e/i} t \exp(-t\kappa_{e/i}) \tag{4.28}$$

where H determines the maximum amplitude of the excitatory or inhibitory post synaptic potential and κ are the rate constants. The first operation expressing transfers occurring at the synaptic junction leads to a second order differential equation of the form:

$$\ddot{v}(t) = H_{e/i}\kappa_{e/i}u(t) - 2\kappa_{e/i}\dot{v}(t) - \kappa_{e/i}^2 v(t) \tag{4.29}$$

which can be rewritten in state space :

$$\begin{aligned} \dot{v}_t &= x(t) \\ \dot{x}_t &= H_{e/i}\kappa_{e/i}u(t) - 2\kappa_{e/i}x(t) - \kappa_{e/i}^2 v(t) \end{aligned} \tag{4.30}$$

2. The second operation is non linear since neurons "fire" action potentials only when the post-synaptic membrane potential reaches a threshold (cfr. section 2.2.1). This operation is represented by a sigmoid function :

$$S(v) = \frac{1}{1+\exp(-\rho_1(v-\rho_2))} - \frac{1}{1+\exp(\rho_1\rho_2)} \tag{4.31}$$

where ρ_1 and ρ_2 determine the firing threshold and the slope of the curve.

By generalizing Eq. 4.30 to the cortical source of Jansen and Rit [164] described above, the following equations are obtained for each of the three subpopulation:

1. Membrane potentials of inhibitory cells (v_7) in supragranular layers are driven by 1) excitatory postsynaptic potentials from pyramidal cells in infragaranular layers mediated by coupling strengths γ_3, (intrinsic connection) A^B, (backward connection) and A^L (lateral connection). 2) recurrent inhibitory input from the inhibitory population itself mediated by a coupling strength γ_5 . Hence the state of this subpopulation is the membrane potential v_7 and the inputs are the action potentials $S(v_6)$ and $S(v_7)$:

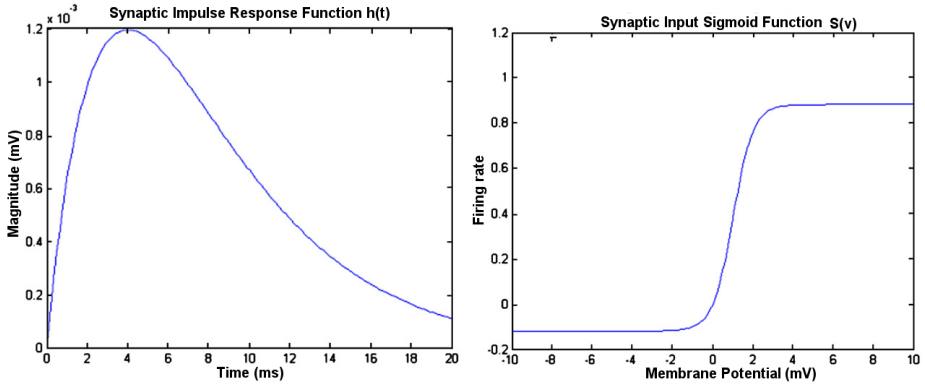

Figure 4.2 Left: the synaptic impulse function, when convolved with firing rate it produces postsynaptic potentials. Right : Sigmoid function which transforms post synaptic potentials to firing rates(Figures modified from [165])

$$
\begin{aligned}
\dot{v}_4 &= i_4 \\
\dot{i}_4 &= \kappa_e H_e (A^B + A^L + \gamma_3) S(v_6) - 2\kappa_e i_4 - \kappa_e^2 v_4 \\
\dot{v}_5 &= i_5 \\
\dot{i}_5 &= \kappa_i H_i \gamma_5 S(v_7) - 2\kappa_i i_5 - \kappa_i^2 v_5 \\
\dot{v}_7 &= i_4 - i_5
\end{aligned}
\tag{4.32}
$$

2. The macro column receives exogenous input (u) at the excitatory spiny cell population. Membrane potentials of excitatory spiny cells (v_1) in granular layers are driven by the exogenous input and excitatory postsynaptic potentials from pyramidal cells in infragaranular layers mediated by coupling strength γ_1:

$$
\begin{aligned}
\dot{v}_1 &= i_1 \\
\dot{i}_1 &= \kappa_e H_e (\gamma_1 S(v_6) + u) - 2\kappa_e i_1 - \kappa_e^2 v_1
\end{aligned}
\tag{4.33}
$$

3. Excitatory pyramidal cells in infragranular layers are driven by: 1) action potentials from excitatory spiny cells ($S(v_1)$) through a connection mediated by γ_1 and by backward and lateral connections mediated by A^B and A^L from pyramidal cells of other columns. 2) inhibitory inputs ($S(v_7)$) from interneurons mediated by γ_4

$$
\begin{aligned}
\dot{v}_2 &= i_2 \\
\dot{i}_2 &= \kappa_e H_e ((A^B + A^L) S(v_6) + \gamma_2 S(v_1)) - 2\kappa_e i_2 - \kappa_e^2 v_2 \\
\dot{v}_3 &= i_3 \\
\dot{i}_3 &= \kappa_i H_i \gamma_4 S(v_7) - 2\kappa_i i_3 - \kappa_i^2 v_3 \\
\dot{v}_6 &= i_2 - i_3
\end{aligned}
\tag{4.34}
$$

These equations can be resumed in a state-space formulation:

$$\begin{aligned}\dot{\mathbf{x}} &= f(\mathbf{x}) + \mathbf{Bu} \\ \mathbf{y} &= \mathbf{Cx} + \mathbf{Du}\end{aligned} \tag{4.35}$$

As stated in section 2.4, pyramidal neurons are the main EEG generators, hence the output y of our state-space formulation corresponds to the membrane potential of pyramidal neurons (v_6). The hidden variables are included in $\mathbf{x}$ ($v_1, v_2, v_3, v_4, v_5, v_6, v_7, i_1, i_2, i_3, i_4, i_5$). From this point we are only interested in a steady state response DCM applied on resting state data as used in chapter 5. The non linear part $f(x)$ in Eq. (4.35) is due to the sigmoid function. If we consider the system's dynamic behavior around a specific operating point corresponding to S(0)=0, the mean firing rate is zero when the membrane potential is zero. Hence the states have resting values $\mathbf{x}_0$ of zero. The dynamics around this point depend on the slope of $S(0)$:

$$\frac{\delta S(0)}{\delta v} = \frac{\rho_1 \exp \rho_1 \rho_2}{(1 + \exp \rho_1 \rho_2)^2} = g \tag{4.36}$$

where g is coined the sigmoid gain. We can now linearize (4.35):

$$\begin{aligned}\dot{\mathbf{x}} &= \mathbf{Ax} + \mathbf{Bu} \\ \mathbf{y} &= \mathbf{Cx} + \mathbf{Du}\end{aligned} \tag{4.37}$$

We can obtain the system transfer function with the Laplace Transform:

$$\begin{aligned}sX(s) &= AX(s) + BU(s) \\ Y(s) &= CX(s) + DU(s)\end{aligned} \tag{4.38}$$

which leads to:

$$\begin{aligned}X(s) &= (sI - A)^{-1} BU(s) \\ Y(s) &= H(s)U(s)\end{aligned} \tag{4.39}$$

with

$$H(s) = C(sI - A)^{-1} B + D \tag{4.40}$$

Evaluating at $s = j\omega$ gives the frequency output of the system. Given that the cross-spectrum for two signals i and j is defined as $S_{ij} = Y_i Y_j$ and that inputs to the system are seen by both sources, we can write the output cross-spectral density as

$$S_{ij} = H_i H_j^* |U_j| \tag{4.41}$$

Model inversion The equations described above provide a generative model of cross spectral features of local field potentials. To invert the model it is necessary to obtain cross-spectral features from the data. This is achieved by using parametric

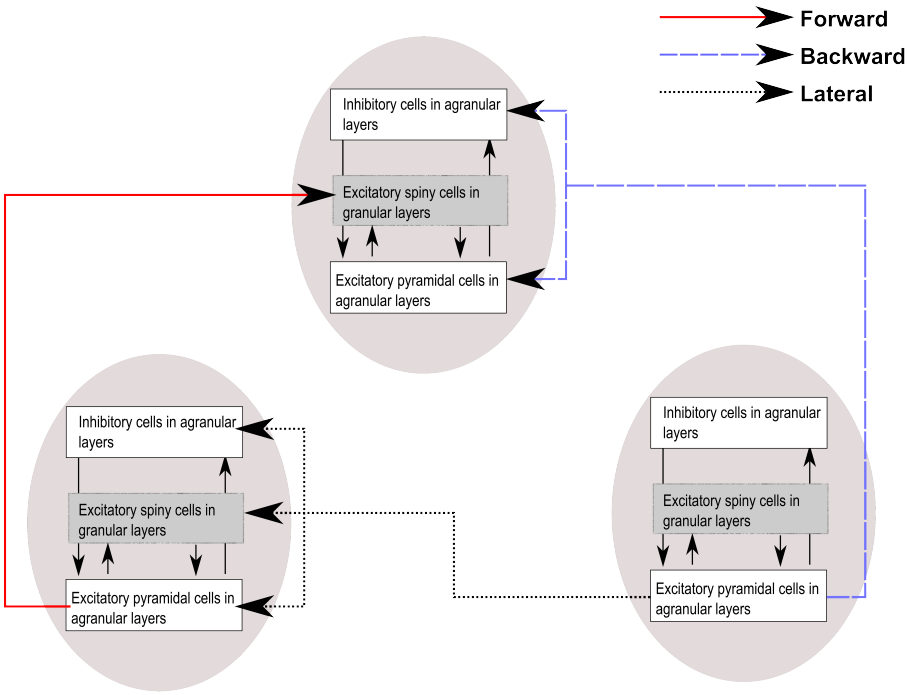

Figure 4.3 Illustration of the different types of connection. First intrinsic connections allow communication inside a cortical column between the three subpopulation of cells. Second, cortical columns can communicate between each other via three types of extrinsic connections. Forward (or bottom-up) (in red continuous lines) connections originate from agranular pyramidal cells and connect to the spiny cells in granular layers. Backward (or top down connections) (in blue dashed lines) connect excitatory pyramidal cells from agranular layers to excitatory or inhibitory cells from agranular layers. Lateral connections (in black dotted lines) originate from excitatory pyramidal cells and connect to any other layer.

modelling as described in section (4.2.5). Let $\mathbf{g_y}$ be the cross-spectral density estimated from the data and ϑ the unknown parameters of model m. Inverting the model requires to estimate the conditional density $p(\vartheta|\mathbf{g_y}, m)$ which can be achieved through variational Bayes as described in Friston et al. 2007 [166]. Variational Bayes approximates the conditional density $p(\vartheta|\mathbf{g_y}, m)$ of some model parameters ϑ, given a model m and data $\mathbf{g_y}$. Furthermore, it provides the evidence of the model $p(\mathbf{g_y}|m)$. The conditional density is approximated by the variational density $q(\vartheta)$ obtained by maximizing the free energy F defined as follows:

$$\begin{aligned} \ln p(\mathbf{g_y}, m) &= F + D(q(\vartheta)||p(\vartheta)||\mathbf{g_y}, m) \\ F &= \langle L(\vartheta)\rangle_q - \langle \ln (q(\vartheta)))\rangle_q \\ L &= \ln p(\mathbf{g_y}, \vartheta) \end{aligned} \tag{4.42}$$

where $\langle L(\vartheta)\rangle_q$ is the expected energy and $-\langle \ln (q(\vartheta)))\rangle_q$ is the entropy. The log evidence $p(\mathbf{g_y}, m)$ is used for model selection.

4.3.3 Discussion

Functional connectivity measures are useful when there are no possible assumptions on what neuronal mechanisms caused the observed data. Standard coherence measurements are widely used in clinical studies [167] [35] [168] [169] [170], they require careful interpretation as they do not necessarily represent true neuronal connectivity but artificial connectivity caused by volume conduction and the reference. Specific methods have been developed in an attempt to avoid these pitfalls. Measures such as the IC and the PLI are not affected by the volume conduction problem but they might remove non zero lagged neuronal information. When recording at multiple electrodes site, it is recommended to use PDC or DTF as they take into account all the signals simultaneously instead then two by two [171] [172]. When a specific assumption can be made on the observed data, models of underlying neuronal mechanisms can be used to assess effective connectivity between neuronal assemblies. This can be achieved with DCM.

4.4 Inverse problems

There are plenty of occurrences of inverse problems in nature. For example, the study of seismic activity with seismographs (surface activity) allows to measure with precision the location of the epicenter of an earthquake. Similarly, measuring the electrical activity of the brain with electrodes placed on the surface of the scalp can lead to measures of the entire brain volume. The first attempts to describe the relation between surface voltages and dipoles date from the early 1950s with a forward interpretation by Wilson and Bayley [173]. Their article derived the electric field

produced by a dipole inside a sphere. This contribution paved the way to the first attempts to compute an inverse solution from the scalp measurements. These first attempts consisted in computing the localization and strength of a single dipole (a moving dipole) [174] from the scalp measurements. This was also done by Schneider in his PhD thesis [175] and described in an article published in IEEE transactions on biomedical engineering [176]. These simple models were used to identify neural sources that accounts for evoked potentials, for example, in [177], the authors identify one or a few equivalent dipoles responsible for visual evoked potentials. Although they acknowledge the fact that these representations may have no relationship with physiological processes underway, they show the feasibility of such reconstructions. Spherical models were used until 1987 when [178] described a realistic head model based on the Boundary Element Method (BEM). Tested with a single moving dipole solution, it proved to be more accurate than a spherical model. A few years later Cuffin [179] built 3 realistic head models based on modern imaging techniques such as MRI on three subjects. Once more these models proved to offer better localization accuracies. Until then, only localization of a limited number of dipoles had been studied, this limitation was overcome with the paper by Pascual-Marqui et al. [180] introducing a distributed linear inverse solution that computes a current distribution throughout the brain volume. The following decade foresaw a full palette of different techniques for improving, the head model, the localization of limited dipoles and imaging techniques with distributed models. In the following section we will describe briefly the forward model of EEG generation and how sources are reconstructed.

4.4.1 Head models and the forward problem

Head models can have ranging complexities. Depending on the application and on availability of the subject's MRI data, one can use simple models consisting on one to four concentric spheres or realistic head models based on the MRI images of the subject's head and brain. Once the source space has been defined, a lead field matrix needs to be computed. The lead field matrix is the operator which transforms the current at the source level to scalp potentials value. It is obtained by solving the quasi static approximation of the Maxwell's equation taking into account regions with different conductivities of the brain. The forward model is then given by :

$$\mathbf{e} = \mathbf{L}\mathbf{j} + \nu \tag{4.43}$$

Where $\mathbf{e}$ is the data vector at a given time of size m, $\mathbf{L}$ a $m \times n$ matrix is the lead field, $\mathbf{j}$ are the n sources and ν some additive noise. The inverse problem is ill-posed since the source space is between 10 and 1000 times bigger then the scalp space. Therefore, at one time instant, different configurations of sources can explain the measured potential at the scalp surface.

4.4.2 Inverse solutions

There are two main families of inverse solutions. Parametric methods assume that a limited number of dipoles are active at the same time. The goal of these methods is to find the location, orientation and amplitude of the limited number of active dipoles. The second family of inverse methods are coined imaging or distributed methods since their aim is to represent the entire brain activity with distributed sources throughout the brain volume. In imaging methods, the location of dipoles is fixed but not their location and amplitude. Dipoles located in the gray matter can have a restricted orientation perpendicular to the cortex to mimic pyramidal neurons (see section 2.4). In these cases the only unknown is the amplitude of the source. Still, since typical imaging methods involve 10 to 1000 times more sources than electrodes, finding the amplitude of the sources requires solving an underdetermined problem. Hence prior assumptions on the data must be taken to favor plausible solutions. The first proposed solution to Eq. 4.43 is the minimum norm method which favors the solution with the minimum overall activity. It favors weak and localized surface activity. Yet the constraint of minimum activity has no physiological validation hence a regularization term needs to be added to input a priori information on the sources. Such a priori can be achieved with the Tikhonov regularization problem [181]:

$$\hat{\mathbf{j}} = min_{\mathbf{j}}(||\mathbf{e} - \mathbf{L}\mathbf{j}||^2 + \lambda^2||\mathbf{H}\mathbf{j}||^2) \tag{4.44}$$

where $\mathbf{H}$ is the regularization matrix and λ the regularization parameter. In the minimum norm method $\mathbf{H}$ is an identity matrix. Priors can be introduced in $\mathbf{H}$ in order to favor regions or voxels of interest. Minimizing the right hand side of Eq. 4.44 involves setting it's derivative to zero, which gives the following estimate $\hat{\mathbf{j}}$:

$$\hat{\mathbf{j}} = (\mathbf{L}^T\mathbf{L} + \lambda^2\mathbf{H}^T\mathbf{H})^{-1}\mathbf{L}^T\mathbf{e} \tag{4.45}$$

Equation 4.44 can also be obtained through a Bayesian inference problem formulation which offers also the advantage of estimating a goodness of fit of the solution. Following Bayes rule we have:

$$p(\mathbf{j}|\mathbf{e}) = \frac{p(\mathbf{e}|\mathbf{j})p(\mathbf{j})}{p(\mathbf{e})} \tag{4.46}$$

where $p(\mathbf{j}|\mathbf{e})$ is *a posteriori* probability of observing the sources $\mathbf{j}$ knowing the measurements $\mathbf{e}$. $p(\mathbf{e}|\mathbf{j}$ is the *likelihood*, the probability of obtaining the measures $\mathbf{e}$ given the source activity $\mathbf{j}$ $p(\mathbf{j})$ is the *a priori* probability of having a given source distribution $\mathbf{j}$. Finally $p(\mathbf{e})$ is the *evidence*, the probability of measuring $\mathbf{e}$. The evidence can be fixed arbitrarily to 1. It is trivial to expect that the most realistic solution would be the one with the maximum *likelihood* and the maximum *a priori*, hence also the maximum *a posteriori* (MAP estimator):

$$\hat{\mathbf{j}} = argmax_{\mathbf{j}}[p(\mathbf{e}|\mathbf{j})p(\mathbf{j})] \tag{4.47}$$

which can be rewritten using the log-likelihood:

$$\hat{\mathbf{j}} = argmin_{\mathbf{j}}[-\ln(p(\mathbf{e}|\mathbf{j})) - \ln(p(\mathbf{j}))] \tag{4.48}$$

To solve Eq. 4.48 we need to define the *likelihood* and the *a priori*:

- The *likelihood* is linked to the noise which is most often expressed as a gaussian distribution with zero mean and covariance matrix C_η:

$$(p(\mathbf{e}|\mathbf{j})) = \frac{1}{\sqrt{2\pi}C_\eta} \exp\left(-\frac{1}{2}(\mathbf{e} - L\mathbf{j})^T C_\eta (\mathbf{e} - L\mathbf{j})\right) \tag{4.49}$$

  The log-likelihood can now be written as:

$$\ln(p(\mathbf{e}|\mathbf{j})) = \frac{1}{\sqrt{2\pi}C_\eta} \exp\left(-\frac{1}{2}(\mathbf{e} - L\mathbf{j})^T C_\eta (\mathbf{e} - L\mathbf{j})\right) \tag{4.50}$$

  the log likelihood is then:

$$\ln(p(\mathbf{e}|\mathbf{j})) = -\frac{1}{2\mathbf{C}_{eta}}||\mathbf{e} - \mathbf{L}\mathbf{j}||^2 + \text{cte} \tag{4.51}$$

- the *a priori* can also be expressed as a gaussian with zero mean and covariance matrix $\mathbf{C}_j$:

$$\ln(p(\mathbf{j})) = -\frac{1}{2\mathbf{C}_\mathbf{j}}||\mathbf{j}||^2 + \text{cte} \tag{4.52}$$

If we write $C_j^{-1} = \sigma^2 \mathbf{H}^T\mathbf{H}$ the source estimate $\hat{\mathbf{j}}$ is given by the minimization of the following expression:

$$\hat{\mathbf{j}} = argmin_j(\mathbf{C}_\eta^{-1}||\mathbf{e} - \mathbf{L}\mathbf{j}||^2 + \sigma^2||\mathbf{H}\mathbf{j}||^2) \tag{4.53}$$

which leads to the following linear solution:

$$\hat{\mathbf{j}} = (\mathbf{L}^T\mathbf{C}_\eta^{-1}\mathbf{L} + \sigma^2\mathbf{H}^T\mathbf{H})^{-1}\mathbf{L}^T\mathbf{C}_\eta^{-1}\mathbf{e} \tag{4.54}$$

when $\mathbf{C}_\eta = \sigma_\eta^2\mathbf{I}$ we obtain the same result as in Eq. 4.45:

$$\hat{\mathbf{j}} = (\mathbf{L}^T\mathbf{L} + \lambda^2\mathbf{H}^T\mathbf{H})^{-1}\mathbf{L}^T\mathbf{e} \tag{4.55}$$

with $\lambda^2 = \sigma_v^2\sigma$. Constraints on the solution are introduced in $\mathbf{H}$:

- $\mathbf{H} = \mathbf{I}$, we obtain the minimum norm solution
- $\mathbf{H} = diag(\frac{1}{||L_i||})$ compensates the small contribution of deep sources. Hence, they receive a stronger weight which can be given by the norm of the column of the lead field matrix [182].
- $\mathbf{H}$ is a laplacian matrix which imposes a smoothness constraint on the sources hence avoiding sparse focal activity.

- **H** is a diagonal matrix which elements reflect the a priori that the experimenter has on the source. This favors any desired source.

Interestingly, Eq. 4.55 can be partly precomputed since

$$pL = (\mathbf{L}^T\mathbf{L} + \lambda^2\mathbf{H}^T\mathbf{H})^{-1}\mathbf{L}^T \tag{4.56}$$

does not depend on the data, but only on the lead field and the constraint matrix. Hence inverting incoming data at time n only requires a matrix multiplication.

In this thesis, a source reconstruction approach is used in chapter 5 and in chapter 7. In chapter 5, a source reconstruction on realistic head models of 6 healthy volunteers is achieved to find differences at the source level between wakeful state and ketamine induced loss of consciousness. In chapter 7, the use of a four shell approximation of the brain is studied in a BCI setting and compared to scalp-based BCI methods.

Part II

Applications

Electrophysiologic correlates of ketamine induced loss of responsiveness

5

Essentially, all models are wrong, but some are useful [1]

This chapter presents an exploratory study (under submission [183]) on neural correlates of ketamine loss of responsiveness. Anesthetic agents provide a unique opportunity to study correlates of consciousness on an experimental basis hence potentially leading to a better understanding of brain states of patients with disorders of consciousness.

5.1 Introduction

Ketamine is a dissociative anesthetic agent whose molecular targets are very different from classical hypnotics. Ketamine is seldom used in clinical settings because of its side effects (hallucinations, out of body experiences). However it offers numerous advantages, which makes it an ideal field anesthetic. Indeed, it does not require ventilation; it can be administered in different forms and its effect can be controlled through its dosage [184]. Furthermore reports have shown that it could work as an antidepressant [185] and is also effective as a therapy for alcoholism [186]. Ketamine acts as a NMDA receptor antagonist and at sub anesthetic doses has a negative effect on attention and memory [187]. Its effect on clinical EEG has been described in the literature. After injection of Ketamine, three phases can be observed in the EEG, in phase I, the alpha waves are suppressed, in phase II theta waves are observed and in phase III delta waves [19]. While the increase in theta waves is well documented [188] even at sub-anesthetic doses [186], studies also report a concomitant superimposed fast rhythm in the beta and/or gamma band. Monitoring the level of

[1] Box and Draper 1987

anesthesia under ketamine with EEG features such as entropy has proven difficult due to the high frequency component [189] [190] [191]. The influence of Ketamine on brain metabolism has been described with Pet studies and tend to favor a hyper activation of frontal areas [192] [193] [194], and at sub-anesthetic levels of ketamine, a higher activity was detected in the frontal, parietal and thalamus [195]. Specific brain processes have also been studied under ketamine such as mismatch negativity [196], visual oddball task [197], and auditory steady state response [198]. A recent study modelling the effect of ketamine [199] predicts an increase in theta and gamma oscillations. Our objectives in this prospective study were to explore resting state EEG under ketamine at the scalp and source level and to infer effective connectivity between frontal, parietal and thalamus using Dynamic Current Modelling (DCM).

5.2 Materials and methods

5.2.1 Subjects

This study was approved by the Ethics Committee of the Faculty of Medicine of the University of Liege, and written informed consent was obtained from all participants. The subjects were recruited through advertisement in an internet forum and underwent a medical history and physical examination before participating in the study. Women were tested for pregnancy the day of the experiment (urine test) and were asked if they were using contraception. None of the subjects had a history of head trauma or surgery, mental illness, drug addiction, asthma, motion sickness, or previous problems during anesthesia. All volunteers received financial compensation for inconvenience and time lost during the experiment. Subjects fasted 6 h for solids and 2 h for liquids prior to sedation. Fifteen-minute spontaneous 60-electrode EEG recordings (Nexstim's eXimia TMS-compatible 60-channel EEG unit) were acquired in 6 subjects (mean age (years) 24,72 $\pm$ 2,64, 2 males) in 3 different states: normal wakefulness, LOC with clinical unconsciousness (no response to command, Ramsay scale score 5), and recovery of consciousness. The subject was asked to strongly squeeze the hand of the investigator. She/he was considered fully awake or having recovered consciousness if the response to verbal command (squeeze my hand!) was clear and strong (Ramsay 2); in sedation if the response to verbal command was clear but slow (Ramsay 3); and in LOC if there was no response to verbal command (Ramsay 5-6). For each consciousness level assessment, Ramsay scale verbal commands were repeated twice. The most comfortable supine position was sought to avoid painful stimulation related to position

Subject #	Experience
1	Out of room experience - Did not have the impression of being in LOC - Travelled with the anesthetic agent through the catheter
2	Spatial navigation, feelings of being immortal, traveling in it's own body vessels
3	Acute sensory experiences, spatial navigation and body image (viewing itself in other rooms), feelings of enlightenment and pleasure
4	Dreamy-like stage, spatial navigation, real sensation of beauty, body image
5	Spatial navigation, heroic fantasy-like experience
6	Spatial navigation, picturing himself as a box in chain of boxes.

Table 5.1 Subjective experience of volunteers during ketamine LOC

5.2.2 EEG

The EEG was first manually checked for bad channels exclusion, and then all channels were high passed filtered with a cutoff frequency of 0.5 Hz before being low-passed with a 40Hz cutoff frequency. A Butterworth filter of order 5 was used for both filtering operations. Subsequently the EEG was down sampled to 200Hz and re-referenced to a common average. Ocular channels were automatically inspected and all activity above three standard deviations was marked as artifacts. Continuous data were epoched and windows lasting 4 seconds outside of ocular artifacts were extracted with a 50% overlap. Each epoch was then carefully inspected and rejected if it contained remaining artifacts.

5.2.3 Source Modelling

An anatomical MRI scan was obtained for each subject and a cortical mesh of 8196 vertices was created. Electrode position was digitized to match the subject's scalp. Coregistration was achieved with 3 fiducials, the nose, the left and the right tragus. A boundary element model (BEM) was used as a forward model on which the lead field matrix was computed. The sources were reconstructed with a minimum norm solution with smooth priors, as implemented in SPM8.

5.2.4 DCM

A dynamic causal model was used to assess the connectivity between two sources that presented the most differences between wake and ketamine induced loss of consciousness. These two sources were chosen based on statistical differences at the source level in the theta band and were located in the superior frontal gyrus and in the inferior parietal lobule. A steady state response DCM modelling was used to

assess connectivity between the two regions of interest and three different models were tested to explore the influence of the thalamus in ketamine induced loss of consciousness. The first model only included the frontal and parietal source connected by frontal and backward connections. The second model included a hidden thalamus connected with frontal and backward connections to the two sources. The third model consists in two hidden thalamus modules with identical properties which are separately connected to the two sources (cfr. figure 5.1.A). In order to perform the bayesian model selection at the group level, we use the fixed effects assumption that the optimal model is identical for all subjects [200]. Physiologically, this implies that the effect of ketamine will not vary accross the subject.

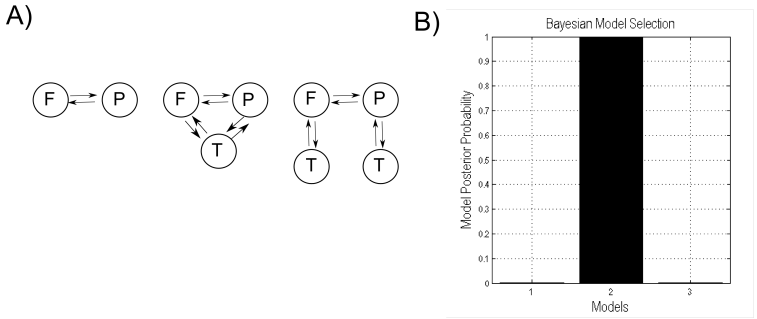

Figure 5.1 A) Three models for DCM, the first one models forward and backward connections between a frontal and a parietal source. The second model includes an additional thalamus with forward and backward connections to the two sources. In the third one, the thalamus has independent connections to the two sources. B) Bayesian model selection under the fixed effects assumption shows that model 2 is the most probable model.

5.3 Results

5.3.1 Subjective experience under ketamine induced loss of responsiveness

While provoking a total loss of clinical responsiveness (Ramsay scale score 5), ketamine infusion induced in our volunteers a vivid visual and emotional mental imagery state, combined with a total sensory disconnection from the environment (Table 5.1). None of the subjects reported any awareness of experimental events having occurred during the sedation. Ketamine thus induced a dissociated state with preserved internal awareness and altered mentation combined with a total loss of awareness of the environment.

5.3.2 Higher amplitude of slow and fast waves in ketamine induced loss of consciousness versus wake

During wakeful resting, the EEG of all but one subject resembles that of normal waking adults as widely acknowledged in the literature. Subjects display alpha waves oscillations between 8-12 Hz with a higher amplitude in the posterior regions. The mean power spectra averaged for the 6 subjects is displayed in figure 5.2.B and the alpha peak is clearly visible and centers around 10Hz. Under ketamine, visual inspection of the EEG reveals high amplitude slow theta waves oscillating around 5-7Hz mingled with slow waves and faster oscillations with an overall higher power in frequencies over 30Hz. The topography of the theta waves displays a posterior distribution with some activity in anterior regions; it is similar to the one of the alpha waves at rest. Finally, the EEG during recovery is less structured than during wake. As it is displayed in figure 5.2.D the alpha peak is attenuated compared to the rest condition before injection of ketamine. However it also displays a peak at higher frequencies 26-29 Hz in posterior regions. In order to extract statistical differences between the three conditions, one tail t-tests were performed. Figure 5.2.C displays in green significant results ($p<0.05$). The top row shows the distribution of higher power in rest versus ketamine condition. Significant differences are found in the alpha band in posterior and anterior regions. The second row shows the distribution of higher power in ketamine versus wake condition. Significant differences are found frontal posterior and occipital regions on the scalp in delta, theta and gamma bands. Similar results are found in the Ketamine > recovery setting. Testing for higher power in the recovery settings over wake does not yield any results.

5.3.3 Higher activation in theta parietal and frontal sources in ketamine- induced loss of consciousness versus wake

Results at the source level follow the same line as on the scalp level. Higher activations are found in wake in occipital and parietal sources at the voxel level ($p<0.05$) while during ketamine, there is an increase in theta power, and in gamma power ($p<0.05$) (Figure 4). No effect is seen during recovery. At the cluster level, the superior frontal gyrus of the left hemisphere and the inferior parietal lobule of the right hemisphere display a significant increase of theta power ($p<0.001$ family wise error corrected) (Table 5.2). In the gamma band the same two sources have higher activations but they do not stand out at the cluster level (Figure 5.4).

5.3.4 Higher intrinsic frontal connectivity as assessed with DCM

Bayesian model selection under the fixed effect assumption showed that model 2 has the highest probability (cfr. figure 5.1.B). Subsequently, connections strengths

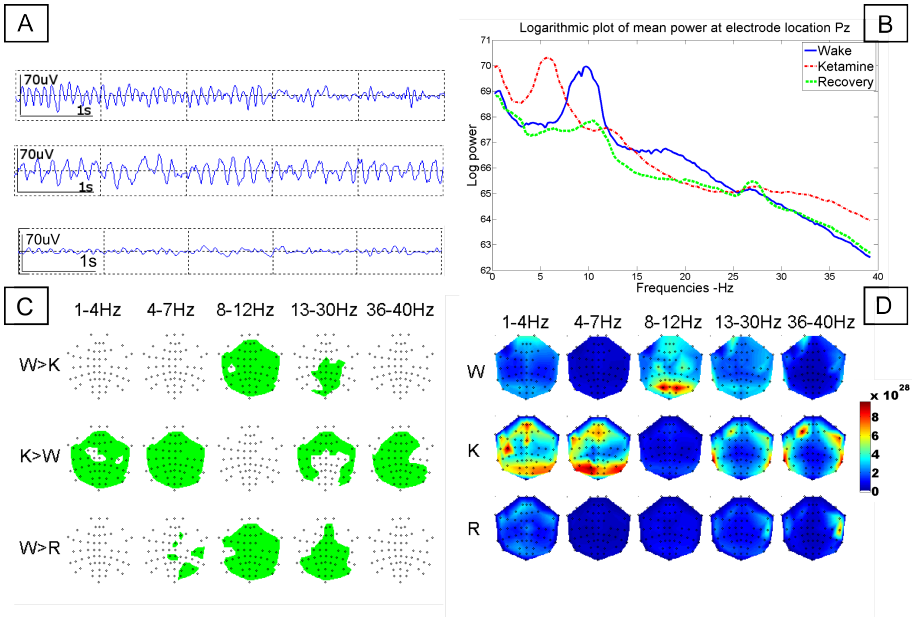

Figure 5.2 A) EEG traces of a subject on electrode Pz in the three conditions (from top to bottom , wake, ketamine and recovery). B) Log of power in rest (blue), ketamine (red) and recovery (green) conditions averaged for electrode Pz. C) Significative ($p<0.05$) differences (in green) for one tail t-tests assessing wake >ketamine (top), ketamine > wake (middle), wake>recovery (down) in 5 frequency bands. D) Topographic plots in five frequency bands for the three conditions (W,K,R)

	Center of gravity			NoV	side	lobe	AS	BA	Cp	Vp
	X	Y	Z							
Theta	-28	22	50	1729	Left	Frontal	SPG	BA8	0.001	0.027
	54	-30	48	1755	Right	Parietal	IPL	BA40	0.001	0.245
	26	-2	46	810	Right	Premotor	MFG	BA6	0.021	0.266

Table 5.2 Three clusters show significative ($p<0.05$ family wise error correction) increase in theta band power during ketamine versus wake. The center of gravity (in cartesian coordinates), number of voxels (NoV), side and lobe of the clusters, anatomical structure (AS), Brodmann area (BA), cluster p-value (Cp) and voxel p-value (Vp) are indicated. The 3 clusters are located in the superior frontal gyrus (SFG), the inferior parietal lobule (IPL) and the middle frontal gyrus (MFG)

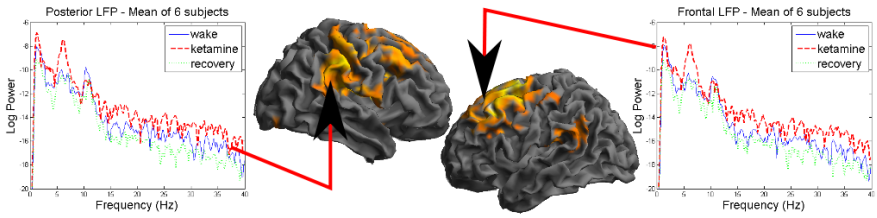

Figure 5.3 Two sets of clusters at the source level in the theta band show higher activations in ketamine versus wake at p<0.001 under family wise error correction. The first source is located in a centro-parietal region of the right hemisphere (displayed on the left of the figure with associated power spectra). The second source is located in a frontal region of the left hemisphere (displayed on the right of the figure with associated power spectra).

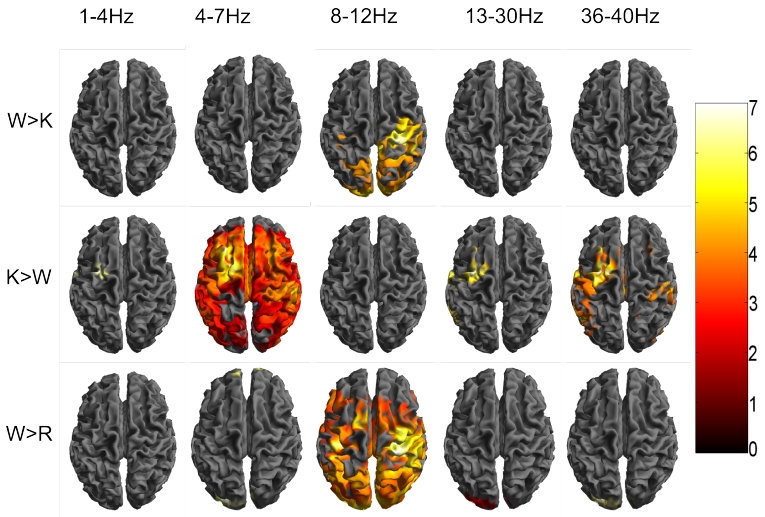

Figure 5.4 Voxels with statistically higher activations (p<0.05) in the five frequency bands and for three different statistical tests: 1) wake versus ketamine 2) ketamine versus wake 3) wake versus recovery.

in model 2 were examined and a higher intrinsic frontal connectivity was observed in all six subjects ($p<0.05$ corrected) with an average increase of 24% in the ketamine state compared to wake. A trend of higher connection strength in ketamine versus wake($p<0.05$ uncorrected) was also observed in the intrinsic parietal connectivity and in the forward connection from the parietal source to the thalamus. During recovery a drop in connection strength is observed ($p<0.05$ uncorrected).

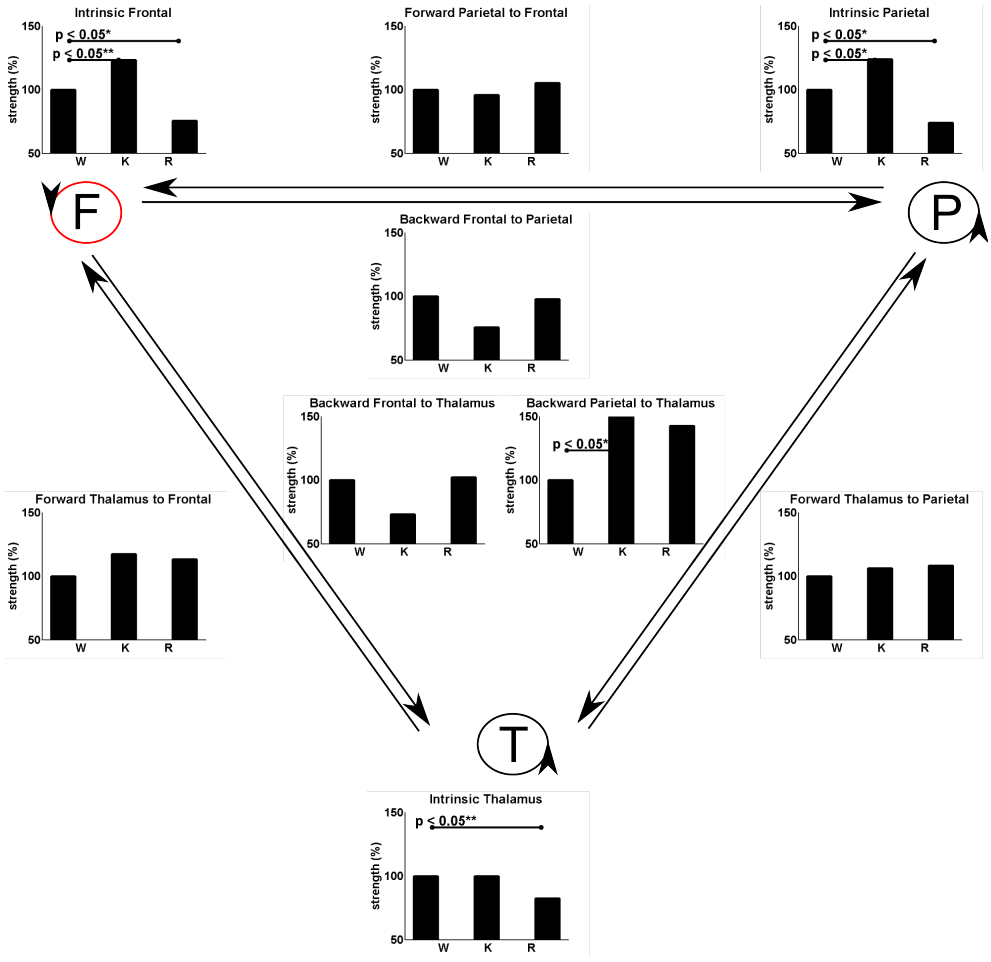

Figure 5.5 Changes in intrinsic frontal, parietal and thalamus connection strengths between wake, ketamine and recovery conditions. Statistically different conditions are marked by a star ($p<0.05$) or by two stars ($p<0.05$ corrected for multiple comparisons).

5.4 Discussion

5.4.1 Concomitant increase in slow (theta) and fast (gamma) oscillations

Ketamine-induced disconnected state was associated with an increase in theta, high beta and gamma power originating in lateral frontal and posterior regions. Understanding the role of gamma oscillations is a recurring subject in many studies. Gamma was associated with consciousness [201], but has also been found in anesthesia induced loss of consciousness with propofol [202]. In our case, it appears that the increase of gamma oscillations in lateral cortex is linked to impaired cortical function, since it is associated with loss of external awareness.

5.4.2 Intra-frontal cortical loop

Dynamical causal modelling analyses suggested an instrisic mechanism for explaining these changes in power spectrum. Increased intrinsic connectivity in the frontal cortex matches previous findings showing increased metabolism in frontal regions [194] [193] during ketamine infusion as compared to wakefulness. Interestingly, this differs from a study using propofol where thalamus was involved in mild sedation. This suggests that loss of consciousness can be triggered by different mechanisms. It has been demonstrated that gamma oscillations are produced by fast spiking cells while activation of pyramidal neurons only triggers low frequency oscillations [203]. The observed concomitant increase in slow and fast oscillations would therefore be due to the activation of two distinct cell types. More complex DCM models could differentiate that. DCM models specifically designed to pinpoint the effect of ketamine on NMDA receptors might give better insights on the biophysical mechanisms underlying this frontal intrinsic excitability [204].

5.5 Conclusion

Ketamine sedation induced a total disconnection from the environment, paired with preserved dream-like mentation (internal content). In line with this phenomenon, source reconstruction results revealed that ketamine preferentially altered oscillatory activity in lateral frontoparietal cortices (involved in 'external' awareness) [205], while default network function (involved in 'internal' awareness) was relatively preserved. Our DCM findings corroborate previous studies showing increase in metabolism in frontal regions [194] [192] during ketamine infusion as compared to wakefulness. Interestingly, in contrast to results previously obtained during propofol-induced loss of consciousness [206], ketamine-induced power spectral

changes and decrease in responsiveness seem not to involve changes in thalamo-cortical interactions, but rather to be linked to an intra-cortical action mechanism. Further studies should include a larger population and use more specifically designed DCM models.

Differences between VS/UWS and MCS patients from an EEG connectivity and EEG spectral power viewpoint

6

It is important to distinguish patients in MCS from those in coma and VS/UWS because preliminary findings suggest that there are meaningful differences in outcome.[1]

This chapter presents results published in *Functional Neurology* [39]. The aim of this study was to look for differences in the power spectra and in EEG connectivity measures between patients in the vegetative state (VS/UWS) and patients in the minimally conscious state (MCS). We showed that (VS/UWS) patients had increased delta power but decreased alpha power compared with the MCS patients. Connectivity measures revealed that patients in the VS/UWS state had significantly lower connectivity than MCS patients in the theta and alpha bands. This study demonstrates that standard EEG recorded in clinical conditions could be used as a tool to help the clinician in the diagnosis of disorders of consciousness.

6.1 Introduction

Patients emerging from coma can go through varying states of consciousness. The vegetative state / unresponsive wakefulness syndrome (VS/UWS) [5] is characterized by wakefulness but absence of both self and environmental awareness [207] 'The minimally conscious state (MCS) is a condition of severely altered consciousness in which minimal but definite behavioral evidence of self or environmental awareness is demonstrated' [8] The importance of a correct diagnosis of these two

[1] J.T. Giacino et al. [8]

states is two-fold. First, MCS have better recovery chances than VS/UWS patients [208]. Secondly, different treatments are needed depending on the state of the patient. In clinical practice, several scales [209] are used to evaluate the state of consciousness of a patient based on behavioral reactions to different stimuli. The Glasgow coma scale [210] is widely used however recent studies show that for chronic patients, more advanced scales such as the coma recovery scale revised (CRS-R) [9] improves considerably the diagnosis of patients emerging from coma [10]. Still, bedside evaluation is difficult, requires expertise and can be dependent to the subjectivity of the assessor. Thus, an automated method providing a paraclinical measure allowing a correct diagnosis of VS/UWS and MCS patients would prove helpful [90]. Several steps have been achieved towards this goal using external stimulations in passive and active paradigms with different imaging and neurophysiologic tools. Studies based on passive stimulation have shown that MCS patients have bigger and wider activations than VS/UWS patients [211], [212], [89], [86], [76]. Still VS/UWS patients can also display significant activations showing that they retain some islands of preserved cognitive function [213]. Proof of higher level cognitive function can be assessed with active stimulation [214], [215], [98] but in this case the absence of activation is not a proof of absence of cognitive function as it is not possible to know if the patient tried to achieve the task or not. Hence, researchers are exploring resting-state activity, which is stimulus independent and therefore does not depend on the reaction of the patient. One step has been achieved toward this goal using the bi-spectral index, which was found lower for VS/UWS patients than for MCS patients [45]. These results are promising, still they only provide a general measure but no physiological details, thus a logical step forward would be to identify more precisely correlates of consciousness in the EEG signal.

The objective of this study is to investigate the possible differences in low-density EEG of MCS and VS/UWS patients recorded in resting state conditions. In the following, we present demographic and clinical data, the pre-processing steps and the studied electrode montages. Three main results are presented, the comparison between MCS and VS/UWS, the etiology analysis and the longitudinal analysis.

6.2 Materials and Methods

We prospectively studied 31 brain-damaged patients with disorders of consciousness (DOC). Patients were free of sedative drugs at the time of the recording. Three MCS patients were excluded due to movement or ocular artifacts (only patients showing at least 10 artifact-free 4 second-epochs were included). We assessed the effect of time, comparing 15 patients studied in the acute/subacute phase (i.e., <3 months post-injury) and 13 patients studied in the chronic phase. The effect of etiology was assessed by comparing the 15 non-traumatic with 13 traumatic patients.

Finally, the influence of clinical diagnosis compared the 18 MCS (15 males, aged 39 $\pm$ 11 years; 10 chronic (>3 months post-injury); 8 non-traumatic) with the 10 VS/UWS patients (6 males, 50 $\pm$ 13 years; 5 chronic; 8 non-traumatic). The study was approved by the Ethics Committee of the Medical School of the University of Liege. Informed consent was obtained from the legal surrogate of the patients. All the patients were evaluated in the University hospital of Liege, Liege, Belgium. The diagnosis of patients was based on repeated Coma Recovery Scale - Revised assessments [216]. Table 6.1 shows clinical and demographic data.

Fifteen minutes of EEG were recorded in resting state conditions at 500Hz sampling rate using a Vamp amplifier (Brain Products GmbH, Munich, Germany). Ten cephalic EEG recording (using the 10-20 positioning system Fz, F3, F4, Cz, C3, C4, Pz, P3, P4, Oz; referenced to the nose) and 2 electrooculogram (EOG) and chin electromyography (EMG) were obtained. EEG recordings were visually inspected for artifact removal using the FASsT toolbox [217] and band-passed into three frequency bands: delta [0.5-4Hz], theta [4-8Hz], alpha [8-12Hz], using a first-order Butterworth filter. A low-order filter was chosen to minimize phase distortions due to filtering. Artifact-free epochs lasting at least 4 seconds were extracted and power spectra, coherence, imaginary part of coherency [54] and phase lag index [55] were computed for each epoch and next averaged over all data for each subject and for different combinations of electrodes. Power spectra of EEG and EMG were computed for each epoch with a frequency resolution of 1Hz. The average power spectra were then taken over all the epochs for each subject and for each frequency band. A multitaper method [218] was used with 7 discrete prolate spheroidal sequences as data tapers. Relative power values were obtained for each band by computing the fraction of power at each band divided by the sum of power across 1-48 Hz. We calculated mean relative power spectra for frontal (i.e., F3 C3 P3), posterior (F4 C4 P4), left-hemisphere (F3 C3 P3) and right hemisphere (F4 C4 P4) derivations. Connectivity studies measured coherence (C), imaginary part of coherency (IC) [54] and phase lag index (PLI) [55] as described in section 4.3.1. These measures were computed for each epoch (values were next averaged over all epochs) for each frequency band and for each subject. All three connectivity measures were bounded between 0 (no connectivity) and 1 (total connectivity). The aim of using the IC and the PLI was to diminish the influence of common sources due to the volume conduction effect [34] (see sections 4.3.1.3 and 4.3.1.4).

For connectivity assessments, data were analyzed with four constructed bipolar montages, avoiding influence of the reference, assessing (i) left-right interhemispheric (employing F3 C3 P3, F4 C4 P4), (ii) front-to-back (i.e., F3 Fz F4,P3 Pz P4) and (iii) left-hemisphere (F3,C3,P3) and (iv) right hemisphere (F4,C4,P4). Average connectivity values were computed on all these subsets for the different fre-

State	n°	Age	G	CRS-R	Etio	ISI	AfS	VfS	Mfs	OfS	CS	AS
VS	1	62	M	6	A	260	AS	N	FW	ORM	N	Eo
	2	35	F	7	A	125	AS	BtT	FW	ORM	N	Eo
	3	45	F	4	CVA	77	AS	N	AP	V	N	Eo
	4	47	M	3	A	7	AS	N	N	ORM	N	EoWS
	5	54	M	4	A	169	AS	N	AP	ORM	N	EoWS
	6	61	M	4	E	16	AS	N	FW	ORM	N	EoWS
	7	37	M	7	A	262	AS	F	AP	ORM	N	Eo
	8	31	M	3	T	184	N	N	AP	ORM	N	Eo
	9	69	F	3	T	8	AS	N	AP	ORM	N	EoWS
	10	61	F	5	A	34	N	N	FW	ORM	N	Eo
MCS	11	28	M	11	T	2299	RMC	VP	FW	ORM	N	Eo
	12	31	M	11	A	604	AS	VP	AP	V	N	Eo
	13	28	F	11	T	800	RMC	VP	FW	V	N	Eo
	14	48	M	18	CVA	43	RMC	OR	AMR	V	NF	Eo
	15	35	M	9	T	8602	AS	VP	FW	V	N	Eo
	16	62	M	8	T	66	N	PEM	FW	ORM	N	Eo
	17	31	F	11	CVA	44	LtS	PEM	FW	V	N	Eo
	18	36	M	6	T	340	N	VP	N	ORM	N	Eo
	19	48	M	14	T	16	RMC	VS	LNS	IV	F	Eo
	20	24	M	8	T	71	N	VP	FW	ORM	N	Eo
	21	46	M	21	CVA	569	CMC	OR	AMR	IV	NfI	A
	22	24	M	8	T	318	RMC	VP	FW	ORM	N	Eo
	23	41	M	12	A	47	RMC	VP	N	V	NfI	Eo
	24	37	M	11	T	128	RMC	VP	FW	ORM	N	Eo
	25	38	M	10	A	4542	N	VP	AMR	ORM	N	Eo
	26	44	F	10	CVA	80	AS	VP	FW	V	N	Eo
	27	58	M	9	T	56	AS	VP	FW	ORM	N	Eo
	28	35	M	14	T	24	RMC	VP	OM	V	N	Eo
	29	53	F	12	T	80	RMC	VP	FW	ORM	NfI	Eo
	30	42	F	15	CVA	23	RMC	VP	FW	ORM	NfI	Eo
	31	21	F	10	T	743	AS	VP	FW	V	N	Eo

Table 6.1 Demographic and clinical information encompassing age (years), gender (G), coma recovery scale - revised total score (CRS-R), Etiology (Etio; A=anoxic; T=traumatic; CVA=cerebrovascular accident; E=encephalitis), interval since insult (ISI : in days), Auditory function Scale (AfS; CMC = consistent movement to command; RMC=reproducible movement to command; LtS = Localization to Sound; AS=auditory startle ; N = none), Visual function Scale (VfS; OR = object recognition; VR = Visual Pursuit; F = fixation; BtT=blink to threat), Motor function Scale (MfS; AMR = automatic motor response; OM = object manipulation; FW = flexion withdrawal; AP = abnormal posturing; N = none), Oromotor/Verbal function Scale (OfS; IV = intelligible verbalization; V = vocalization ; ORM = oral reflexive movement), Communication Scale (CS; NfI = non functional : intentional; N = none) and Arousal Scale (AS; A = attention; Eo = eye opening without stimulation; EoWS = Eye opening with stimulation).

quency bands. Averages were made for all relevant connections. Bipolar montages are illustrated in figure 1.

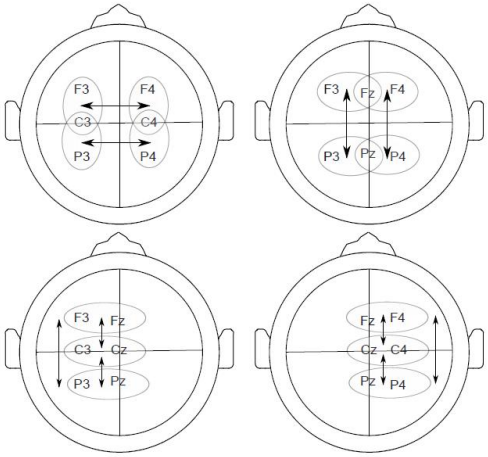

Figure 6.1 Bipolar montages representation for inter-hemispheric, front to back connectivity (top left and top right figures) and for connectivity in left and right hemispheres (bottom left and right figures).

Statistical analyses were performed in Matlab R2007b (MATLAB version 7.5 Natick, Massachusetts: The MathWorks Inc., 2007). Permutation testing (10000 permutations) compared relative power spectra for frontal, posterior, left and right averaged electrodes and connectivity measures for back-to-front, left-right inter-hemispheric, left-hemisphere and right-hemisphere montages, looking for the effect of time (acute/subacute vs chronic), etiology (traumatic vs non-traumatic) and diagnosis (MCS vs VS/UWS). Since most of the VS/UWS patients are non traumatic, the effect of etiology is only assessed on MCS patients. Results were thresholded for significance at $p<0.05$ and corrected for multiple comparisons.

6.3 Results

Relative power spectra were higher in VS/UWS patients as compared to MCS patients in the delta band in all electrodes. There was a marked difference in right hemisphere electrodes (0.223 +/- 0.04; 0.165 +/- 0.07; $p<0.05$**). Relative power spectra were higher in MCS patients as compared to VS/UWS patients in the alpha band for all electrodes with a marked difference in right hemisphere electrodes (0.0173 +/- 0.007; 0.0106 +/- 0.006; $p<0.05$ **). None of the frequency bands in EEG and EMG showed any difference between acute/subacute DOC patients and chronic patients. No differences were found between traumatic and non-traumatic DOC patients. Connectivity measures (C, IC and PLI) showed no differences be-

tween acute/subacute and chronic DOC patients and between traumatic and non-traumatic etiology. Connectivity assessments based on classical coherence showed no difference between diagnostic groups for any frequency band. There was a higher front to back connectivity in MCS as compared to VS/UWS groups in the theta band as measured by the PLI (0.127 +/- 0.03; 0.103 +/- 0.03; p<0.05 **) and the IC (0.134 +/- 0.02; 0.108 +/- 0.03; p<0.05 **). The PLI also identified a higher alpha connectivity between hemispheres (0.0995 +/- 0.01; 0.0869 +/- 0.009; p<0.05 **). An illustration of the power and connectivity results is given in figure 6.2.

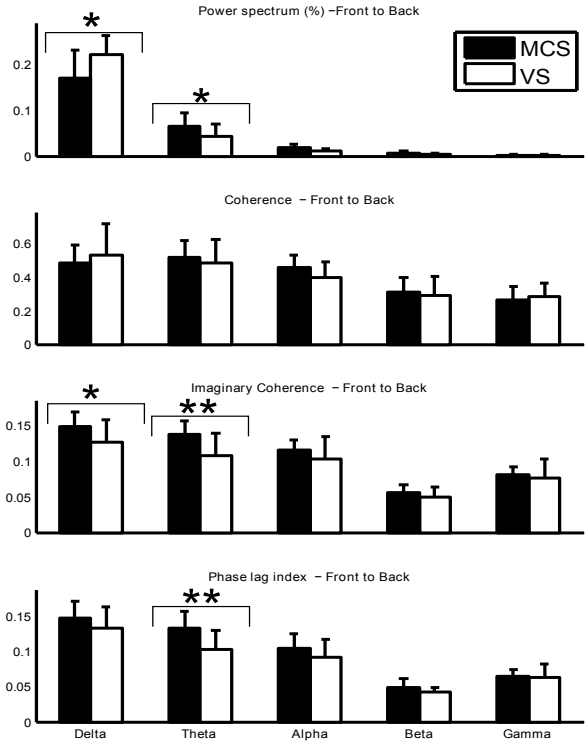

Figure 6.2 Power spectra (at Back location), coherence, imaginary part of coherence and phase lag index (of the left hemisphere) in patients in minimally conscious state (MCS; n=18; in black) and vegetative/unresponsive state (VS/UWS; n=10; in white). Values are means and standard deviations. * uncorrected $p < 0.05$; ** $p < 0.05$ corrected for multiple comparisons.

6.4 Conclusion

Quantitative analysis of the EEG of 28 DOC patient revealed that the relative power in the delta band is higher for the VS/UWS group than for the MCS group.

	PLI			IC		
	MCS	VS	sig	MCS	VS	sig
Inter Hemisphere						
Delta	0.133 +/- 0.02	0.151 +/- 0.04	-	0.138 +/- 0.02	0.149 +/- 0.02	-
Theta	0.108 +/- 0.02	0.108 +/- 0.03	-	0.118 +/- 0.02	0.111 +/- 0.02	-
Alpha	0.0995 +/- 0.01	0.0869 +/- 0.009	**	0.114 +/- 0.02	0.0994 +/- 0.01	*
Front to Back						
Delta	0.144 +/- 0.02	0.133 +/- 0.03	-	0.147 +/- 0.02	0.127 +/- 0.03	*
Theta	0.127 +/- 0.03	0.103 +/- 0.03	**	0.134 +/- 0.02	0.108 +/- 0.03	**
Alpha	0.101 +/- 0.02	0.0918 +/- 0.03	-	0.114 +/- 0.01	0.103 +/- 0.03	-
Left Hemisphere						
Delta	0.155 +/- 0.03	0.155 +/- 0.03	-	0.137 +/- 0.02	0.122 +/- 0.03	*
Theta	0.136 +/- 0.03	0.113 +/- 0.02	*	0.12 +/- 0.03	0.1 +/- 0.02	*
Alpha	0.114 +/- 0.02	0.1 +/- 0.02	*	0.107 +/- 0.01	0.0971 +/- 0.02	-
Right Hemisphere						
Delta	0.158 +/- 0.03	0.157 +/- 0.03	-	0.128 +/- 0.01	0.121 +/- 0.02	-
Theta	0.135 +/- 0.03	0.124 +/- 0.03	-	0.114 +/- 0.02	0.104 +/- 0.02	-
Alpha	0.114 +/- 0.02	0.104 +/- 0.03	-	0.103 +/- 0.02	0.0966 +/- 0.02	-

Table 6.2 Connectivity comparisons between MCS and VS/UWS. Values are means and standard deviations of the phase lag index and imaginary part of coherency in three frequency bands (delta, theta, alpha) for all bipolar montages (inter-hemisphere, front to back, left and right hemisphere). * uncorrected $p < 0.05$; ** $p < 0.05$ corrected for multiple comparisons.

However a drop in alpha power is observed in VS/UWS patients compared to MCS patients. Connectivity measurements showed that MCS patients had a better connected network in the theta and in the alpha band. No differences were found in the acute/chronic or in the trauma /non trauma patients. However, both of these results are subject to limitations. Indeed the etiology study only compared MCS patients since the VS/UWS group had unbalanced etiologies (80% non traumatic). It should also be stressed that the study on the effect of time looked for between-patient variability and not for within-patient changes in the acute and subacute phase. Further longitudinal studies should aim to quantify the temporal dynamics of the EEG changes and neuronal plasticity in the recovery of consciousness after coma and related disorders. The results based on the relative power in the delta band are in line with a previous study [38] which compared a group of MCS patients and patients with severe neurocognitive disorders (SND) showing that the power in the delta band increased with the severity of the disorder while it decreased in higher frequency bands. VS/UWS patients thus have a more important slowing of the brain electrical activity than MCS. Such observations have already been acknowledged

	Comparison MCS-VS		
	MCS	VS	sig
Front			
Delta	0.172 +/- 0.07	0.22 +/- 0.04	*
Theta	0.0523 +/- 0.02	0.0412 +/- 0.03	-
Alpha	0.0142 +/- 0.005	0.011 +/- 0.006	-
Back			
Delta	0.171 +/- 0.06	0.224 +/- 0.04	*
Theta	0.0648 +/- 0.03	0.0435 +/- 0.03	*
Alpha	0.0176 +/- 0.008	0.0115 +/- 0.005	*
Left Hemisphere			
Delta	0.173 +/- 0.07	0.221 +/- 0.04	*
Theta	0.0589 +/- 0.03	0.0409 +/- 0.03	-
Alpha	0.0154 +/- 0.007	0.0109 +/- 0.005	*
Right Hemisphere			
Delta	0.165 +/- 0.07	0.223 +/- 0.04	**
Theta	0.058 +/- 0.02	0.0409 +/- 0.03	*
Alpha	0.0173 +/- 0.007	0.0106 +/- 0.006	**
EMG			
Delta	0.113 +/- 0.08	0.0848 +/- 0.09	-
Theta	0.0348 +/- 0.02	0.0272 +/- 0.02	-
Alpha	0.0166 +/- 0.01	0.0211 +/- 0.01	-

Table 6.3 Power spectra and significance between MCS and VS/UWS in front, back, left and right hemisphere and EMG. Values are means and standard deviations. * uncorrected $p < 0.05$; ** $p < 0.05$ corrected for multiple comparisons.

by clinical EEG inspection [17] [219], and delta activity is known to be a malignant pattern in VS/UWS [86]. Furthermore, EEG connectivity showed that MCS patients have better connected networks than VS/UWS. This result goes in the same direction as a recent study which stated that SND patients consistently displayed a higher number of connections than MCS patients [56] thus the level of connectivity could be related to the severity of the disorder. It is interesting to note that theta and alpha connectivity in MCS have different locations. This finding should be further investigated but it could be due to the limited number of electrodes (i.e., inter-hemisphere and front to back bipolar montages share four out of six electrodes). A previous study reported that EEG could be used to diagnose DOC patients using the bi-spectral index [45], which is originally used to monitor the level of anesthesia and provides a unit-less number between 0 (death) and 100 (fully awake). The advantage of the approach presented herein is that it offers features that can be interpreted from a physiological point of view and thus can provide a better understanding of the underpinning brain electrical activity. The IC and the PLI had never been used previously with DOC patients, they succeeded in finding differences between MCS and VS/UWS while standard coherence did not. Still, these results have been obtained at the group level, and further work has to be done to disentangle VS/UWS and MCS patients at the individual level. Further improvements will include a higher density electrode cap to allow the use of source reconstruction techniques for better localization of the brain activity.

Investigating the usefulness of source reconstruction in Brain Computer Interfaces

7

A BCI is a communication system in which messages or commands that an individual sends to the external world do not pass through the brain's normal output pathways of peripheral nerves and muscles [1]

In the preceding chapter we saw that it was possible to differentiate VS/UWS patients and MCS patients with electrophysiological measurements. Once that a patient demonstrates signs of consciousness, the next step is to establish a communication mean with a brain computer interface (BCI). The quality of a BCI is judged on the information transfer rate it can achieve. Improving the information transfer rate requires improving feature extraction for better classification accuracies. In this chapter we investigate the use of source reconstruction methods to extract features possibly offering more discriminative power than features extracted from scalp measurements.

7.1 Introduction

The last two decades have foreseen an increasing interest in Brain-machine interfaces (BMI) or Brain computer interfaces (BCI). Different modalities have been used to obtain reliable signals from which commands can be derived. These modalities can be seen as corresponding to three hierarchical levels in the brain [220]. First, macroscopic level, with the EEG, from which one can have a blurred and spatially filtered electric activity of the brain, then the mesoscopic level which corresponds to local field potentials (LFP) measured with local intra-cranial electrodes (Electrocorticograms - ECoG). Finally the microscopic level can be investigated with arrays

[1] J.R. Wolpaw et al. [12]

of micro electrodes that are inserted in the neo-cortex and allow the measurement of multiple spike activity (MSA). Direct measures at microscopic and mesoscopic levels are promising but highly invasive. Furthermore, there are physical limitations to the use of long-term intra-cranial micro-electrodes since they tend to oxide and to be rejected by body cells. It is possible to improve the spatial resolution of recordings at the scalp level by using an inverse solution. Extracting features from the source space instead of the scalp space might improve BCI performances. To date, five contributions have been made in this direction. In [221], the author use the inverse problem as classifier. Parametric and imaging methods are tested. Classification rates are 78,9% for the first case and 80,6% for the second. In [222] results are 80% for four subjects. Both of these results are not compared with electrode-based methods. In [223], the use of an inverse problem shows improvements compared to electrode-based methods. However the latter are not optimal. Similarly in [224] the use of the inverse problem elicits better results on a benchmark dataset, but again the electrode based method is not optimal and gives weaker results than the ones obtained in the literature. These results therefore raises the question whether or not the inverse problem can truly improve classification rates compared to standard BCI electrode-based methods. Indeed although these methods can be seen as alternatives to current state of the art methods, they add complicated parameter tuning except in [225] where the use of the inverse problem leads to an untrained classifier. The following study is thus a comparison of the common spatial patterns (CSP) approach, a well-known method in the BCI community, and inverse solutions.

7.2 Materials

7.2.1 Data : Dataset IV from BCI competition 2003

The data is provided by the Berlin brain computer interface lab and can be downloaded online on the BCI competition pages. It was provided during the BCI competition 2003. The dataset consists of one subject that has to type on a computer keyboard with his index and little fingers. The typing is done at a rate of one key every second in a 'self-paced key typing' paradigm. For the BCI competition, the organizers kept 416 epochs of 500ms ending 130ms before movement onset. This is to avoid EMG artefacts in the EEG and make sure that the analyzed feature is the movement preparation. The 416 epochs were divided in 316 training trials and 100 trials for testing purposes. While the competition was running, labels were available only for the training trials and the participants had to submit the labels on the test set for the competition. Once the competition was closed and final results announced, the labels for the test set were posted on line. The data was recorded at 1000Hz than downsampled to 100Hz. The EEG was recorded with a 28 channel cap according to the 10-20 system [226].

7.2.2 The Bereitschaft Potential (BP)

The first report of a potential change measured consecutively a finger movement dates back to 1951, when Bates and colleagues demonstrated a contralateral desynchronisation [227] *following* movement. This interesting result was confirmed ten years later and complemented with the observation that a slow drift occurs *preceding* movement onset [228]. This slow drift is termed the bereitschaft potential (BP), the german word for readiness potential as it was discovered by a german team. One interesting feature of this potential is that it is increased by intentional engagement. The BP is composed of an early part starting up to 1.5 seconds before movement onset and a later part centering around 0.5 seconds before the movement [229] [230] [231] [232]. The BP is a low frequency potential (0.4 - 3.5 Hz) belonging to the family of slow cortical potentials (SCP). Features extracted from SCPs can be used to classify finger movement or imagination [233] [234]. Finger movement or imagination do not only involve the BP but also other complex processing involving alpha, beta and gamma oscillations [235]. In the present study, only features extracted from the BP will be used.

7.3 Methods

7.3.1 Preprocessing and filtering

This part is common to the two approaches, first the signal is re-referenced to a common average reference. Then, since the movement related signal appears near the end of each trial, each trials are multiplied by a one-sided cosine function :

$$w(n) = 1 - cos(n\pi/128) \text{ for } n = 0, ..., 99 \tag{7.1}$$

Then the signal is zero-padded in order to apply a 512 points fast Fourier transformation, followed by an inverse fast Fourier transformation, keeping only the coefficient between 0.4 and 3.5 Hz.

7.3.2 Electrode-based analysis

7.3.2.1 Common Spatial Patterns(CSP)

The CSP approach to discriminating two events in EEG recordings has been presented in [236] and consists in maximizing the differences between two conditions. The spatial filters are built from the joint diagonalization of two covariance matrices which result in eigenvectors (which are the spatial filters) that are a linear combination of all the electrodes available. The selection of these filters is made based on their corresponding eigenvalue. These values are comprised between 0 and 1. A

value close to 0 or 1 indicates a good discrimination between classes. A value close to 0.5 indicates no discriminability. This method is widely used in the BCI community and has been derived in multiple variants where temporal and spectral aspects are included. For example, the common spatial subspace decomposition (CSSD) [237], the common spatio spectral patterns (CSSP) [238], the common spatio temporal pattern (CSTP) [239] used in a P300-speller BCI and extracts the spatio-temporal pattern of a P300. The CSP algorithm and it's different variants has received great success in all the BCI competitions that have taken place until now. Recently Grosse-Wentrup and Busse [240] showed the relationship between CSP and the minimal classification error in the framework of information theoretic feature extraction (ITFE). They proved that in a 2-class problem, the CSP algorithm is equivalent to ITFE and can be considered as optimal. In practical however, CSP suffers from a main drawback, it is sensitive to artefacts. Indeed, when computing the spatial filters from training data, artefacts in the signal can cause a misplaced spatial filter. This problem could be overcome by computing a ratio of medians as described in [241]. Another solution presented by [242] would be to build the filters using predefined regions of interest (ROI) based on real anatomical a priori given by a head model. This way, the filters are not built from training data but can be built once and for all for any head model and corresponding lead field matrix. The following steps will describe the CSP algorithm briefly. In order to use the CSP method,the signal is centered and scaled : Let $\mathbf{X}_{band-pass} \in \Re^{X \times T}$ be the band passed EEG signal of a trial with X the number of electrodes and T the number of trials. The centered and scaled signal $\mathbf{X}$ is obtained as follows :

$$\mathbf{X} = \frac{1}{\sqrt{T}} \mathbf{X}_{band-pass} (\mathbf{I}_T - \mathbf{1}_T \mathbf{1}_T^t) \tag{7.2}$$

Where $\mathbf{I}_T$ is a $T * T$ identity matrix and $\mathbf{1}_T$ is a T-dimensional vector of ones. Then the Common Spatial Patterns is a 3-step operation :

1. Compute the covariance matrix for each class :

$$\mathbf{C}_l = \frac{1}{n} \sum \mathbf{X}_i \mathbf{X}_i^t \tag{7.3}$$

2. Compute the simultaneous diagonalization of $\mathbf{C}1$ and $\mathbf{C}2$

$$\mathbf{w}^T \mathbf{C}_1 \mathbf{w} = \mathbf{D}_1 \tag{7.4}$$

$$\mathbf{w}^T \mathbf{C}_2 \mathbf{w} = \mathbf{D}_2 \tag{7.5}$$

3. Filter EEG with W :

$$\mathbf{X}_{CSP} = \mathbf{w}^T \mathbf{X} \tag{7.6}$$

7.3.2.2 feature extraction

Once the spatial filters ($\mathbf{w}$) have been computed, the best filters maximizing the variance of one condition versus the other are kept and features are taken as the mean over 5 time windows of the signal. These features are then classified with a Proximal Support Vector Machine (PSVM) algorithm

7.3.3 Inverse Problem-based analysis

7.3.3.1 Head model

A four shell head model was used to represent the brain, the cerebro spinal fluid, the skull and the scalp [243] . The radius of the scalp was set arbitrarily to 100mm. The number of dipoles were set to 400 since it gave the best results on the validation set of a previous study [224]. Dipole orientation was fixed perpendicular to the surface in order to mimic orientation of pyramidal cells. Dipoles are located 2mm under the surface of the scalp, inside the gray matter. They have equiangular distribution (see Fig. 7.1).

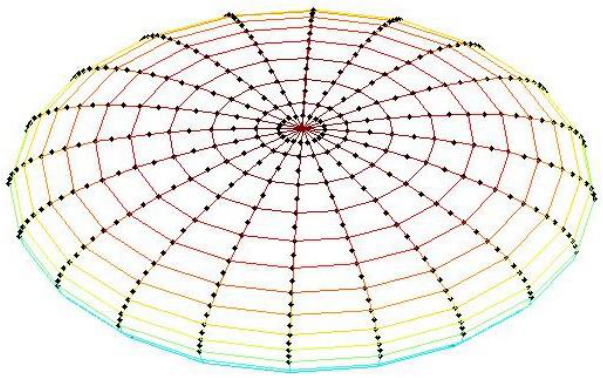

Figure 7.1 Dipole position illustration. Dipoles have equiangular distribution and are placed 2mm below the cortex surface

7.3.3.2 Inverse solutions

In the following, two inverse solutions were tested, the minimum norm source reconstruction approach and the minimum norm with a laplacian prior.

7.3.3.3 Spatial prefiltering before using an inverse solution

In order to carry out a thorough comparison between electrode analysis and inverse problem analysis we need to follow a similar approach. Logically, CSP should

be applied at the scalp level and identically at the source level. However, the simultaneous diagonalization step of the CSP algorithm becomes computationally demanding when the size of the matrices increase. Hence a CSP filtering step is introduced before the source reconstruction. This is implemented by building a single spatial filter encompassing the activity corresponding to left and right movement. This can be interpreted as denoising the signal from activity not related to the movements of interest. This filter is computed as follows :

$$\mathbf{f} = [\overline{\mathbf{w}_1}...\overline{\mathbf{w}_i}\overline{\mathbf{w}_{N-i}}...\overline{\mathbf{w}_N}] \tag{7.7}$$

where $\mathbf{w}_i$ are the best filters corresponding to the first class and $\mathbf{w}_{N-i}$ the best filters corresponding to the second class. All filters $\mathbf{w}_i$ are normalized so as to have equal weights. The inverse solution procedure is then carried out by computing :

$$si(t) = \mathbf{G} \times \mathbf{f} \times \mathbf{f}^T \times s(t) \tag{7.8}$$

7.3.3.4 Feature extraction with the inverse problem

Since the inverse problem yields a much higher dimensional feature space, a supplementary feature selection step is needed to extract the most relevant features. These features consist in the mean over 5 time windows over all the voxels. The method used is termed Discriminant Power (DP) presented by [9]. It ranks all the features (mean of voxels over each time window) along their capacity to discriminate two tasks. The DP is computed once and for all during a training phase and consists in computing the number of true positives yielded by each single feature separately, knowing that the false positives are set to zero. The DP is given by the following equation :

$$DP = \frac{card(a < b_{min}) + card(b > a_{max})}{card(a) + card(b)} \times 100 \tag{7.9}$$

where a (resp. b) is the feature vector for class A (res. B). card(.) stands for the number of elements in a set.

7.4 Results

The data available for the BCI competition is already partitioned in a training set of 316 trials and a testing set of 100 trials. All results presented below are acquired by training the classifier with a ten fold cross-validation. Once the training step is achieved, the trained classifier is used on the test set.

7.4.1 Results with electrodes

There is only one parameter to tune which is the number of spatial filters used. Between 2 and 6 features, the results are comparable and yield a 85% accurate classi-

fication on the test set. Training and validation are slightly better with 6 filters (table 7.1).

filters	validation	test
1	83,51 $\pm$ 11,39	83
2	84,19 $\pm$ 10,94	85
3	84,16 $\pm$ 6,61	85
6	**84,54 $\pm$ 9.30**	**85**

Table 7.1 Classification results of electrode-based bereitschaft potential features when increasing the number of CSP filters.

We also used a method to prevent outliers into the filters. This method provides median filters [241]. Results using median filters are comparable with results obtained with normal CSP filters (table 7.2)

filters	validation	test
1	84,49 $\pm$ 9,40	83
2	**84,49 $\pm$8,06**	**85**
3	83,22 $\pm$6,65	85
6	84,20 $\pm$ 13.05	86

Table 7.2 Classification results of electrode-based bereitschaft potential features when increasing the number of CSP median filters.

7.4.1.1 Discussion

Only Bereitschaft potential features were used and classification results are comparable to the best results obtained by the winner of the competition (84%) who used bereitschaft features combined to frequency features with a CSP filtering. Furthermore these results outperform those obtained by [224] who used a conjoint Bereitschaft and frequency features ranked by mutual information. However, [224] did not use any spatial filtering. Furthermore, the results presented by [244] based on frequency features ranked by the DP are better (87 %), however they did not use the downsampled version of the dataset but the original 1000Hz data which seemingly yields better frequency features than the downsampled version. We can expect that adding frequency features to our analysis will improve the results. Furthermore, using normal filters or median filters does not seem to influence much the results.

7.4.2 Results with the inverse problem

The introduction of inverse problem methods into BCI applications adds three more parameters to tune. First, the method itself (Minimum Norm, Tikhonov Regularization with or without Location Priors, Laplacian etc..). Then the parameter λ which gives the degree of confidence in the model or in the data. Finally, the last parameter is the number of features sent to the classifier. The results are surprisingly quite insensitive to the first two parameters. Furthermore, very few features are needed to achieve comparable results to the one obtained with the electrodes.

7.4.2.1 Minimum Norm

We try here to assess the influence of CSP filtering before applying a linear inverse transform. Therefore we computed the Minimum Norm inverse method with and without a CSP filtering

Minimum Norm Features extracted from sources obtained with a minimum norm solution yielded 83% accuracy. Interestingly, five voxels are sufficient to obtain this result (Table 7.3)

voxels	validation	test
5	**85,05 $\pm$ 11,45**	**83**
10	84.14 $\pm$ 8,10	83
20	82,93 $\pm$ 9.85	83
30	83,54 $\pm$ 7.72	83
40	80,67 $\pm$ 10.23	82
50	76,63 $\pm$ 12.14	66

Table 7.3 Classification results of bereitschaft potential features extracted from source reconstructed data with a minimum norm solution. The varying parameter is the number of voxels used based on their discriminant power

Minimum Norm with CSP filtering We tested the Minimum Norm when refiltering the scalp data using 3 CSP filters. The results obtained are similar to those obtained with the electrodes. A small number of voxels is sufficient to achieve a good accuracy (Table 7.4).

voxels	validation	test
5	**84,53 ± 10,28**	**83**
10	84,50 ± 9,52	85
20	83,55 ± 11,86	84
30	83,51 ± 8,38	86
40	81,64 ± 10,71	81
50	74,38 ± 11,93	69

Table 7.4 Classification results of bereitschaft potential features extracted at the source level. Minimum norm solution is used after CSP filtering of scalp data. Varying parameter is the number of voxels used based on their discriminant power

7.4.2.2 Laplacian

Using a laplacian prior adds an additional parameter λ. Varying λ has little influence on the classification results. The best classification obtained with this method is 84% using 20 voxels and $\lambda = 1000$ (Table 7.5).

voxels	validation	test	λ
10	83,85 ± 10,43	84	0.01
10	83,52 ± 10,11	84	100
10	83,54 ± 10,87	82	1000
20	83,88 ± 11,13	82	0.01
20	83,83 ± 10,34	84	100
20	**84,45 ± 9,92**	**84**	1000

Table 7.5 Classification results of bereitschaft potential features extracted at the source level using a laplacian inverse solution.

7.5 Conclusion

Classification of bereitschaft potential features extracted both at the scalp and at the source level were computed. Spatially filtered features at the scalp level yielded similar and better results (85% correct classifications) than the winner of the BCI competition (84% correct classifications). At the source level, both the minimum norm solution and the laplacian solution gave similar results on the training and validation set but underperformed by 2% classification accuracy compared to the scalp analysis. Interestingly, when spatially filtering the data with aggregate CSP filters of both classes, classification rates improved at the source level. Although results obtained with the source reconstruction approach is comparable to the best result at

the time of the competition, no improvement could be demonstrated over the traditional and widely used CSP method. This can be explained by the coarse head model approximation which was used and by the limited number of electrodes used for the recording. Furthermore, the transformation from the scalp space to the source space, while possibly generating more discriminant features, increases considerably the amount of data thus requiring an additional feature selection step. These results are also limited by the fact that only bereitschaft potential features were used. Including features such as band power might have added further improvements. Data from only one subject was analyzed, consistency of the results should be assessed on a larger database. In the current study, the discriminant power approach should be replaced by state of the art machine learning techniques. While this could improve classification accuracy, it might however increase the complexity and computational load of source reconstruction approach which therefore might not be suited for real time BCI approaches. Finally, CSP is optimized for two-class problems but there are currently no equivalent of CSP for n-class problems (n>2). In such cases, classification accuracies might benefit from a source reconstruction approach.

Conclusions and future work

8

Cerebellum-type organization can never give rise to conscious experience, no matter the size. On the other hand, the cerebral cortex, with its self-organized, persistent oscillations and global computational principles, can create qualities fundamentally different from those provided by input-dependent local processing. It may turn out that the rhythms of the brain are also the rhythms of the mind[1]

In this thesis we have presented our work on electrophysiological correlates of consciousness in DOC patients and healthy subjects.

First, we investigated mechanisms of ketamine induced loss of consciousness in healthy subjects. Indeed anaesthetic agents provide a unique opportunity to follow in real time fluctuations of consciousness. Our study, using state of the art dynamical causal modelling, demonstrated that loss of consciousness under ketamine seemingly involves a frontal intra-cortical loop. Interestingly this mechanism differs from propofol induced loss of consciousness which was associated with changes in thalamo-cortical interactions [206]. Hence, there is no single substrate for consciousness which can be viewed as an integrated global network requiring correct functioning of all it's part. Breaking down parts of the network breaks down the entire network, only leaving islands of preserved functional networks.

Second, power spectra and connectivity patterns were extracted from resting state EEG of 31 DOC patients. The power spectra measurements confirmed visual assessments in the sense that patients with minimal consciousness displayed faster oscillating patterns than patients in vegetative/unresponsive wakefulness. VS/UWS patients had slower oscillations. Connectivity assessments could also disentangle VS/UWS from MCS patients at the group level, MCS patients displaying stronger connections in the alpha and theta band in front to back and inter hemispheric connections. Although these results are encouraging, individual classification of patients is not yet possible. Further improvements will require multimodal measure-

[1] György Buzsáki, Rhythms of the Brain, 2006 [245]

ments taking advantage of the spatial resolution of fMRI and PET, and the time resolution of HD-EEG. Integration of features extracted from these brain imaging techniques will provide a unique window for brain assessments, double-crossing underlying physiological mechanisms, the haemodynamic response, the metabolic activity and electric current generation. We contributed to a first attempt towards this goal by comparing results obtained with the three modalities in two case studies of patients with asymmetrical brain damage [246].

Finally, the use of source reconstruction methods were investigated and compared to CSP, a renowned method in the BCI field. Results obtained with the two approaches gave similar results but the CSP approach is easier to use and seems more suited. However, high density EEG recordings, recommended for better accuracy of the source reconstructions were not used. Moreover state of the art machine learning approaches could have improved feature extraction and classification in the source space. These improvements should be examined in the future.

Interestingly, while localization of brain function with a source reconstruction approach helped us identify regions involved during ketamine loss of consciousness, it did not improve classification rates in a brain computer interface application. We explain these seemingly contradictory results by the inherent differences in the two study. Indeed, in the ketamine experiment we used the source reconstruction approach to *localize* brain function while in the BCI task the aim was to *classify* brain function. Furthermore, while ketamine induced visually drastic changes in the EEG of the subject, movement preparation as studied in the BCI task only induces very subtle changes. Finally, even if results were not improved compared to CSP, the source reconstruction approach presented in chapter 7 is computationally viable as it mainly involves a multiplication of the data with a precomputed matrix. Hence it offers an alternative to the CSP approach.

Epilogue

EEG is an interdisciplinary field that can hardly be entirely self taught. Correct interpretation of results require a sound understanding of a large panel of skills. The modern EEG user should have knowledge of the rich oscillatory content of EEG signals and of their underlying physiological basis, apprehend parameter tuning of the qEEG method used and a strong statistical background to find significant attributes deciphering the different states of consciousness. Furthermore, integration of the different brain imaging modalities into a multimodal assessment will also require knowledge of fMRI and PET. Therefore a unifying course on the brain and the different windows to view it's functionalities should and hopefully would yield interest for students from different backgrounds.

As discussed in section 4.3, the view that we have of the brain is inspired by the society we live in. In future years, with the advent of cloud computing we could imagine not only studying neuron networks, but also brain networks ! BCIs might become Brain to Brain Computer Interfaces and in a sense fulfill the dream of Berger to find a mental energy allowing direct communication between human brains.

List of Publications

Journal papers

- R. Lehembre, O. Gosseries, Z. Lugo, Z. Jedidi, C. Chatelle, B. Sadzot, S. Laureys, Q. Noirhomme, "Electrophysiological investigations of brain function in coma, vegetative and minimally conscious patients" *Archives Italiennes de Biologie*, 2012, in press.
- R. Lehembre, M-A. Bruno, A. Vanhaudenhuyse, C. Chatelle, V. Cologan, Y. Leclercq, A. Soddu, B. Macq, S. Laureys, Q. Noirhomme, "Resting state EEG in disorders of consciousness: differences in spectral power and connectivity measures in vegetative/unresponsive and minimally conscious states" *Functional Neurology*, 2012, Jan-Mar;27(1):40-47.
- R. Lehembre, O. Gosseries, R. Moran, M. Massimini, M. Rosanova, A.Vanhaudenhuyse, M.A. Bruno, V. Bonhomme, J.F. Brichant, P. Boveroux, A.Soddu, C.Phillips, Q.Noirhomme, S.Laureys, M.Boly "Electrophysiological correlates of ketamine induced loss of responsiveness", , 2012, to be submitted.
- M.A. Bruno, D. Fernández-Espejo, R. Lehembre, L. Tshibanda, A. Vanhaudenhuyse, O. Gosseries, E. Lommers, M Napolitani, Q. Noirhomme, M. Boly, M. Papa, A. Owen, P. Maquet, S. Laureys, A. Soddu, "Multimodal neuroimaging in patients with disorders of consciousness showing "functional hemispherectomy"", *Progress in Brain Research*, 2011 193:323-333.
- O. Gosseries, C. Schnakers, D. Ledoux, A. Vanhaudenhuyse, M-A. Bruno, A. Demertzi, Q. Noirhomme, R. Lehembre, P. Damas, S. Goldman, E. Peeters, G. Moonen, S. Laureys, "Automated EEG entropy measurements in coma, vegetative state/unresponsive wakefulness syndrome and minimally conscious state", *Functional Neurology*, 2011 Jan-Mar;26(1):25-30.
- Q. Noirhomme, A. Soddu, R. Lehembre, A. Vanhaudenhuyse, P. Boveroux, M. Boly, S. Laureys, "Brain connectivity in pathological and pharmacological coma", *Frontiers in Systems Neuroscience*, 2010 Dec 20;4:160

Conference papers

- R. Lehembre, O. Gosseries, R. Moran, M. Massimini, M. Rosanova, A. Vanhaudenhuyse, M.A. Bruno, V. Bonhomme, J.F. Brichant, P. Boveroux, A. Soddu, C. Phillips, Q. Noirhomme, S. Laureys, M. Boly, "Electrophysiological correlates of ketamine-induced behavioral unresponsiveness", in *HBM 2012, Beijing, China, June 2012*

- D. Lesenfants, N. Partoune, A. Soddu, R. Lehembre, G. Müller-Putz, S. Laureys, Q. Noirhomme, "Design of a covert SSVEP-based BCI for the diagnosis of unresponsive patients", in *Proceedings of the 5th Internationnal Brain Computer Interface Workshop and Training Course 2011, Graz University of Technology, Austria, 2011*

- R. Lehembre, M-A. Bruno, V. Cologan, C. Chatelle, A. Vanhaudenhuyse, Y. Leclercq, B. Macq, A. Soddu, S. Laureys, Q. Noirhomme, "Resting-state EEG functional connectivity in vegetative and minimally conscious states", in *HBM 2010, Barcelona, Spain, May 2010*,

- C. Erkut, J-J. Filatriau, R.Lehembre, I. Ekman, "Sonic Interaction Design with Physiological Interfaces in a Workshop Setting", in *Proceedings of the CHI'08 Sonic Interaction Design workshop, Florence, Italy, 2008*,

- R. Lehembre, C. Mühl, U. Gundogdu, A. Sayin, M. Soleymani, C. Erkut "Auditory vs Visual Feedback in an Asynchronous Brain-Computer-Interface", in *MAIA Workshop 'BCI Meets Robotics: Challenging Issues in Brain-Computer Interaction and Shared Control', Leuven, Belgium, November 2007*

- B. Arslan, A. Brouse, J. Castet, J-J. Filatriau, R. Lehembre, Q. Noirhomme, C. Simon, "A real-time music synthesis environment driven with biological signals", in *Proceedings of the 2006 IEEE International Conference on Acoustics, Speech and Signal Processing (ICASSP'06), Toulouse, France, 2006*

- J-J. Filatriau, R. Lehembre, Q. Noirhomme, C. Simon, B. Arslan, A. Brouse, J. Castet, "Using physiological signals for sound creation", in *Proceedings of the 11th International Conference Speech and Computer (SPECOM'06), Saint-Petersburg, Russia, 2006*

- R. Lehembre, Q. Noirhomme, B. Macq, "Inverse Problem Applied to BCI's : Keeping Track of the EEG's Brain Dynamics Using Kalman Filtering", in *Proceedings of the 3rd Internationnal Brain Computer Interface Workshop and Training Course 2006, Graz University of Technology, Austria, 2006*

Book Chapters

- Q. Noirhomme, R. Lehembre, "Electrophysiology and disorders of consciousness", in "Coma and disorders of consciousness", C. Schnakers, S. Laureys (eds), Springer, 2012

Workshop Proceedings

- M. Benovoy, A. Brouse, T. Corcoran, H. Drayson, C. Erkut, J-J. Filatriau, C. Frisson, C. Gundogdu, B. Knapp, R. Lehembre, C. Müehl, M.A. Ortiz Pérez, A. Sayin, K. Tahiroglu, "Audiovisual content generation controlled by physiological signals for clinical and artistic applications," in *Proceedings of the 3rd summer workshop on multimodal interfaces (eNTERFACE'07), Istanbul, Turkey, 2007*,

- A. Brouse, J-J. Filatriau, K. Gaitanis, R. Lehembre, B. Macq, E. Miranda, A. Zenon, "An instrument of sound and visual creation driven by biological signals" in *Proceedings of the 2nd summer workshop on multimodal interfaces (eNTERFACE'06), Dubrovnik, Croatia, 2006*,

- B. Arslan, A. Brouse, J. Castet, J-J. Filatriau, R. Lehembre, Q. Noirhomme, C. Simon, "A biologically-driven musical instrument" in *Proceedings of the 1st summer workshop on multimodal interfaces (eNTERFACE'05), Mons, Belgium, 2005*,

Bibliography

[1] G. Nolte, O. Bai, L. Wheaton, Z. Mari, S. Vorbach, and M. Hallett, "Identifying true brain interaction from eeg data using the imaginary part of coherency," *Clinical Neurophysiology*, vol. 115, pp. 2292–2307, 2004.

[2] R. Moran, S. Kiebel, K. Stephan, R. Reilly, J. Daunizeau, and K. Friston, "A neural mass model of spectral responses in electrophysiology," *NeuroImage*, vol. 37, pp. 706–720, 2007.

[3] R. Frackowiak, K. Friston, C. Frith, R. Dolan, C. Price, S. Zeki, J. Ashburner, and W. Penny, *Human Brain Function*, 2nd ed. Academic Press, 2003.

[4] H. Berger, "Uber das elektrenkephalogramm des menschen," *European Archives of Psychiatry and Clinical Neuroscience*, vol. 87, no. 1, pp. 527–570, 1929.

[5] R. Plonsey, *Bioelectric phenomena*. New York: McGraw-Hill, 1969.

[6] R. Lehembre, O. Gosseries, Z. Lugo, Z. Jedidi, C. Chatelle, B. Sadzot, S. Laureys, and Q. Noirhomme, "Electrophysiological investigations of brain function in coma, vegetative and minimally conscious patients," *Archives Italiennes de Biologie*, 2012, in press.

[7] S. Laureys, G. Celesia, F. Cohadon, J. Lavrijsen, J. Leon-Carrion, W. Sannita, L. Sazbon, E. Schmutzhard, K. von Wild, A. Zeman, G. Dolce, and the European Task Force on Disorders of Consciousness, "Unresponsive wakefulness syndrome: a new name for the vegetative state or apallic syndrome," *BMC Medicine*, vol. 8, no. 1, p. 68, 2010.

[8] J.-M. Guérit, "Electroencephalography: the worst traditionally recommended tool for brain death confirmation," *Intensive Care Medicine*, vol. 33, pp. 9–10, 2007, 10.1007/s00134-006-0430-0.

[9] E. Zandbergen, R. de Haan, C. Stoutenbeek, J. Koelman, and A. Hijdra, "Systematic review of early prediction of poor outcome in anoxicischaemic coma," *The Lancet*, vol. 352, no. 9143, pp. 1808–1812, 1998.

[10] J. Giacino, S. Ashwal, N. Childs, M. R. Cranford, B. Jennett, D. Katz, J. Kelly, J. Rosenberg, J. Whyte, R. Zafonte, and N. Zasler, "The minimally conscious state : Definition and diagnostic criteria," *Neurology*, vol. 58, no. 3, pp. 349–353, 2002.

[11] J. T. Giacino, K. Kalmar, and J. Whyte, "The jfk coma recovery scale-revised: measurement characteristics and diagnostic utility," *Arch Phys Med Rehabil*, vol. 85, no. 12, pp. 2020–2029, 2004.

[12] C. Schnakers, A. Vanhaudenhuyse, J. Giacino, M. Ventura, M. Boly, S. Majerus, G. Moonen, and S. Laureys, "Diagnostic accuracy of the vegetative and minimally conscious state: Clinical consensus versus standardized neurobehavioral assessment," *BMC Neurology*, vol. 9, no. 35, 2009.

[13] R. Thatcher, "Validity and reliability of quantitative electroencephalography (qeeg)," *Journal of Neurotherapy*, vol. 14, pp. 122–152, 2010.

[14] J. R. Wolpaw, N. Birbaumer, D. J. McFarland, G. Pfurtscheller, and T. M. Vaughan, "Brain-computer interfaces for communication and control," *Clinical Neurophysiology*, vol. 113, pp. 767–791, 2002.

[15] N. Birbaumer and L. G. Cohen, "Brain-computer-interfaces(bci): Communication and restoration of movement in paralysis," *The Journal of Physiology*, vol. 579, pp. 621–636, 2007.

[16] D. L. Schomer, "The normal eeg in an adult," *The Clinical Neurophysiology Primer*, pp. 57–71, 2007.

[17] E. Niedermeyer and F. Da Silva, *Electroencephalography: basic principles, clinical applications, and related fields*. Lippincott Williams & Wilkins, 2005.

[18] P. W. Kaplan, D. Genoud, T. W. Ho, and P. Jallon, "Etiology, neurologic correlations, and prognosis in alpha coma," *Clinical Neurophysiology*, vol. 110, pp. 205–213, 1999.

[19] R. P. Brenner, "The interpretation of the eeg in stupor and coma," *Neurologist*, vol. 11, no. 5, pp. 271–284, 2005.

[20] O. N. Markand, "Electroencephalogram in "locked-in" syndrome," *Electroencephalography and Clinical Neurophysiology*, vol. 40, no. 5, pp. 529 – 534, 1976.

[21] J. Patterson and M. Grabois, "Locked-in syndrome: a review of 139 cases," *Stroke*, vol. 17, no. 4, pp. 758–764, 1986.

[22] D. Jacome and D. Morilla-Pastor, "Unreactive eeg : pattern in locked-in syndrome," *Clinical Electroencephalography*, vol. 21, no. 1, pp. 31–36, 1990, anglais.

[23] C. Bassetti, J. Mathis, and C. Hess, "Multimodal electrophysiological studies including motor evoked potentials in patients with locked-in syndrome: report of six patients," *British Medical Journal*, vol. 57, no. 11, p. 1403, 1994.

[24] E. Gutling, S. Isenmann, and W. Wichmann, "Electrophysiology in the locked-in-syndrome," *Neurology*, vol. 46, no. 4, pp. 1092–1101, 1996.

[25] O. Gosseries, M. Bruno, A. Vanhaudenhuyse, S. Laureys, and C. Schnakers, *The Neurology of Consciousness: Cognitive Neuroscience and Neuropathology*. Oxford, Elsevier, 2009, ch. Consciousness in the Locked-in Syndrome, pp. 191–203.

[26] A. M. Husain, "Electroencephalographic assessment of coma," *Journal of Clinical Neurophysiology*, vol. 23, no. 3, pp. 208–220, 2006.

[27] A. O. Rossetti, L. A. Urbano, F. Delodder, P. W. Kaplan, and M. Oddo, "Prognostic value of continuous eeg monitoring during therapeutic hypothermia after cardiac arrest," *Critical Care Medicine*, vol. 14, 2010.

[28] V. Synek, "Prognostically important eeg coma patterns in diffuse anoxic and traumatic encephalopathies in adults," *Journal of Clinical Neurophysiology*, vol. 5, pp. 161–174, 1988.

[29] G. B. Young, R. S. McLachlan, J. Kreeft, and J. Demelo, "An electroencephalographic classification for coma," *Canadian Journal of Neurological Science*, vol. 24, no. 4, pp. 320–325, 1997.

[30] L. Hirsch, R. Brenner, F. Drislane, P. Kaplan, K. Jordan, S. Herman, S. LaRoche, B. Young, T. Bleck, M. Scheuer, and R. Emerson, "The acns subcommittee on research terminology for continuous eeg monitoring: proposed standardized terminology for rhythmic and periodic eeg patterns encountered in critically ill patients," *Journal of Clinical Neurophysiology*, vol. 22, no. 2, pp. 128–135, 2005.

[31] V. Kulkarni, K. Lin, and S. Benbadis, "Eeg findings in the persistent vegetative state," *Journal of Clinical Neurophysiology*, vol. 24, no. 6, p. 433, 2007.

[32] E. A. Thenayan, M. Savard, M. D. Sharpe, L. Norton, and B. Young, "Electroencephalogram for prognosis after cardiac arrest," *Journal of Critical Care*, vol. 25, pp. 300–304, 2010.

[33] S. Bagnato, C. Boccagni, C. Prestandrea, A. Sant'Angelo, A. Castiglione, and G. Galardi, "Prognostic value of standard eeg in traumatic and non-traumatic disorders of consciousness following coma," *Clinical Neurophysiology*, vol. 121, no. 3, pp. 274–280, March 2010.

[34] M. Berkhoff, F. Donati, and C. Bassetti, "Postanoxic alpha (theta) coma: a reappraisal of its prognostic significance," *Clinical Neurophysiology*, vol. 111, no. 2, pp. 297 – 304, 2000.

[35] M. Valente, F. Placidi, A. J. Oliveira, A. Bigagli, I. Morghen, R. Proietti, and G. L. Gigli, "Sleep organization pattern as a prognostic marker at the subacute stage of post-traumatic coma," *Clinical Neurophysiology*, vol. 113, no. 11, pp. 1798 – 1805, 2002.

[36] P. L. Nunez, R. Srinivasan, A. F. Westdorp, R. S. Wijesinghe, D. M. Tucker, R. B. Silberstein, and P. J. Cadusch, "Eeg coherency i: statistics, reference electrode, volume conduction, laplacians, cortical imaging, and interpretation at multiple scales," *Electroencephalography and clinical neurophysiology*, vol. 103, pp. 499–515, 1997.

[37] P. L. Nunez, R. B. Silberstein, Z. Shi, M. R. Carpenter, R. Srinivasan, D. M. Tucker, S. M. Doran, P. J. Cadusch, and R. S. Wijesinghe, "Eeg coherency ii: experimental comparisons of multiple measures," *Clinical Neurophysiology*, vol. 110, pp. 469–486, 1999.

[38] P. Comon, "Independent component analysis, a new concept," *Signal processing*, vol. 36, no. 3, pp. 287–314, 1994.

[39] S. Tong and N. V. Thakor, Eds., *Quantitative EEG Analysis Methods and Clinical Applications*. Artech House, 2009.

[40] J.Leon-Carrion, J.F.Martin-Rodriguez, J. Damas-Lopez, J. B. y Martina, and M. Dominguez-Morales, "Brain function in the minimally conscious state: A quantitative neurophysiological study," *Clinical Neurophysiology*, vol. 119, pp. 1506–1514, 2008.

[41] R. Lehembre, M.-A. Bruno, A. Vanhaudenhuyse, C. Chatelle, V. Cologan, Y. Leclercq, A. Soddu, B. Macq, S. Laureys, and Q. Noirhomme, "Resting state eeg study of comatose patients: a connectivity and frequency analysis to find differences between vegetative and minimally conscious states," *Functional Neurology*, vol. 27, no. 1, pp. 41–47, 2012.

[42] J. W. Johansen and P. S. Sebel, "Development and clinical application of electroencephalographic bispectrum monitoring," *Anesthesiology*, vol. 93, no. 5, pp. 1336–1344, 2000.

[43] C. Rosow and P. Manberg, "Bispectral index monitoring." *Anesthesiol Clin North America*, vol. 19, no. 4, pp. 947–966, 2001.

[44] I. Rampil, "A primer for eeg signal processing in anesthesia," *Anesthesiology*, vol. 89, no. 4, p. 980, 1998.

[45] Q. Noirhomme, M. Boly, V. Bonhomme, P. Boveroux, C. Phillips, P. Peigneux, A. Soddu, A. Luxen, G. Moonen, P. Maquet, and S. Laureys, "Bispectral index correlates with regional cerebral blood flow during sleep in distinct cortical

and subcortical structures in humans," *Archives Italiennes de Biologie*, vol. 147, pp. 51–57, 2009.

[46] M. Gill, S. M. Green, and B. Krauss, "Can the bispectral index monitor quantify altered level of consciousness in emergency department patients?" *Academic Emergency Medicine*, vol. 10, no. 2, pp. 175–179, 2003.

[47] C. Schnakers, D. Ledoux, S. Majerus, P. Damas, F. Damas, B. Lambermont, M. Lamy, M. Boly, A. Vanhaudenhuyse, G. Moonen, and S. Laureys, "Diagnostic and prognostic use of bispectral index in coma, vegetative state and related disorders," *Brain Injury*, vol. 22, no. 12, pp. 926–931, November 2008.

[48] O. Gosseries, C. Schnakers, D. Ledoux, A. Vanhaudenhuyse, M.-A. Bruno, A. Demertzi, Q. Noirhomme, R. Lehembre, P. Damas, S. Goldman, E. Peeters, G. Moonen, and S. Laureys, "Automated eeg entropy measurements in coma, vegetative state/unresponsive wakefulness syndrome and minimally conscious state," *Functional Neurology*, vol. 26, no. 1, pp. 25–30, 2011.

[49] M. Sarà and F. Pistoia, "Complexity loss in physiological time series of patients in a vegetative state." *Nonlinear Dynamics Psychol Life Sci*, vol. 14, no. 1, pp. 1–13, 2010.

[50] D. Y. Wu, G. Cai, Y. Yuan, L. Liu, G. qing Li, W. qun Song, and M. bin Wang, "Application of nonlinear dynamics analysis in assessing unconsciousness: A preliminary study," *Clinical Neurophysiology*, 2010.

[51] E. Pereda, R. Q. Quiroga, and J. Bhattacharya, "Nonlinear multivariate analysis of neurophysiological signals," *Progress in Neurobiology*, vol. 77, pp. 1–37, 2005.

[52] S. Laureys, "The neural correlate of (un) awareness: lessons from the vegetative state," *Trends in cognitive sciences*, vol. 9, no. 12, pp. 556–559, 2005.

[53] R. Thatcher, D. Cantor, R. McAlaster, F. Geisler, and P. Krause, "Comprehensive predictions of outcome in closed head-injured patients the development of prognostic equations," *Ann N Y Acad Sci*, vol. 620, pp. 82–101, 1991.

[54] M. P. Davey, J. D. Victor, and N. D. Schiff, "Power spectra and coherence in the eeg of a vegetative patient with severe asymmetric brain damage," *Clinical Neurophysiology*, vol. 111, pp. 1949–1954, 2000.

[55] N. D. Schiff, J. T. Giacino, K. Kalmar, J. D. Victor, K. Baker, M. Gerber, B. Fritz, B. Eisenberg, J. O/'Connor, E. J. Kobylarz, S. Farris, A. Machado, C. McCagg, F. Plum, J. J. Fins, and A. R. Rezai, "Behavioural improvements with thalamic stimulation after severe traumatic brain injury," *Nature*, vol. 448, no. 7153, pp. 600–603, Aug. 2007.

[56] C. J. Stam, G. Nolte, and A. Daffertshofer, "Phase lag index: Assessment of functional connectivity from multi channel eeg and meg with diminished bias from common sources," *Human Brain Mapping*, vol. 28, pp. 1178–1193, 2007.

[57] L. Pollonini, S. Pophale, N. Situ, M. Wu, R. Frye, J. Leon-Carrion, and G. Zouridakis, "Information communication networks in severe traumatic brain injury," *Brain Topography*, 2010.

[58] C. M. Michel, M. M. Murray, G. Lantz, S. Gonzalez, L. Spinelli, and R. G. de Peralta, "Eeg source imaging," *Clinical Neurophysiology*, vol. 115, no. 10, pp. 2195–2222, 2004.

[59] C. Babiloni, M. Sarà, F. Vecchio, F. Pistoia, F. Sebastiano, P. Onorati, G. Albertini, P. Pasqualetti, G. Cibelli, P. Buffo, and P. M. Rossini, "Cortical sources of resting-state alpha rhythms are abnormal in persistent vegetative state patients," *Clinical Neurophysiology*, vol. 120, pp. 719–729, 2009.

[60] S. J. Luck, *An Introduction to Event-Related Potential Technique*, 2005.

[61] S. Laureys, F. Perrin, C. Schnakers, M. Boly, and S. Majerus, "Residual cognitive function in comatose, vegetative and minimally conscious states," *Current Opinion in Neurology*, vol. 18, pp. 726–733, 2005.

[62] H. auditory evoked potentials. I Evaluation of components., "T.w. picton and s.a hillyard and h.i krausz and r. galambos," *Electroencephalography and clinical Neurophysiology*, vol. 36, no. 2, pp. 179–190, 1974.

[63] C. Fischer, V. Ibanez, C. Jourdan, A. Grau, F. Mauguiere, and F. Artru, "Early and middle latency auditory evoked potentials and somatosensory evoked potentials in the vital and functional prognosis of severe brain injuries in intensive care," *Agressologie*, vol. 29, no. 5, pp. 359–363, 1988.

[64] L. García-Larrea, F. Artru, O. Bertrand, J. Pernier, and F. Mauguière, "The combined monitoring of brain stem auditory evoked potentials and intracranial pressure in coma. a study of 57 patients." *Journal of Neurology, Neurosurgery & Psychiatry*, vol. 55, no. 9, pp. 792–798, 1992.

[65] J. Guérit, M. de Tourtchaninoff, L. Soveges, and P. Mahieu, "The prognostic value of three-modality evoked potentials (tmeps) in anoxic and traumatic comas," *Clinical Neurophysiology*, vol. 23, no. 2-3, pp. 209 – 226, 1993.

[66] C. Fischer, J. Luaute, F. Salord, C. Jourdan, and D. Morlet, *Valeur pronostique des PEA au stade aigu du coma. PE auditifs precoces,de latence moyenne, tardifs et negativite de discordance (MMN)*. Marseille, Solal, 2001, vol. L'evaluation neurophysiologique des comas, de la mort encephalique et des etats vegetatifs., pp. 169–181.

[67] B. Cant, A. L. Hume, J. Judson, and N. Shaw, "The assessment of severe head injury by short-latency somatosensory and brain-stem auditory evoked potentials," *Electroencephalography and Clinical Neurophysiology*, vol. 65, no. 3, pp. 188–195, May 1986.

[68] H. L. Lew, S. Dikmen, J. Slimp, N. Temkin, E. H. Lee, D. Newell, and L. R. Robinson, "Use of somatosensory-evoked potentials and cognitive event-related potentials in predicting outcomes of patients with severe traumatic brain injury," *American Journal of Physical Medicine and Rehabilitation*, vol. 82, no. 1, pp. 53–61, 2003.

[69] F. Logi, C. Fischer, L. Murri, and F. Mauguière, "The prognostic value of evoked responses from primary somatosensory and auditory cortex in comatose patients," *Clinical Neurophysiology*, vol. 114, no. 9, pp. 1615–1627, Sept 2003.

[70] L. R. Robinson, P. J. Micklesen, D. L. Tirschwell, and H. L. Lew, "Predictive value of somatosensory evoked potentials for awakening from coma," *Critical Care Medicine*, vol. 31, no. 3, pp. 960–967, 2003.

[71] L. R. Robinson and P. J. Micklesen, "Somatosensory evoked potentials in coma prognosis." *Physical medicine and rehabilitation clinics of North America*, vol. 15, no. 1, pp. 43–61, 2004.

[72] C. De Giorgio, A. Rabinowicz, and P. Gott, "Predictive value of p300 event-related potentials compared with eeg and somatosensory evoked potentials in non-traumatic coma." *Acta Neurol Scand*, vol. 87, no. 5, pp. 423–427, 1993.

[73] B. G. Carter and W. Butt, "Review of the use of somatosensory evoked potentials in the prediction of outcome after severe brain injury," *Critical Care Medicine*, vol. 29, no. 1, pp. 178–186, 2001.

[74] A. Amantini, A. Grippo, S. Fossi, C. Cesaretti, A. Piccioli, A. Peris, A. Ragazzoni, and F. Pinto, "Prediction of awakening and outcome in prolonged acute coma from severe traumatic brain injury: evidence for validity of short latency seps," *Clinical Neurophysiology*, vol. 116, pp. 229–235, 2005.

[75] C. Fischer, J. Luauté, C. Némoz, D. Morlet, G. Kirkorian, and F. Mauguière, "Improved prediction of awakening or nonawakening from severe anoxic coma using tree-based classification analysis *," *Critical Care Medicine*, vol. 34, no. 5, pp. 1520–1524, 2006.

[76] A. Vanhaudenhuyse, S. Laureys, and F. Perrin, "Cognitive event-related potentials in comatose and post-comatose states," *Neurocritical Care*, vol. 8, pp. 262–270, 2008, 10.1007/s12028-007-9016-0.

[77] J. Daltrozzo, N. Wioland, V. Mutschler, and B. Kotchoubey, "Predicting coma and other low responsive patients outcome using event-related brain potentials: A meta-analysis," *Clinical Neurophysiology*, vol. 118, pp. 606–614, 2007.

[78] S. A. Hillyard, R. F. Hink, V. L. Schwent, and T. W. Picton, "Electrical signs of selective attention in the human brain," *Science*, vol. 182, no. 4108, pp. 177–180, 1973.

[79] R. Näätänen and T. Picton, "The n1 wave of the human electric and magnetic response to sound: A review and an analysis of the component structure," *Psychophysiology*, vol. 24, no. 4, pp. 375–425, 1987.

[80] H. L. Lew, S. Dikmen, J. Slimp, N. Temkin, E. H. Lee, D. Newell, and L. R. Robinson, "Use of somatosensory-evoked potentials and cognitive event-related potentials in predicting outcomes of patients with severe traumatic brain injury," *American Journal of Physical Medicine and Rehabilitation*, vol. 82, no. 1, pp. 53–61, 2003.

[81] C. Fischer, J. Luauté, P. Adeleine, and D. Morlet, "Predictive value of sensory and cognitive evoked potentials for awakening from coma," *Neurology*, vol. 63, no. 4, pp. 669–673, 2004.

[82] I. Glass, L. Sazbon, and Z. Groswasser, "Mapping "cognitive" event-related potentials in prolonged postcoma unawareness state," *Clinical Electroencephalography*, vol. 29, no. 1, pp. 19–30, 1998.

[83] J.-M. Guérit, D. Verougstraete, M. de Tourtchaninoff, D. Debatisse, and C. Witdoeckt, "Erps obtained with the auditory oddball paradigm in coma and altered states of consciousness: clinical relationships, prognostic value, and origin of components," *Clinical Neurophysiology*, vol. 110, no. 7, pp. 1260–1269, July 1999.

[84] R. Naatanen, A. Lehtokoski, M. Lennes, M. Cheour, M. Huotilainen, A. Iivonen, M. Vainio, P. Alku, R. J. Ilmoniemi, A. Luuk, J. Allik, J. Sinkkonen, and K. Alho, "Language-specific phoneme representations revealed by electric and magnetic brain responses," *Nature*, vol. 385, no. 6615, pp. 432–434, Jan. 1997.

[85] K. Alho, "Cerebral generators of mismatch negativity (mmn) and its magnetic counterpart (mmnm) elicited by sound changes." *Ear Hear*, vol. 16, no. 1, pp. 38–51, 1995.

[86] N. M. Kane, S. H. Curry, C. A. Rowlands, A. R. Manara, T. Lewis, T. Moss, B. H. Cummins, and S. R. Butler, "Event-related potentials - neurophysiological tools for predicting emergence and early outcome from traumatic coma," *Intensive Care Medicine*, vol. 22, pp. 39–46, 1996, 10.1007/BF01728329.

[87] B. Kotchoubey, S. Lang, G. Mezger, D. Schmalohr, M. Schneck, A. Semmler, V. Bostanov, and N. Birbaumer, "Information processing in severe disorders of consciousness: Vegetative state and minimally conscious state," *Clinical Neurophysiology*, vol. 116, pp. 2441–2453, 2005.

[88] L. Naccache, L. Puybasset, R. Gaillard, E. Serve, and J.-C. Willer, "Auditory mismatch negativity is a good predictor of awakening in comatose patients: a fast and reliable procedure," *Clinical Neurophysiology*, vol. 116, no. 4, pp. 988–989, Apr. 2005.

[89] P. Qin, H. Di, X. Yan, S. Yu, D. Yu, S. Laureys, and X. Weng, "Mismatch negativity to the patient's own name in chronic disorders of consciousness," *Neuroscience Letters*, vol. 448, no. 1, pp. 24 – 28, 2008.

[90] V. Wijnen, G. van Boxtel, H. Eilander, and B. de Gelder, "Mismatch negativity predicts recovery from the vegetative state," *Clinical Neurophysiology*, vol. 118, pp. 597–605, 2007.

[91] J. Luauté, D. Maucort-Boulch, L. Tell, F. Quelard, T. Sarraf, J. Iwaz, D. Boisson, and C.Fischer, "Long-term outcomes of chronic minimally conscious and vegetative states," *Neurology*, vol. 75, pp. 246–252, 2010.

[92] S. Sutton, M. Braren, J. Zubin, and E. R. John, "Evoked-potential correlates of stimulus uncertainty," *Science*, vol. 150, no. 3700, pp. 1187–1188, 1965.

[93] F. Pegado, T. Bekinschtein, N. Chausson, S. Dehaene, L. Cohen, and L. Naccache, "Probing the lifetimes of auditory novelty detection processes," *Neuropsychologia*, vol. 48, no. 10, pp. 3145 – 3154, 2010.

[94] B. Kotchoubey and S. Lang, "Event-related potentials in an auditory semantic oddball task in humans," *Neuroscience Letters*, vol. 310, no. 23, pp. 93 – 96, 2001.

[95] L. Mazzini, M. Zaccala, F. Gareri, A. Giordano, and E. Angelino, "Long-latency auditory-evoked potentials in severe traumatic brain injury," *Arch Phys Med Rehabil*, vol. 82, no. 1, pp. 57–65, Jan. 2001.

[96] M. Marosi, T. Prevec, C. Masala, M. Bramanti, R. Giorganni, G. Luef, K. Berek, and L. Saltuari, "Event-related potentials in vegetative state," *Lancet*, vol. 341, no. 8858, pp. 1473–, June 1993.

[97] M. Signorino, S. D'Acunto, S. Cercaci, P. Pietropaoli, and F. Angeleri, "The p300 in traumatic coma: Conditioning of the odd-ball paradigm," *Journal of Psychophysiology*, vol. 11, pp. 59–70, 1997.

[98] F. Perrin, C. Schnakers, M. Schabus, C. Degueldre, S. Goldman, S. Bredart, M.-E. Faymonville, M. Lamy, G. Moonen, A. Luxen, P. Maquet, and S. Laureys,

"Brain response to one's own name in vegetative state, minimally conscious state, and locked-in syndrome," *Arch Neurol*, vol. 63, no. 4, pp. 562–569, 2006.

[99] C. Schnakers, F. Perrin, M. Schabus, S. Majerus, D. Ledoux, P. Damas, M. Boly, A. Vanhaudenhuyse, M.-A. Bruno, G. Moonen, and S. Laureys, "Voluntary brain processing in disorders of consciousness," *Neurology*, vol. 71, pp. 1614–1620, 2008.

[100] D. O'Mahony, M. Rowan, J. Walsh, and D. Coakley, "P300 as a predictor of recovery from coma," *Lancet*, vol. 336, no. 8725, pp. 1265–1266, Nov. 1990.

[101] P. S. Gott, A. L. Rabinowicz, and C. M. DeGiorgio, "P300 auditory event-related potentials in nontraumatic coma: Association with glasgow coma score and awakening," *Arch Neurol*, vol. 48, no. 12, pp. 1267–1270, 1991.

[102] C. Fischer, F. Dailler, and D. Morlet, "Novelty p3 elicited by the subject's own name in comatose patients," *Clinical Neurophysiology*, vol. 119, no. 10, pp. 2224 – 2230, 2008.

[103] M. Cavinato, U. Freo, C. Ori, M. Zorzi, P. Tonin, F. Piccione, and A. Merico, "Post-acute p300 predicts recovery of consciousness from traumatic vegetative state," *Brain Injury*, vol. 23, no. 12, pp. 973–980, 2009, pMID: 19831494.

[104] M. Kutas and S. Hillyard, "Reading senseless sentences: brain potentials reflect semantic incongruity," *Science*, vol. 207, no. 4427, pp. 203–205, 1980.

[105] M. E. Smith, J. M. Stapleton, and E. Halgren, "Human medial temporal lobe potentials evoked in memory and language tasks," *Electroencephalography and Clinical Neurophysiology*, vol. 63, no. 2, pp. 145 – 159, 1986.

[106] P. Hagoort, C. M. Brown, and T. Y. Swaab, "Lexical - semantic event - related potential effects in patients with left hemisphere lesions and aphasia, and patients with right hemisphere lesions without aphasia," *Brain*, vol. 119, no. 2, pp. 627–649, 1996.

[107] F. Perrin and L. Garcia-Larrea, "Modulation of the n400 potential during auditory phonological/semantic interaction," *Cognitive Brain Research*, vol. 17, no. 1, pp. 36 – 47, 2003.

[108] P. W. Schoenle and W. Witzke, "How vegetative is the vegetative state? preserved semantic processing in vs patients - evidence from n 400 event-related potentials," *NeuroRehabilitation*, vol. 19, no. 4, pp. 329–334, Jan 2004.

[109] B. Kotchoubey, J. Kaiser, V. Bostanov, W. Lutzenberger, and N. Birbaumer, "Recognition of affective prosody in brain-damaged patients and healthy

controls: A neurophysiological study using eeg and whole-head meg," *Cognitive, Affective, & Behavioral Neuroscience*, vol. 9, pp. 153–167, 2009, 10.3758/CABN.9.2.153.

[110] A. Kübler, *Brain-Computer Interfaces for Communication in Paralysed Patients and Implications for Disorders of Consciousness*. Oxford, Elsevier, 2009, ch. 17, pp. 217–233.

[111] J. del R. Millàn, R. Rupp, G. Mueller-Putz, R. Murray-Smith, C. Giugliemma, M. Tangermann, C. Vidaurre, F. Cincotti, A. Kubler, R. Leeb, C. Neuper, K. R. Mueller, and D. Mattia, "Combining brain-computer interfaces and assistive technologies: State-of-the-art and challenges," *Frontiers in Neuroscience*, vol. 4, no. 00161, 2010.

[112] C. Schnakers, F. Perrin, M. Schabus, R. Hustinx, S. Majerus, G. Moonen, M. Boly, A. Vanhaudenhuyse, M.-A. Bruno, and S. Laureys, "Detecting consciousness in a total locked-in syndrome: An active event-related paradigm," *Neurocase*, vol. 15, no. 4, pp. 271–277, 2009.

[113] T. A. Bekinschtein, S. Dehaene, B. Rohaut, F. Tadel, L. Cohen, and L. Naccache, "Neural signature of the conscious processing of auditory regularities," *Proceedings of the National Academy of Sciences*, vol. 106, no. 5, pp. 1672–1677, 2009.

[114] J. R. Wolpaw, "Brain-computer interface research comes of age: Traditional assumptions meet emerging realities," *Journal of Motor Behavior*, vol. 42, no. 6, pp. 351–353, 2010.

[115] E. Donchin, K. Spencer, and R. Wijesinghe, "The mental prosthesis: assessing the speed of a p300-based brain-computer interface," *Rehabilitation Engineering, IEEE Transactions on*, vol. 8, no. 2, pp. 174 –179, jun 2000.

[116] F. Nijboer, E. Sellers, J. Mellinger, M. Jordan, T. Matuz, A. Furdea, S. Halder, U. Mochty, D. Krusienski, T. Vaughan, J. Wolpaw, N. Birbaumer, and A. KÃ$\frac{1}{4}$bler, "A p300-based brain-computer interface for people with amyotrophic lateral sclerosis," *Clinical Neurophysiology*, vol. 119, no. 8, pp. 1909–1916, Aug. 2008.

[117] A. Furdea, S. Halder, D. Krusienski, D. Bross, F. Nijboer, N. Birbaumer, and A. Kübler, "An auditory oddball (p300) spelling system for brain-computer interfaces," *Psychophysiology*, vol. 46, no. 3, pp. 617–625, 2009.

[118] A. Kübler, A. Furdea, S. Halder, E. M. Hammer, F. Nijboer, and B. Kotchoubey, "A brain-computer interface controlled auditory event-related potential (p300) spelling system for locked-in patients," *Annals of the New York Academy of Sciences*, vol. 1157, no. 1, pp. 90–100, 2009.

[119] E. W. Sellers and E. Donchin, "A p300-based brain-computer interface: Initial tests by als patients," *Clinical Neurophysiology*, vol. 117, no. 3, pp. 538 – 548, 2006.

[120] Q. Noirhomme, C. Chatelle, S. Kleih, M. Thonnard, A. Demertzi, M. Bruno, A. Vanhaudenhuyse, O. Gosseries, C. Schnakers, R. Lehembre, A. Soddu, A. Kübler, S. Laureys, and D. Lulé, "Probing command following in patients with disorders of consciousness using a brain-computer interface." in *European Neurological Society, Berlin, Germany*, 2010.

[121] S. Halder, M. Rea, R. Andreoni, F. Nijboer, E. Hammer, S. Kleih, N. Birbaumer, and A. Kübler, "An auditory oddball brain-computer interface for binary choices," *Clinical Neurophysiology*, vol. 121, no. 4, pp. 516–523, Apr. 2010.

[122] J. I. Muenssinger, S. Halder, S. C. Kleih, A. Furdea, V. Raco, A. Hoesle, and A. Kubler, "Brain painting: first evaluation of a new brain-computer interface application with als patients and healthy volunteers," *Frontiers in Neuroscience*, vol. 4, no. 00182, 2010.

[123] G. Pfurtscheller and F. L. da Silva, "Event-related eeg/meg synchronization and desynchronization: basic principles," *Clinical Neurophysiology*, vol. 110, pp. 1842–1857, 1999.

[124] G. Pfurtscheller, C. Neuper, D. Flotzinger, and M. Pregenzer, "Eeg-based discrimination between imagination of right and left hand movement," *Electroencephalography and Clinical Neurophysiology*, vol. 103, no. 6, pp. 642 – 651, 1997.

[125] R. Scherer, G. R. Muller, C. Neuper, B. Graimann, and G. Pfurtscheller, "An asynchronously controlled eeg-based virtual keyboard: improvement of the spelling rate," *IEEE Transactions on Biomedical Engineering*, vol. 51, no. 6, pp. 979–984, June 2004.

[126] F. Nijboer, A. Furdea, I. Gunst, J. Mellinger, D. J. McFarland, N. Birbaumer, and A. Kübler, "An auditory brain-computer interface (bci)," *Journal of Neuroscience Methods*, vol. 167, no. 1, pp. 43 – 50, 2008, <ce:title>Brain-Computer Interfaces (BCIs)</ce:title>.

[127] N. Birbaumer, N. Ghanayim, T. Hinterberger, I. Iversen, B. Kotchoubey, A. Kubler, J. Perelmouter, E. Taub, and H. Flor, "A spelling device for the paralysed," *Nature*, vol. 398, no. 6725, pp. 297–298, Mar. 1999.

[128] C. Neuper, G. Müller, A. Kübler, N. Birbaumer, and G. Pfurtscheller, "Clinical application of an eeg-based brain-computer interface: a case study in a patient with severe motor impairment," *Clinical Neurophysiology*, vol. 114, no. 3, pp. 399 – 409, 2003.

[129] D. Cruse, S. Chennu, C. Chatelle, T. A. Bekinschtein, D. Fernández-Espejo, J. D. Pickard, S. Laureys, and A. M. Owen, "Bedside detection of awareness in the vegetative state: a cohort study," *Lancet*, vol. 378, no. 9809, pp. 2088–2094, Dec. 2011.

[130] N. Birbaumer, "Slow cortical potentials: their origin, meaning, and clinical use," *Brain and Behavior Past, Present, and Future*, pp. 25–39, 1997.

[131] T. Elbert, B. Rockstroh, W. Lutzenberger, and N. Birbaumer, "Biofeedback of slow cortical potentials. i," *Electroencephalography and Clinical Neurophysiology*, vol. 48, no. 3, pp. 293 – 301, 1980.

[132] A. Kübler, B. Kotchoubey, T. Hinterberger, N. Ghanayim, J. Perelmouter, M. Schauer, C. Fritsch, E. Taub, and N. Birbaumer, "The thought translation device: a neurophysiological approach to communication in total motor paralysis," *Experimental Brain Research*, vol. 124, pp. 223–232, 1999, 10.1007/s002210050617.

[133] J. W. Cooley and J. W. Tukey, "An algorithm for the machine calculation of complex fourier series," *Mathematics of Computation*, vol. 19, no. 90, pp. 297–301, 1965.

[134] F. Harris, "On the use of windows for harmonic analysis with the discrete fourier transform," *Proc IEEE*, vol. 66, pp. 51–83, Jan 1978.

[135] N. E. Huang, Z. Shen, S. R. Long, M. C. Wu, H. H. Shih, Q. Zheng, N.-C. Yen, C. C. Tung, and H. H. Liu, "The empirical mode decomposition and the hilbert spectrum for nonlinear and non-stationary time series analysis," *Proc. R. Soc. Lond. A*, vol. 454, pp. 903–995, 1998.

[136] G. Rilling, P. Flandrin, and P. Goncalves, "On empirical mode decomposition and its algorithms," in *IEEE-Eurasip Workshop on Nonlinear Signal and Image Processing NSIP*, 2003.

[137] N. E. Huang, *Hilbert-Huang Transform and It's Applications*, N. E. Huang and S. S. Shen, Eds. World Scientific Publishing Co. Pte. Ltd., 2005.

[138] J. G. Proakis and D. G. Manolakis, *Digital Signal Processing. Principles, Algorithms, and Applications*, 3rd ed. Prentice-Hall, 1996.

[139] A. Bruns, "Fourier-, hilbert- and wavelet-based signal analysis : are they really different approaches?" *Journal of Neuroscience Methods*, vol. 137, pp. 321–332, 2004.

[140] M. L. V. Quyen, J. Foucher, J.-P. Lachaux, E. Rodriguez, A. Lutz, J. Martinerie, and F. J. Varela, "Comparison of hilbert transform and wavelet methods for

the analysis of neuronal synchrony," *Journal of Neuroscience Methods*, vol. 111, pp. 83–98, 2001.

[141] Q. Gu, "Neuromodulatory transmitter systems in the cortex and their role in cortical plasticity," *Neuroscience*, vol. 111, no. 4, pp. 815 – 835, 2002.

[142] J. N. J. Reynolds, B. I. Hyland, and J. R. Wickens, "A cellular mechanism of reward-related learning," *Nature*, vol. 413, no. 6851, pp. 67–70, Sept. 2001.

[143] B. Horwitz, "The elusive concept of brain connectivity," *NeuroImage*, vol. 19, no. 2, pp. 466 – 470, 2003.

[144] A. A. Fingelkurts, A. A. Fingelkurts, and S. Kähkönen, "Functional connectivity in the brain : is it an elusive concept?" *Neuroscience & Biobehavioral Reviews*, vol. 28, no. 8, pp. 827–836, 2005.

[145] K. J. Friston, C. D. Frith, P. F. Liddle, and R. S. J. Frackowiak, "Functional connectivity: The principal-component analysis of large (pet) data sets," *Journal of Cerebral Blood Flow & Metabolism*, vol. 13, no. 1, pp. 5–14, Jan. 1993.

[146] K. J. Friston, C. D. Frith, and R. S. J. Frackowiak, "Time-dependent changes in effective connectivity measured with pet," *Human Brain Mapping*, vol. 1, no. 1, pp. 69–79, 1993.

[147] V. Sakkalis, "Review of advanced techniques for the estimation of brain connectivity measured with eeg/meg," *Computers in Biology and Medicine*, vol. 41, no. 12, pp. 1110–1117, 2011.

[148] R. Srinivasan, P. L. Nunez, and R. B. Silberstein, "Spatial filtering and neocortical dynamics: Estimates of eeg coherence," *IEEE Transactions on Biomedical Engineering*, vol. 45, no. 7, pp. 814–826, July 1998.

[149] R. Srinivasan, W. R. Winter, J. Ding, and P. L. Nunez, "Eeg and meg coherence: Measures of functional connectivity at distinct spatial scales of neocortical dynamics," *Journal of Neuroscience Methods*, vol. 166, pp. 41–52, 2007.

[150] G. Fein, J. Raz, F. Brown, and E. Merrin, "Common reference coherence data are confounded by power and phase effects," *Electroencephalography and clinical Neurophysiology*, vol. 69, pp. 581–584, 1988.

[151] G. Florian, C. Andrew, and G. Pfurtschellera, "Do changes in coherence always reflect changes in functional coupling?" *Electroencephalography and clinical Neurophysiology*, vol. 106, pp. 87–91, 1998.

[152] J.-P. Lachaux, E. Rodriguez, J. Martinerie, and F. J. Varela, "Measuring phase synchrony in brain signals," *Human Brain Mapping*, vol. 8, pp. 194–208, 1999.

[153] C. M. Sweeney-Reed and S. J. Nasuto, "A novel approach to the detection of synchronisation in eeg based on empirical mode decomposition," *Journal of Computational Neuroscience*, vol. 23, pp. 79–111, 2007.

[154] F. Mormann, K. Lehnertz, P. David, and C. E. Elger, "Mean phase coherence as a measure for phase synchronization and its application to the eeg of epilepsy patients," *Physica D*, vol. 144, pp. 358–369, 2000.

[155] R. Kus, M. Kaminski, and K. J. Blinowska, "Determination of eeg activity propagation: Pair-wise versus multichannel estimate," *IEEE Transactions on Biomedical Engineering*, vol. 51, no. 9, pp. 1501–1510, Sept 2004.

[156] K. Sameshima and L. A. Baccala, "Using partial directed coherence to describe neuronal ensemble interactions," *Journal of Neuroscience Methods*, vol. 94, pp. 93–103, 1999.

[157] B. Schelter, M. Winterhalder, M. Eichler, M. Peifer, B. Hellwig, B. Guschlbauer, C. H. Lücking, R. Dahlhaus, and J. Timmer, "Testing for directed influences among neural signals using partial directed coherence," *Journal of Neuroscience Methods*, vol. 152, pp. 210–219, 2005.

[158] A. Korzeniewska, M. gorzata Manczak, M. Kaminski, K. J. Blinowska, and S. Kasicki, "Determination of information flow direction among brain structures by a modified directed transfer function (ddtf) method," *Journal of Neuroscience Methods*, vol. 125, pp. 195–207, 2003.

[159] M. J. Kaminski and K. J. Blinowska, "A new method of the description of the information flow in the brain structures," *Biol. Cybern.*, vol. 65, pp. 203–210, 1991.

[160] L. Astolfi, F. Cincotti, D. Mattia, F. De Vico Fallani, A. Tocci, A. Colosimo, S. Salinari, M. Marciani, W. Hesse, H. Witte, M. Ursino, M. Zavaglia, and F. Babiloni, "Tracking the time-varying cortical connectivity patterns by adaptive multivariate estimators," *IEEE Transactions on Biomedical Engineering*, vol. 55, no. 3, pp. 902 –913, march 2008.

[161] K. Friston, L. Harrison, and W. Penny, "Dynamic causal modelling," *NeuroImage*, vol. 19, no. 4, pp. 1273–1302, Aug. 2003.

[162] O. David, S. J. Kiebel, L. M. Harrison, J. Mattout, J. M. Kilner, and K. J. Friston, "Dynamic causal modeling of evoked responses in eeg and meg," *NeuroImage*, vol. 30, pp. 1255–1272, 2006.

[163] R. Moran, K. Stephan, T. Seidenbecher, H.-C. Pape, R. Dolan, and K. Friston, "Dynamic causal models of steady-state responses," *NeuroImage*, vol. 44, pp. 796–811, 2009.

[164] C. Chen, S. Kiebel, and K. Friston, "Dynamic causal modelling of induced responses," *NeuroImage*, vol. 41, pp. 1293–1312, 2008.

[165] B. H. Jansen and V. G. Rit, "Electroencephalogram and visual evoked potential generation in a mathematical model of coupled cortical columns," *Biol. Cybern.*, vol. 73, pp. 357–366, 1995.

[166] K. Friston, J. Mattout, N. Trujillo-Barreto, J. Ashburner, and W. Penny, "Variational free energy and the laplace approximation," *NeuroImage*, vol. 34, no. 1, pp. 220 – 234, 2007.

[167] D. Ruchkin, "Eeg coherence," *International Journal of Psychophysiology*, vol. 57, pp. 83–85, 2005.

[168] R. Thatcher, D. North, and C. Biver, "Eeg and intelligence: Relations between eeg coherence, eeg phase delay and power," *Clinical Neurophysiology*, vol. 116, pp. 2129–2141, 2005.

[169] W. R. Winter, P. L. Nunez, J. Ding, and R. Srinivasan, "Comparison of the effect of volume conduction on eeg coherence with the effect of field spread on meg coherence," *Statist. Med.*, vol. 26, pp. 3946–3957, 2007.

[170] R. D. Pascual-Marqui, "Coherence and phase synchronization: generalization to pairs of multivariate time series, and removal of zero-lag contributions," *arXiv:0706.1776v3 [stat.ME]*, 2007.

[171] R. Q. Quiroga, A. Kraskov, T. Kreuz, and P. Grassberger, "Performance of different synchronization measures in real data: A case study on electroencephalographic signals," *Physical Review*, vol. 65, 2002.

[172] L. Astolfi, F. Cincotti, D. Mattia, M. G. Marciani, L. A. Baccala, F. de Vico Fallani, S. Salinari, M. Ursino, M. Zavaglia, L. Ding, J. C. Edgar, G. A. Miller, B. He, and F. Babiloni, "Comparison of different cortical connectivity estimators for high-resolution eeg recordings," *Human Brain Mapping*, vol. 28, pp. 143–157, 2007.

[173] F. N. Wilson and R. H. Bayley, "The electric field of an eccentric dipole in a homogeneous spherical conducting medium," *Circulation*, vol. 1, pp. 84–92, 1950.

[174] S. Rush and D. A. Driscoll, "Current distribution in the brain from surface electrodes," *Anesthesia and Analgesia*, vol. 47, pp. 717–723, Nov-Dec 1968.

[175] M. Schneider and P. Gerin, "Une methode de localization des dipoles cerebraux," *Electroencephalography and clinical neurophysiology*, vol. 28, pp. 68–78, 1970.

[176] M. R. Schneider, "A multistage process for computing virtual dipolar sources of eeg discharges from surface information," *IEEE Transactions on Biomedical Engineering*, vol. 19, no. 1, pp. 1–12, January 1972.

[177] R. N. Kavanagh, T. M. Darcey, D. Lehmann, and D. H. Fender, "Evaluation of methods for three-dimensional localization of electrical sources in the human brain," *IEEE Transactions on Biomedical Engineering*, vol. 25, no. 5, pp. 421–429, September 1978.

[178] B. He, T. Musha, Y. Okamoto, S. Homma, Y. Nakajima, and T. Sato, "Electric dipole tracing in the brain by means of the boundary element method and its accuracy," *IEEE Transactions on Biomedical Engineering*, vol. 34, no. 6, pp. 406–414, June 1987.

[179] B. N. Cuffin, "Eeg localization accuracy improvements using realistically shaped head models," *IEEE Transactions on Biomedical Engineering*, vol. 43, no. 3, pp. 299–303, March 1996.

[180] R. D. Pascual-Marqui, C. M. Michel, and D. Lehmann, "Low resolution electromagnetic tomography : A new method for localizing electrical activity in the brain," *International Journal of Psychophysiology*, vol. 18, pp. 49–65, 1994.

[181] A. N. Tikhonov and V. Y. Arsenin, *Solutions of Ill-Posed Problems*. New-York : Wiley, 1977.

[182] I. F. Gorodnitsky, J. S. George, and B. D. Rao, "Neuromagnetic source imaging with focuss: a recursive weighted minimum norm algorithm," *Electroencephalography and clinical neurophysiology*, vol. 95, pp. 231–251, 1995.

[183] R. Lehembre, O. Gosseries, R. Moran, M. Massimini, M. Rosanova, A.Vanhaudenhuyse, M. Bruno, V. Bonhomme, J. Brichant, P. Boveroux, A.Soddu, C.Phillips, Q.Noirhomme, S.Laureys, and M.Boly, "Electrophysiological correlates of ketamine induced loss of responsiveness," 2012, to be submitted.

[184] K. W. Grathwohl, "Does ketamine improve postoperative analgesia? more questions than answers," *Pain Medicine*, vol. 12, no. 8, pp. 1135–1136, 2011.

[185] E. Check, "Depression: Comfortably numb," *Nature*, vol. 443, no. 7112, pp. 629–631, Oct. 2006.

[186] E. Krupitsky and A. Grinenko, "Ketamine psychedelic therapy (kpt): A review of the results of ten years of research," *Journal of Psychoactive Drugs*, vol. 29, pp. 165–183, 1997.

[187] A. K. Malhotra, D. A. Pinals, H. Weingartner, K. Sirocco, C. D. Missar, D. Pickar, and A. Breier, "Nmda receptor function and human cognition: The

effects of ketamine in healthy volunteers," *Neuropsychopharmacology*, vol. 14, pp. 301–307, 1996.

[188] E. Kochs, E. Scharein, O. Mollenberg, B. Bromm, and J. Schulte Esch, "Analgesic efficacy of low-dose ketamine: Somatosensory-evoked responses in relation to subjective pain ratings," *Anesthesiology*, vol. 85, no. 2, pp. 304–314, 1996.

[189] P. Hans, P.-Y. Dewandre, J. F. Brichant, and V. Bonhomme, "Comparative effects of ketamine on bispectral index and spectral entropy of the electroencephalogram under sevoflurane anaesthesia," *British Journal of Anaesthesia*, vol. 94, no. 3, pp. 336–340, 2005.

[190] A. Maksimow, M. Särkelä, J. Långsjö, E. Salmi, K. Kaisti, A. Yli-Hankala, S. Hinkka-Yli-Salomäki, H. Scheinin, and S. Jääskeläinen, "Increase in high frequency eeg activity explains the poor performance of eeg spectral entropy monitor during s-ketamine anesthesia," *Clinical Neurophysiology*, vol. 117, no. 8, pp. 1660 – 1668, 2006.

[191] T. Sakai, H. Singh, W. D. Mi, T. Kudo, and A. Matsuki, "The effect of ketamine on clinical endpoints of hypnosis and eeg variables during propofol infusion," *Acta Anaesthesiologica Scandinavica*, vol. 43, no. 2, pp. 212–216, 1999.

[192] F. X. Vollenweider, K. L. Leenders, I. Øye, D. Hell, and J. Angst, "Differential psychopathology and patterns of cerebral glucose utilisation produced by (s)- and (r)-ketamine in healthy volunteers using positron emission tomography (pet)," *European Neuropsychopharmacology*, vol. 7, no. 1, pp. 25 – 38, 1997.

[193] F. X. Vollenweider, K. L. Leenders, C. Scharfetter, A. Antonini, P. Maguire, J. Missimer, and J. Angst, "Metabolic hyperfrontality and psychopathology in the ketamine model of psychosis using positron emission tomography (pet) and [18f]fluorodeoxyglucose (fdg)," *European Neuropsychopharmacology*, vol. 7, no. 1, pp. 9 –24, 1997.

[194] A. Breier, A. Malhotra, D. Pinals, N. Weisenfeld, and D. Pickar, "Association of ketamine-induced psychosis with focal activation of the prefrontal cortex in healthy volunteers," *Am J Psychiatry*, vol. 154, no. 6, pp. 805–811, 1997.

[195] J. W. Langsjö, E. Salmi, K. K. Kaisti, S. Aalto, S. Hinkka, R. Aantaa, V. Oikonen, T. Viljanen, T. Kurki, M. Silvanto, and H. Scheinin, "Effects of subanesthetic ketamine on regional cerebral glucose metabolism in humans," *Anesthesiology*, vol. 100, no. 5, pp. 1065–1071, 2004.

[196] I. Kreitschmann-Andermahr, T. Rosburg, U. Demme, E. Gaser, H. Nowak, and H. Sauer, "Effect of ketamine on the neuromagnetic mismatch field in healthy humans," *Cognitive Brain Research*, vol. 12, no. 1, pp. 109 – 116, 2001.

[197] F. Musso, J. Brinkmeyer, D. Ecker, M. K. London, G. Thieme, T. Warbrick, H.-J. Wittsack, A. Saleh, W. Greb, P. de Boer, and G. Winterer, "Ketamine effects on brain function – simultaneous fmri/eeg during a visual oddball task," *NeuroImage*, vol. 58, no. 2, pp. 508 – 525, 2011.

[198] G. Plourde, J. Baribeau, and V. Bonhomme, "Ketamine increases the amplitude of the 40-hz auditory steady-state response in humans." *British Journal of Anaesthesia*, vol. 78, no. 5, pp. 524–529, 1997.

[199] S. A. Neymotin, M. T. Lazarewicz, M. Sherif, D. Contreras, L. H. Finkel, and W. W. Lytton, "Ketamine disrupts theta modulation of gamma in a computer model of hippocampus," *The Journal of Neuroscience*, vol. 31, no. 32, pp. 11 733–11 743, 2011.

[200] K. Stephan, W. Penny, R. Moran, H. den Ouden, J. Daunizeau, and K. Friston, "Ten simple rules for dynamic causal modeling," *NeuroImage*, vol. 49, no. 4, pp. 3099–3109, 2010.

[201] G. Buzsaki, *Cycle 9, The Gamma Buzz. Rhythms of the brain*. Oxford, 2006.

[202] M. Murphy, M.-A. Bruno, B. A. Riedner, P. Boveroux, Q. Noirhomme, E. C. Landsness, J.-F. Brichant, C. Phillips, M. Massimini, S. Laureys, G. Tononi, and M. Boly, "Propofol anesthesia and sleep: a high-density eeg study," *Sleep*, vol. 34, no. 3, pp. 283–291, 2011.

[203] J. A. Cardin, M. Carlen, K. Meletis, U. Knoblich, F. Zhang, K. Deisseroth, L.-H. Tsai, and C. I. Moore, "Driving fast-spiking cells induces gamma rhythm and controls sensory responses," *Nature*, vol. 459, no. 7247, pp. 663–667, June 2009.

[204] R. J. Moran, K. E. Stephan, R. J. Dolan, and K. J. Friston, "Consistent spectral predictors for dynamic causal models of steady-state responses," *NeuroImage*, vol. 55, no. 4, pp. 1694 – 1708, 2011.

[205] A. Vanhaudenhuyse, A. Demertzi, M. Schabus, Q. Noirhomme, S. Bredart, M. Boly, C. Phillips, A. Soddu, A. Luxen, G. Moonen, and S. Laureys, "Two distinct neuronal networks mediate the awareness of environment and of self," *Journal of Cognitive Neuroscience*, vol. 23, no. 3, pp. 570–578, june 2010.

[206] M. Boly, R. Moran, M. Murphy, P. Boveroux, M.-A. Bruno, Q. Noirhomme, D. Ledoux, V. Bonhomme, J.-F. Brichant, G. Tononi, S. Laureys, and K. Friston, "Connectivity changes underlying spectral eeg changes during propofol-induced loss of consciousness," *The Journal of Neuroscience*, vol. 32, no. 20, pp. 7082–7090, 2012.

[207] B. Jennett and F. Plum, "Persistent vegetative state after brain damage. a syndrome in search of a name." *Lancet*, vol. 1, pp. 734–737, April 1972.

[208] J. Giacino and K. Kalmar, "The vegetative and minimally conscious states: A comparison of clinical features and functional outcome," *The Journal of Head Trauma Rehabilitation*, vol. 12, no. 4, pp. 36–54, August 1997.

[209] S. Majerus, H. Gill-Thwaites, K. Andrews, and S. Laureys, "Behavioral evaluation of consciousness in severe brain damage," *Progress in Brain Research*, vol. 150, pp. 397–413, 2005.

[210] G. Teasdale and B. Jennett, "Assessment of coma and impaired consciousness. a practical scale." *The Lancet*, vol. 304, no. 7872, pp. 81–84, July 1974.

[211] N. Schiff, D. Rodriguez-Moreno, A. Kamal, K. Kim, J. Giacino, F. Plum, and J. Hirsch, "fmri reveals large-scale network activation in minimally conscious patients," *Neurology*, vol. 64, pp. 514–523, 2005.

[212] M. Boly, M.-E. Faymonville, P. Peigneux, B. Lambermont, P. Damas, G. D. Fiore, C. Degueldre, G. Franck, A. Luxen, M. Lamy, G. Moonen, P. Maquet, and S. Laureys, "Auditory processing in severely brain injured patients - differences between the minimally conscious state and the persistent vegetative state," *Archive in Neurology*, vol. 61, p. 233, 2004.

[213] M. R. Coleman, J. M.Rodd, M. H. Davis, I. S. Johnsrude, D. K. Menon, J. D. Pickard, and A. M.Owen, "Do vegetative patients retain aspects of language comprehension? evidence from fmri," *Brain*, vol. 130, pp. 2494–2507, 2007.

[214] M. M. Monti, A. Vanhaudenhuyse, M. R. Coleman, M. Boly, J. D. Pickard, L. Tshibanda, A. M. Owen, and S. Laureys, "Willful modulation of brain activity in disorders of consciousness," *The new england journal of medicine*, 2010.

[215] A. M. Owen, M. R. Coleman, M. Boly, M. H. Davis, S. Laureys, and J. D. Pickard, "Detecting awareness in the vegetative state," *Science*, vol. 313, p. 1402, 2006.

[216] C. Schnakers, S. Majerus, J. Giacino, A. Vanhaudenhuyse, M.-A. Bruno, M. Boly, G. Moonen, P. Damas, B. Lambermont, M. Lamy, F. Damas, M. Ventura, and S. Laureys, "The coma recovery scale-revised (crs-r): Validation of the french version," *Brain Injury*, vol. 22, no. 10, pp. 786–792, 2008.

[217] Y. Leclercq, P. Maquet, Q. Noirhomme, and C. Phillips, "fmri artefact rejection and sleep scoring toolbox (fast)," Cyclotron Research Centre, University of Liege, Belgium., http://www.montefiore.ulg.ac.be/ phillips/toolbox.html, Tech. Rep., 2009.

[218] D. Percival and A. Walden, *Spectral Analysis for Physical Applications: Multitaper and Conventional Univariate Techniques*. Cambridge University Press, 1993.

[219] R. Thatcher, "Eeg database-guided neurotherapy. in: Evans jr, abarbanel a, editors. introduction to quantitative eeg and neurofeedback. san diego: Academic press," pp. 29–60, 1999.

[220] W. J. Freeman, "Definitions of state variables and state space for brain-computer interface. part i. multiple hierarchical levels of brain function," *Cognitive Neurodynamics*, vol. 1, pp. 3–14, 2007.

[221] L. Qin, L. Ding, and B. He, "Motor imagery classification by means of source analysis for brain computer interface applicatinos," *Journal of Neural Engineering*, vol. 1, pp. 133–141, 2004.

[222] B. Kamousi, Z. Liu, and B. He, "An eeg inverse solution based brain-computer interface," *International Journal of Bioelectromagnetism*, vol. 7, no. 2, pp. 292–294, 2005.

[223] R. G. de Peralta Menendez, S. G. Andino, L. Perez, P. Ferrez, and J. d.R. Millán, "Non-invasive estimation of local field potentials for neuroprosthesis control," *Cognitive Processing*, vol. 6, pp. 59–64, 2005.

[224] Q. Noirhomme, R. Kitney, and B. Macq, "Single-trial eeg source reconstruction for brain-computer interface," *IEEE Transactions on Biomedical Engineering*, vol. 55, pp. 1592–1601, May 2008.

[225] M. Congedo, F. Lotte, and A. Lécuyer, "Classification of movement intention by spatially filtered electromagnetic inverse solutions," *Physics in Medicine and Biology*, vol. 51, pp. 1971–1989, 2006.

[226] B. Blankertz, G. Curio, and K.-R. Müller, "Classifying single trial eeg: Towards brain computer interfacing," *Advances in Neural Inf. Proc. Systems*, vol. 14, 2002.

[227] J. A. V. Bates, "Electrical activity of the cortex accompanying movement," *Journal of Physiology*, vol. 113, pp. 240–257, 1951.

[228] H. Kornhuber and L. Deecke, "Changes in the brain potential in voluntary movements and passive movements in man: readiness potential and reafferent potentials," *Pflugers Arch Gesamte Physiol Menschen Tiere*, vol. 284, pp. 1–17, 1965.

[229] L. Defebvre, J.-L. Bourriez, K. Dujardin, P. Derambure, A. Destée, and J.-D. Guieu, "Spatiotemporal study of bereitschaflspotential and event-related desynchronization during voluntary movement in parkinson's disease," *Brain Topography*, vol. 6, no. 3, pp. 237–244, 1994.

[230] R. Q. Cui, D. Huter, W. Lang, and L. Deecke, "Neuroimage of voluntary movement: Topography of the bereitschaftspotential, a 64-channel dc current source density study," *NeuroImage*, vol. 9, pp. 129–134, 1999.

[231] R.-Q. Cui and L. Deecke, "High resolution dc eeg of the bereitschaftspotential preceding anatomically congruent versus spatially congruent bimanual finger movements," *Brain Topography*, vol. 12, no. 2, pp. 117–127, 1999.

[232] M. Kukleta and M. Lamarche, "Steep early negative slopes can be demonstrated in pre-movement bereitschaftspotential," *Clinical Neurophysiology*, vol. 112, pp. 1642–1649, 2001.

[233] G. Dornhege, B. Blankertz, and G. Curio, "Speeding up classification of multi-channel brain-computer interfaces: Common spatial patterns for slow cortical potentials," in *First International IEEE EMBS Conference on Neural Engineering*, March 2003, pp. 595–598.

[234] J. Green, P. S. Arnold, L. Rozhkov, D. Strother, and N. Garrott, "Bereitschaft (readiness potential) and supplemental motor area interaction in movement generation: Spinal cord injury and normal subjects," *Journal of Rehabilitation Research and Development*, vol. 40, no. 3, pp. 225–234, 2003.

[235] R. Kus, J. S. Ginter, and K. J. Blinowska, "Propagation of eeg activity during finger movement and its imagination," *Acta Neurobiol Exp*, vol. 66, pp. 195–206, 2006.

[236] Z. J. Koles, M. S. Lazar, and S. Z. Zhou, "Spatial patterns underlying population differences in the background eeg," *Brain Topography*, vol. 2, no. 4, pp. 275–284, 1990.

[237] Y. Wang, P. Berg, and M. Scherg, "Common spatial subspace decomposition applied to analysis of brain responses under multiple task conditions: a simulation study," *Clinical Neurophysiology*, vol. 110, pp. 604–614, 1999.

[238] S. Lemm, B. Blankertz, G. Curio, and K.-R. Müller, "Spatio-spectral filters for improving the classification of single trial eeg," *IEEE Transactions on Biomedical Engineering*, vol. 52, pp. 1541–1548, 2005.

[239] D. Krusienski, E. Sellers, and T. Vaughan, "Common spatio-temporal patterns for the p300 speller," in *3rd International IEEE/EMBS Conference on Neural Engineering*, ser. 5, no. 2, May 2007, pp. 427–424.

[240] M. Grosse-Wentrup and M. Buss, "Multiclass common spatial patterns and information theoretic feature extraction," *IEEE Transactions on Biomedical Engineering*, vol. 55, no. 8, pp. 1991–2000, August 2008.

[241] B. Blankertz, R. Tomioka, S. Lemm, M. Kawanabe, and K.-R. Müller, "Optimizing spatial filters for robust eeg single-trial analysis," *IEEE Signal Processing Magazine*, vol. 25, pp. 41–56, 2008.

[242] M. Grosse-Wentrup, K. Gramann, and M. Buss, "Adaptive spatial filters with predefined region of interest for eeg based brain-computer-interfaces," *Advances in neural information processing systems*, vol. 19, pp. 537–544, 2007.

[243] J. Mosher, R. Leahy, and P. Lewis, "Eeg and meg : Forward solutions for inverse methods," *IEEE Transactions on Biomedical Engineering*, vol. 46, no. 3, pp. 245–259, March 1999.

[244] R. G. de Peralta Menendez, Q. Noirhomme, F. Cincotti, D. Mattia, F. Aloise, and S. G. Andino, "Modern electrophysiological methods for brain-computer interfaces," *Computational Intelligence and Neuroscience*, 2007.

[245] G. Buzsáki, *Rhythms of the Brain*. Oxford University Press, 2006.

[246] M.-A. Bruno, D. Fernandez-Espejo, R. Lehembre, L. Tshibanda, A. Vanhaudenhuyse, O. Gosseries, E. Lommers, M. Napolitani, Q. Noirhomme, M. Boly, M. Papa, A. Owen, P. Maquet, S. Laureys, and A. Soddu, "Multimodal neuroimaging in patients with disorders of consciousness showing "functional hemispherectomy"." *Progress in Brain Research*, vol. 193, no. 0079-6123 (Linking), pp. 323–333, 2011.